Universidade Nova de Lisboa

Instituto de Higiene e Medicina Tropical

ABC efflux pumps in eukaryotic cells

From function to regulation

Ana Maria Buttle de Mendonça Mourão Possidónio de Armada

TESE PARA A OBTENÇÃO DO GRAU DE DOUTOR EM CIÊNCIAS BIOMÉDICAS ESPECIALIDADE DE GENÉTICA

FEVEREIRO, 2019

Universidade Nova de Lisboa

Instituto de Higiene e Medicina Tropical

ABC efflux pumps in eukaryotic cells

From function to regulation

Ana Maria Buttle de Mendonça Mourão Possidónio de Armada

Supervisor: Professor Doutor Miguel Viveiros Bettencourt (IHMT/UNL**)**

Co-supervisor: Professor Doutor António Sebastião Rodrigues (NMS/FCM/UNL)

Tese apresentada para cumprimento dos requisitos necessários à obtenção do grau de Doutor em Ciências Biomédicas, especialidade de Genética.

Thesis presented in fulfillment of the necessary requirements to obtain the PhD degree in Biomedical Sciences, specialization Genetics

Curso de Doutoramento em Genética Humana e Doenças Infeciosas, em associação entre o IHMT e a Faculdade de Ciências Médicas (NMS/FCM)

Bibliographic elements

This thesis contains data and/or methodologies published in the following peer-reviewed articles:

Armada A, Martins C, Spengler G, Molnar J, Amaral L, Rodrigues AS, Viveiros M. Fluorimetric methods for analysis of permeability, drug transport kinetics and inhibition of the ABCB1 membrane transporter. Cancer Drug Resistance' book- series Springer 'Methods in Molecular Biology'. 2016; 1395:87-103. doi: 10.1007/978-1- 4939-3347-1_7.

Pinto-Almeida A, Mendes T, **Armada A**, Belo S, Carrilho E, Viveiros M, Afonso A. The role of efflux pumps in *Schistosoma mansoni* praziquantel resistant phenotype. PLoS One. 2015; 10: e0140147.

Other papers published during the preparation of this thesis:

Rabna P, Ramos J, Ponce G, Sanca L, Mane M, **Armada A**, Machado D, Vieira F, Gomes V F, Martins E, Colombatti R, Riccardi F, Perdigão J, Sotero J, Portugal I, Couto I, Atouguia J, Rodrigues A, Viveiros M. Direct detection by the Xpert MTB/RIF assay and characterization of multi and poly drug-resistant tuberculosis in Guinea-Bissau, West Africa. PLoS One. 2015; 10. doi: 10.1371/journal.pone.0127536.

The work developed during this thesis was presented in four (4) oral communications and seven (7) posters at national and international conferences:

Oral communications:

Armada A, Costa-Gomes B, Rueff J, Viveiros M, Rodrigues AS. 2017. Evaluation of the modulating effect of miR-203 and miR-200c on drug extrusion by ABCB1. 3rd NOVA Health Genetics Workshop, Universidade Nova de Lisboa (UNL), Reitoria da UNL (Campus de Campolide), 2th October, Lisboa, Portugal. Abstract Book 11.

Santos-Gomes G, Rafael-Fernandes M, **Armada A**, Ruas P, Lago JH, Passero F, Viveiros M. 2017. Eficácia da terapia combinada como estratégia alternativa ao tratamento convencional das leishmanioses. III Encontro Científico. Busca por compostos ativos para as doenças causadas por protozoários. Do conhecimento tradicional à síntese estrutural. Faculdade de Medicina da Universidade de S. Paulo. 21-23 de junho, SP, Brasil.

Armada A, Gomes B, Rueff J, Rodrigues AS, Viveiros M. 2016. MicroRNAs 203 e 200c regulam a expressão das bombas ABCB1 na resistência à doxorrubicina. 2016. Jornadas Científicas do IHMT. Instituto de Higiene e Medicina Tropical, Universidade Nova de Lisboa. 12 dezembro, Lisboa.

Armada A. 2015. Aplicação de técnicas de fluorescência ao estudo dos transportadores de membrana de células eucariotas (tripanosomatídeos). Invited speaker at IHMT 9th November.

Mendes T, Pinto-Almeida A, **Armada A,** Viveiros M, Belo S, Afonso A. 2014. Avaliação do envolvimento das bombas de efluxo na fármaco resistência ao praziquantel em *Schistosoma mansoni*. VII Congresso da Sociedade Paulista de Parasitologia, 14-15 de novembro, Brasil.

Posters:

Armada A, Gomes B, Rueff AJ, Viveiros M, Rodrigues AS. 2017. Evaluation of the modulating effect of miR-203 and miR-200c on drug extrusion by ABCB1 and doxorubicin resistance. Ciência 2017, Science and Technology in Portugal Meeting, Congress Centre, 4-6 July, Lisbon.

Armada A, Gomes B, Rueff AJ, Viveiros M, Rodrigues AS. 2017. Texas United States. Evaluation of the modulating effect of miR-203 and miR-200c on drug extrusion by ABCB1 and doxorubicin resistance. Gordon Research Conferences on Multi-Drug Efflux Systems, 26-31 March, Galveston, Texas, United States.

Armada A, Mendes T, Fernandes MR, Afonso A, Santos-Gomes G, Viveiros M. 2016. Modulation of ABC transporters in unicellular and pluricellular parasites: *L. infantum* and *Schistosoma mansoni*. Ciência 2016, Science and Technology in Portugal Meeting, Lisbon, 4-6 July, Congress Centre. Painel das Ciências Médicas e da Saúde: http://www.ciencia2016.pt/poster/

Armada A, Martins C, Bucar F, Rodrigues S, Viveiros M.2015. Methods of analysis of eukaryotic membrane transporters: application to 6- gingerol. 1rst NOVA Health Genetics Workshop, Universidade Nova de Lisboa (UNL), Reitoria da UNL (Campus de Campolide), 9th October, Lisboa, Portugal.

Armada A, Martins C, Bucar F, Rodrigues S, Viveiros M. 2015. Methods of analysis of eukaryotic membrane transporters: application to 6- gingerol. Microbiotec'15, Congresso Português de Microbiologia e Biotecnologia, Universidade de Évora, 10-12 dezembro, Évora; Portugal.

Gabriel M, **Armada A**, Pereira M, Santos-Gomes G, Viveiros M. 2015. Inflammatory immune response of macrophages in the presence of efflux inhibitors. Microbiotec'15, Congresso Português de Microbiologia e Biotecnologia, Universidade de Évora, 10-12 dezembro, Évora, Portugal.

Armada A, Martins C, Bucar F, Rodrigues AS, Viveiros M. 2015. 6-gingerol como modulador dos transportadores MDR1 humanos: Aplicação de técnicas de fluorescência. Jornadas Científicas do IHMT. Instituto de Higiene e Medicina Tropical, Universidade Nova de Lisboa. 11 dezembro, Lisboa;

Acknowledgements

I would like to express my gratitude to those who, directly or indirectly, have contributed to the development of all the work presented here.

Firstly, I would like to thank my supervisor the Full Professor Miguel Viveiros Bettencourt for the continuous support in my PhD study and related research, for his motivation and knowledge. During the preparation of this manuscript your pertinent suggestions contributed to the improvement of the final document. Thank you for reviewing the manuscript.

To my co-supervisor, Professor António Sebastião Rodrigues for his guidance, support, motivation and for giving me the opportunity to work on a great project in a great laboratory with great people. Thank you for reviewing the manuscript, and thank you for being part of my scientific committee.

I would like to express a special mention to Professor Gabriela Santos-Gomes for all the support and encouragement during the preparation of this manuscript your pertinent suggestions and comments contributed, undoubtedly, for the improvement of the final document. Thank you for reviewing the manuscript, thanks for being part of my scientific committee and helping with *Leishmania* work, and most of all for being my friend, I have learnt a lot from you.

I would also like to express my gratitude to the NOVA Medical School (NMS/FCM/UNL) for being part of this first joint doctoral program of the IHMT, specially to the full Professor José Rueff from Nova Medical School whose expertise and encouragement were inspirational throughout the entire thesis and in particular during miRNA study.

Special thanks to Bruno Costa-Gomes, from NMS/FCM whose vast knowledge and experience in the microRNA field was admirable and inspirational to me. Your unwavering support helped me get through the finish line. It is so easy to work with you.

Besides Bruno and Sebastião, I would also like to thank all the other members of the Genetic group (previous and current) of NMS/FCM/UNL, Michel, Diana, Susana, Isabel, Helena, Joaquim and Francisco for making such a positive work environment. A special thanks to Célia who also helped me when I needed it.

To Researcher Doctor Maria Luisa Vieira who always encouraged me, and gave me help when I needed it, a good colleague and a friend. Thank you for helping. Your help was crucial in a critical moment of this thesis.

To Tiago Mendes and Marta Gabriel, thank you for your collaboration. Thank you Ana Afonso and Tiago, our “worm” study was really one of the most challenging and exciting research works. It all started when I realized it was a “worm”, difficult to put in the rotor-gene!! Thankyou Silvana Belo.

Besides my supervisor, co-supervisor and Gabriela, I would like to thank Doctor Isabel Couto as a colleague and member of my thesis committee, for her advice and helpful comments that pointed this work in the right direction.

To Professor Ana Tomás, from Instituto Biologia Molecular e Celular (IBMC), for providing the GFP-*L. infantum* transformed parasites used in this study. Thank you for your important collaboration.

To Gabriella Spengler and Professor Molnar for providing the breast cancer cell lines (MCF-7 and KCR) used in this study. Thank you for your important collaboration.

To Professor Michael Gottesman for providing the mouse Lymphoma T cells.

To Professor Franz Bucar and Barbara Gröblacher for providing the natural compound 6-gingerol and their important collaboration.

My thanks to Full Professor Lenea Campino and José Manuel for allowing the use of the fluorescence microscope.

To Claudia Andrade from CEDOC, for helping me with the gating strategy (FlowJo).

Thank you Maria for helping me with the *Leishmanias.*

To my colleagues from Microbiology Unit, Paula, Rita, Jorge, Odete, João, Ricardo with a special reference to Aida for letting me use the virology culture room. Thank you João Piedade for your support during these years.

A special thanks to my lunch colleagues, Sofia, Teresa, Sofia Côrtes, Catarina for all the talks and laughs during these years. Teresa, thank you for your help that was crucial in a critical moment of this thesis.

Thankyou Angela for all your support and friendship.

Thankyou Paula Costa for your help, always with me!!

Thank you to the Academic division, specially Paula and Ana Varão for their support, being the first of this PhD wasn't easy.

Thank you Carlos and António, the Informatics team, all the help with the computers during these years.

To GHTM for the acquisition of the Flow Cytometer, it really changed my work, also to the THOP group for their support.

To all the colleagues that work in the other Units of the Institute, thank you for the encouragement given during this thesis, specially Fátima Nogueira, Ana Paula Arez, Ana Domingos, Celso Cunha and Ana Reis.

And finally, my parents, my brothers and sister, parents in law, husband, son and daughter thank you for your support.

Resumo

A resistência à quimioterapia é um problema grave no tratamento de doenças infeciosas e parasitárias e oncológicas. Microrganismos procariotas (bactérias), agentes patogénicos eucariotas (fungos, helmintas e protozoários) e células eucariotas, como é o caso das células tumorais, desenvolvem frequentemente resistência aos agentes quimioterápicos. A resistência a múltiplos fármacos (MDR) está relacionada com o aumento da expressão e atividade do sistema membranar de transportadores de efluxo (bombas ABC). Estas bombas são responsáveis por falhas terapêuticas tanto no cancro como nas doenças infeciosas.

Embora existam diversos moduladores de bombas ABC, estes transportadores são ubiquamente expressos nos tecidos epiteliais humanos, pelo que a aplicação clinica de inibidores de bombas de efluxo causa grave toxicidade sistémica. Permanece, portanto, a necessidade de encontrar moduladores menos tóxicos capazes de reverter o fenótipo MDR, resensibilizando as células resistentes à quimioterapia. O reconhecimento da existência de fitoquímicos capazes de modular os transportadores ABC com menor toxicidade tem gerado novas linhas de investigação.

Este estudo teve como objetivo principal avaliar a influência de bombas de efluxo ABCB1 no desenvolvimento de quimioresistência e analisar a atividade pleiotrópica de moduladores sintéticos e naturais de bombas de efluxo em diversos modelos biológicos: parasita multicelular (*Schistosoma mansoni*), linha macrofágica de murganho infetada por um protozoário intracelular (*Leishmania infantum*) e linhas celulares malignas de origem humana.

Os métodos regularmente utilizados no estudo dos transportadores ABC não permitem determinar a sua eficácia em tempo real. Neste estudo foram aplicadas metodologias baseadas no transporte celular de substratos fluorescentes capazes de avaliar em tempo real a funcionalidade das bombas de efluxo por fluorimetria e por citometria de fluxo. A microscopia de fluorescência e a técnica de PCR quantitativo em tempo real (RT-qPCR) foram também aplicadas.

Nos ensaios *ex vivo* foi possível demonstrar que as bombas ABCB1 de *S. mansoni* estavam envolvidas na resistência ao prazinquantel e que verapamil (VP), modulador sintético de bombas ABCB1, reverte a resistência. Nos macrófagos modificados pela infeção por *L. infantum* foi observado um expressivo incremento de bombas ABCB1 na membrana celular. Inibidores sintéticos de canais iónicos e de bombas de efluxo, como VP, ouabaína, tioridazina e cloropromazina, e o composto natural 6-gingerol (6G) reduziram a atividade de efluxo dos macrófagos não infetados. Complementarmente a atividade destes moduladores foi também relacionada com o stress oxidativo dos macrófagos. O tratamento com inibidores sintéticos de efluxo e com o 6G diminuiu a sobrevivência dos parasitas intracelulares e a sua capacidade de se multiplicar, sugerindo que estes moduladores e o VP, em particular, podem ter um efeito leishmanicida direto ou indireto. Em células de carcinoma mamário resistentes à doxorrubicina e com sobreexpressão de bombas ABCB1, o VP reverteu a resistência ao paclitaxel e o 6G mostrou ser citotóxico para as células resistentes, o que poderá estar relacionado com o

incremento das espécies reativas de oxigénio, e consequentemente com o desequilíbrio homeostático. Nestas células foi possível demonstrar correlação direta entre a atividade de efluxo e a expressão das bombas ABCB1 e que os microRNAs podem modular o fenótipo resistente, interferindo na expressão génica de transportadores ABCB1.

PALAVRAS-CHAVE: Sistemas de efluxo; MDR em modelos células eucariotas, Resistência a múltiplos fármacos; Ensaios de fluorimetria em tempo real, Inibidores efluxo.

Abstract

Resistance to chemotherapy is a serious problem in the treatment of infectious and parasitic and oncological diseases. Prokaryotic microorganisms (bacteria), eukaryotic pathogens (fungi, helminths and protozoa) and eukaryotic cells, such as tumor cells, often develop resistance to chemotherapeutic agents. Multiple drug resistance (MDR) is related to an increased expression and activity of the membrane efflux transporter systems (ABC pumps). These pumps are responsible for therapeutic failures in both cancer and infectious diseases.

Although there are several ABC pump modulators, these transporters are ubiquitously expressed in human epithelial tissues, so the clinical application of efflux pump inhibitors causes severe systemic toxicity. Therefore, there is a need to find less toxic modulators capable of reversing the MDR phenotype and resensitize resistant cells to chemotherapy. The recognition of the existence of phytochemicals capable of modulating ABC transporters with lower toxicity has generated new lines of investigation.

The objective of this study was to evaluate the influence of ABCB1 efflux pumps on the development of chemoresistance and to analyze the pleiotropic activity of synthetic and natural modulators of efflux pumps in several biological models: multicellular parasite (*Schistosoma mansoni*), murine macrophage cell lines infected by an intracellular protozoan (*Leishmania infantum*) and malignant cell lines of human origin.

The methods regularly used in the study of ABC transporters are not able to determine their effectiveness in real-time. In this study, methodologies based on the cellular transport of fluorescent substrates capable of evaluating in real time the functionality of the efflux pumps by fluorometry and by flow cytometry were used. Fluorescence microscopy and the quantitative real-time PCR technique (RT-qPCR) were also applied.

In the *ex vivo* assays it was possible to demonstrate that *S. mansoni* ABCB1 pumps were involved in praziquantel resistance and that verapamil (VP), synthetic pump modulator ABCB1, reverses the resistance. In macrophages modified by infection by *L. infantum* an expressive increase of ABCB1 pumps in the cell membrane was observed. Synthetic ion channel inhibitors and efflux pumps, such as VP, ouabain, thioridazine and chlorpromazine, and natural compound 6-gingerol (6G) reduced the efflux activity of uninfected macrophages. In addition, the activity of these modulators was also related to the oxidative stress of the macrophages. Treatment with synthetic inhibitors of efflux and with 6G decreased the survival of intracellular parasites and their ability to multiply, suggesting that these modulators and VP in particular may have a direct or indirect leishmanicidal effect. In breast carcinoma cells resistant to doxorubicin and with overexpression of ABCB1 pumps, VP reversed resistance to paclitaxel and 6G was cytotoxic to resistant cells, which may be related to the increase of reactive oxygen species, and consequently to the homeostatic imbalance. In these cells it was possible to demonstrate a direct correlation between efflux activity and ABCB1 pump expression and that microRNAs can modulate the resistant phenotype by interfering with the gene expression of ABCB1 transporters.

KEY-WORDS: MDR-eukaryotic cell models; real-time-efflux fluorimetric assays; efflux inhibitors; Efflux-pump systems; multi-drug resistance.

Table of contents

List of Figures

List of Tables

Abbreviation list

6G	6-gingerol
ABC	ATP-binding cassette
ABCA	ATP-binding cassette subfamily A
ABCA3	ATP-binding cassette subfamily A member 3
ABCA4	ATP-binding cassette subfamily A member 4
ABCC2	ATP-binding cassette subfamily C member 2
ABCC7	ATP-binding cassette subfamily C member 7
ABCD1	ATP-binding cassette subfamily D member 1
ABCD3	ATP-binding cassette subfamily D member 3
ABCG	ATP-binding cassette subfamily G
ABCG2	ATP-binding cassette subfamily G member 2
ABCG5	ATP-binding cassette subfamily G member 5
ABCG8	ATP-binding cassette subfamily G member 8
ADP	Adenosine-diphosphate
A-MuLV	Abselon Leukaemia Virus
ANOVA	Analysis of variance
AO	Acridine orange
AP-1	Activator protein-1
ATP	Adenosine triphosphate
BCRP	Breast cancer resistant protein (ABCG2)
BP	Band pass
CC	Cytotoxic concentration
cDNA	Complementary DNA
CDR	Cancer drug resistance
CL	Cutaneous Leishmaniosis
CO_2	Carbon dioxide
CPZ	Chlorpromazine
CS	Collateral sensitivity
CypA	Cyclosporine A

DAPI	4',6-diamidino-2-phenylindole dihydrochloride
DHR	Dihydrorhodamine
$DiOC_2$	3,3'-Diethyloxacarbocyanine Iodide
DMSO	Dimethyl sulfoxide
DNA	Deoxyribonucleic acid
DOX	Doxorubicin
DR	Drug resistance
EB	Ethidium bromide
EC_{50}	Half-maximal inhibition efflux concentration
ELISA	Enzyme-Linked Immunosorbent Assay
EMT	Epithelial-to-mesenchymal transition
EP	Efflux pump
EPI	Efflux pump inhibitor
FAR	Fluorescence activity ratio
FBS	Fetal bovine serum
FCS	Fetal calf serum
FDA	Food and Drug Administration
FITC	Fluorescein isothiocyanate
FSC-A	Forward scatter area
FSC-H	forward scatter height
FOXO1	Forkhead fox-containing protein O1 subfamily transcription factors
GAPDH	Glyceraldehyde-3-Phosphate Dehydrogenase
GCS	Glucosylceramide synthase
GFP	Green fluorescent protein
Glc-Cer	Glucosylceramide
H+	Hydrogen ion
HAT	Histone Acetyltransferases
HDAC	Histone Deacetylase Inhibitors
HEPES	4-(2-hydroxyethyl)-1-piperazineethanesulfonic acid
HSF1	Heat-shock transcription factor 1
IC_{50}	Half inhibitory concentration
ID50	Half inhibitory dose

iNOS	Inducible nitric oxide synthase
Ld	*Leishmania donovani*
LdMRP2	*Leishmania donovani* multidrug resistance protein 2 (LdABCC2)
LiABCG4	*Leishmania infantum* ABC subfamily G (ABCG)-like transporter
LD50	Lethal dose of 50 %
LD90	Lethal dose of 90 %
LD99	Lethal dose of 99 %
Li	*Leishmania infantum*
LmrA	ATP binding cassette (ABC) multidrug transporter in *Lactococcus lactis*
LPS	Lipopolysaccharide
LTR	LysoTracker® Red DND-99
LtrMDR1	*Leishmania tropica* P-glycoprotein (Pgp)-like transporter
M-site	Modulator site
MATE	Multi-antimicrobial extrusion protein family
MDR	Multidrug resistance
MET	Multidrug endosomal transporter
MFS	Major facilitator superfamily
miRNA	microRNA
microRNA	microRNA
miRs	microRNA
MRP	Multidrug resistance protein
MØ	Macrophage
MTT	3-[4,5-dimethylthiazol-2-yl]-2,5-diphenyl tetrazolium bromide
Na+	Sodium cation
NBDs	Cytosolic nucleotide-binding domains
NC	Negative control
NF-κB	Nuclear factor of Kappa Light Polypeptide Gene Enhancer in B-Cells
NO	Nitric oxide
O3a	Forkhead box protein O3a
OM	Optical Microscopy
OUAB	Ouabain

PAR	Parental
PAX	Paclitaxel
PBS	Phosphate-buffered saline
Pfmdr1	*Plasmodium falciparum* multidrug drug resistance gene 1
Pgh1	P-glycoprotein homologue 1
P-gp	P-glycoprotein
pH	Potential of hydrogen
PMA	Phorbol 12-myristate 13-acetate
PMF	Proton motive force
PVDF	Polyvinylidene difluoride
prom	Promastigotes
PV	Parasitophorous vacuole
PXR	Pregnane-X-receptor
PZQ	Praziquantel
RNA	Ribonucleic acid
RT-qPCR	Quantitative reverse transcription polymerase chain reaction
RF	Relative fluorescence
RFF	Relative final fluorescence
Rh123	Rhodamine 123
RND	Resistance-nodulation cell division super family
ROS	Reactive oxygen species
RPMI	Roswell Park Memorial Institute (medium)
SD	Standard deviation
SMDR2	*Schistosoma* Pgp-like transporters
SMR	Small multidrug resistance family
SNAI1	Snail family transcriptional repressor 1
SSC-A	Side scatter-area
TbMRPA	*Trypanosom brucei* Multidrug resistance protein A
TM	Transmembrane domains
TMDs	Transmembrane domains
TZ	Thioridazine
UV	Ultra-violet

V-ATPase	Vacuolar (H^+)-ATPases
VL	Visceral leishmaniosis
VP	Verapamil
WB	Western blot
WHO	World Health Organization

1. General Introduction

1.1. Multidrug Resistance (MDR) in infectious and malignant diseases

The growing resistance to the available therapeutic drugs is one of the main obstacles for the successful treatment of patients with infectious and malignant diseases. Identifying the mechanisms leading to intrinsic or acquired multidrug resistance (MDR) is important in developing more effective therapies.

MDR refers to mechanisms by which cells resistant to one type of drug become resistance to a number of structurally and/or functionally unrelated compounds. This phenomenon can occur during treatment of infections caused by prokaryotic and eukaryotic pathogens as well as in neoplastic cells.

These mechanisms include reduced intracellular drug accumulation (increase drug efflux, decreased drug uptake), resistance to apoptosis, induction of autophagy, abnormal activation of the DNA repair mechanisms, activation of detoxifying systems, modification of drug targets, drug compartmentalization and defects in cellular pathways such as gene regulation by microRNAs (miRNAs) (1, 2).

Regardless of diversity of possible mechanism associated to MDR, upregulation of efflux pumps is the main phenotype, resulting in an increase of drug efflux. Actually, drug efflux has been described as an important mechanism for intrinsic and acquired drug resistance in numerous prokaryotic and eukaryotic cells. Therefore, identifying the mechanisms leading to intrinsic or acquired MDR is crucial in developing more effective therapies.

Figure **1**: Mechanisms that can enable or promote direct or indirect drug resistance in human cancer cells. These mechanisms can act independently or in combination and through various signal transduction pathways. EMT (epithelial to mesenchymal transition), adapted from Housman et al. (3).

Parasitic diseases, caused by protozoan (e.g. *Plasmodium falciparum*, *Leishmania*) and helminths (nematodes, trematodes and cestodes) are responsible for a large number of diseases that affect humans and animals, threatening the lives of more than a third of the world population, especially in subtropical, tropical and equatorial climates and in low income countries (4). Therapeutic options to treat and control parasitic infections are very limited. The emergence of resistance to antiprotozoal drugs limited even more the arsenal of alternative treatment options. Alerted to this reality, in May 2015, the World Health Assembly adopted a global action plan on antimicrobial resistance where the final goal is to ensure treatment and prevention of infectious diseases with quality-assured, safe and effective medicines. Besides this global plan, WHO has been leading multiple initiatives to address antimicrobial resistance.

1.2. **Efflux systems in human diseases**

Membrane transporters play a significant role in normal physiology as well as in disease. They are present in both prokaryotic and eukaryotic cells and play an important role in several cellular functions including, cell metabolism, ion homeostasis and signal transduction pathways by promoting the transport of amino acids, proteins, sugars, xenobiotics including drugs, inorganic ions, water, hormones, nucleic acids, cytokines and endogenous metabolites that are noxious to the cell across cell membrane and endocytic membranes.

Movement of compounds across a biological membrane may occur either passively or actively, depending if their transport is against or along a concentration gradient. The lipid bilayer of cell membranes of most all living organisms, with an amphipathic nature, is a very efficient barrier for polar and charged molecules but permeable to the passage of small hydrophobic molecules which cross the membrane by passive diffusion (simple diffusion, osmosis or facilitated diffusion). Passive transport does not require energy input as transport follows a concentration gradient. On the contrary, in active transport because the movement is against a concentration gradient it requires energy.

Concerning the energy source, active efflux systems (or efflux pumps) can be broadly categorized into two main groups, primary and secondary transporters. The primary active transporters directly use the metabolic free energy (e.g. energy of ATP hydrolysis and/or binding) to mediate the transport of molecules across a membrane. The superfamily of the ATP-binding cassettes (ABC) transporters is included in this group of transporters.

Secondary active transporters utilize the electrochemical potential gradient of the cytoplasmic membrane (driven by ATP-dependent ion-gradient), also known as proton motive force (PMF), to move molecules against their gradients by a drug/H^+ or drug/Na^+ antiporters mechanism. This type of transporter includes pumps of the major facilitator superfamily (MFS), which compromises the largest known groups of solute transporters, which includes a significant number of bacterial efflux pumps. These are the major mediators of antimicrobial resistance. In the prokaryotic kingdom there are five major

families of efflux transporters: MATE, MFS, SMR, RND and ABC (5) (Fig. 2). LmrA was the first bacterial ABC-type transporter found, being described in 1996 in a non-pathogenic bacteria *Lactobacillus lactis* (6), sharing structural and functional homologies with the human multidrug resistance P-glycoprotein MDR1 (ABCB1).

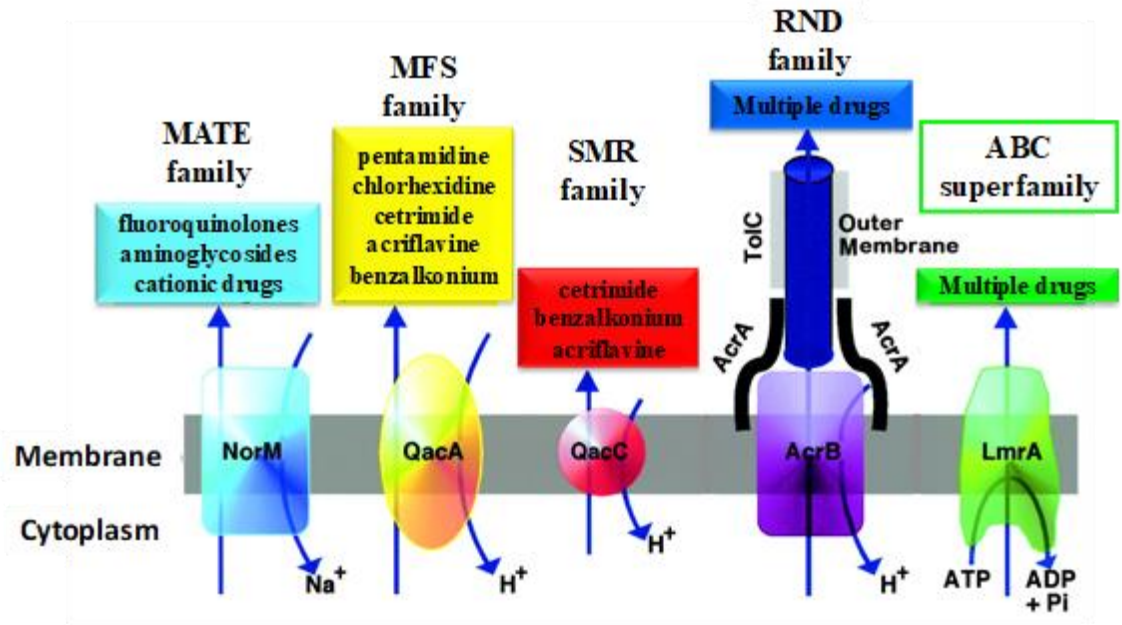

Figure 2: Schematic representation of the five families of efflux pumps, adapted from Piddock et al. (5). ATP-binding cassette super family (ABC), major facilitator super family (MFS), resistance-nodulation cell division super family (RND), small multidrug resistance family (SMR), multi-antimicrobial extrusion protein family (MATE), and multidrug endosomal transporter (MET). NorM, QacA, QacC, AcrB and LmrA, are examples of each family in bacteria.

ABC is one of the largest gene superfamily of transporters among eukaryotes and prokaryotes, being associated with resistance to anti-infective and antitumor drugs and thus of considerable clinical relevance. The biological functions of several ABC proteins have been described in clinically important protozoa and nematode worms and include vesicular trafficking, phospholipid movement and drug resistance. There are more than 100 ABC transporters in both prokaryotes and eukaryote, many are known to play important role in physiology, toxicology, pharmacology and numerous disorders (7).

In humans, dysfunction of ABC transporters has been associated with the development of various diseases, drug disposition (toxicity) and also drug resistance.

Genetic defects in ABC genes are responsible for some inherited human genetic disorders that are not related to drug resistance, like cystic fibrosis (ABCC7), Adrenomyeloneuropathy (ABCD1), Zellweger syndrome 2 (peroxisomal membrane protein or ABCD3), Sitosterolemia (ABCG5 and ABCG8), retinal degeneration (ABCA4), hypercholesterolemia and cholestasis (ABCB4) (8, 9).

1.3. **ABC transporters**

ABC transporters are the largest and most ancient super-family of membrane transport proteins widespread in all forms of life from prokaryotes to higher eukaryotes (including humans). It represents a variety of genes that code for proteins, which perform countless functions, including drug efflux. They are transmembrane proteins responsible for the transport (across cytoplasmic membrane and intracellular membranes) of a wide variety of substrates, ranging from small inorganic and organic molecules to larger organic compounds. In prokaryotic cells these proteins have a role in the influx (importers) of proteins, lipids, drugs and toxins, and in eukaryotic cells are most exclusively efflux pumps (exporters), being expressed in the plasma membrane, intracellular membranes of organelles such as endosomes, multi-vesicular bodies, peroxisomes, mitochondria and endoplasmic reticulum (9).

In humans, ABC proteins are naturally expressed in several tissues (e.g. liver, kidney, colon, adrenal gland, intestine, placenta, hematopoietic precursor cells, and luminal membrane of brain capillary endothelial) and where physiological barriers exist, since its main function is to protect the body from toxic compounds.

Due its role as efflux pumps, ABC are highly associated with several human diseases (Table 1) (10). By decreasing intracellular drug concentration these pumps are associated with treatment failure.

Table 1: Microbial ABC transporters associated with drug resistance in human diseases

Pathogen	ABC transportes	Drug	Reference
Plasmodium falciparum – Malaria	Pfmdr1 or Pgh-1	chloroquine	(11)
Entamoeba histolytica - Amoebiasis	EhPgp1/Pgp5	metronidazole derivatives/emetine	(12)
Trypanosoma brucei - African trypanosomiasis	TbMRPA	melarsoprol	(13, 14)
Trypanosoma cruzi - American trypanosomiasis	ABCC-like ABCG1	benznidazole	(15)
Leishmania major - Cutaneous leishmaniasis	ABCC7 (PRP1)	pentamidine	(16)
Leishmania tropica - Cutaneous leishmaniasis	Pgp-like	alkyl-lysophospholipids.	(17, 18)
Leishmania donovani - Visceral leishmaniasis and *in vitro* studies (infected macrophages)	LtrMDR1 LdMRP2 (ABCC2)/MRP2	miltefosine baicalein (BLN)	(19)
Leishmania infantum - Visceral leishmaniasis	LiABCG4	miltefosin and perifosine	(20)
Leishmania panamensis - in vitro studies (infected macrophages)	ABCA3	miltefosin	(21)
Schistosoma mansoni - Shistosomiasis	SMDR2 in	praziquantel	(22)
Listeria monocytogenes - in vitro studies (infected macrophages)	MRP	ciprofloxacin	(23)

In the human genome, there are 49 known genes encoding for ABC proteins that can be grouped into at least seven family members of transporters (ABCA to ABCG) based on their amino acid sequence and phylogeny.

Among these families, only multidrug resistance-associated proteins (MRP1/ABCC1 and MRP2/ABCC2), breast cancer resistance protein (BCRP/MXR/ABCG2), and multidrug resistance protein 1 (ABCB1/P-gp/MDR1) have shown to be clinically relevant in the efflux of a variety of drugs, and their overexpression confers MDR phenotype to cancer cells (24).

ABCB1 glycoprotein is a mutual ABC transporter present in all studied organisms from parasites (ABCB1-like) to malignant diseases, which suggest the existence of common mechanisms responsible for the development of drug resistance (7).

1.3.1. ABCB1 efflux pumps in drug resistance

ABCB1 transporter is an integral plasma membrane glycoprotein of 1280 amino acid and approximately 170 kDa encoded by the human ABCB1 (MDR1) gene, located on the long arm of chromosome 7 at band 7q21-12 and has 32 exons (GeneBank accession no. NC_000007.14). The corresponding mRNA is about 4718 bp to 4768 bp in length (Ref Seq accession NM_000927.4 and NM001348945.1). This is the best studied member of the ABC transporter super-family of genes and the first to be discovered in 1970 by Biedler et al. (25) and cloned for the first time by Riordan et al. in 1985 (26).

1.3.1.1. Structure and function of ABCB1 efflux pumps

ABC transporters are typically composed of two domains: a cytoplasmic highly conserved nucleotide binding domains (NBDs, ATP-binding cassettes or ABC domain), with about 200 amino acid residues long, bound to the cytosolic face of a hydrophobic integral transmembrane domain (TMDs) (Fig. 3). NBDs, are responsible for the substrate translocation through the membrane by using the energy released by ATP-hydrolysis,

acting as an ATPase, while the TMDs contribute to the substrate translocation events (recognition, translocation and release). Typically, a functional ABC transporter is constituted by a pair of highly conserved NBDs and two TMDs with limited sequence homology containing, each monomer, six membrane spanning α-helices (TMD1-TMD12) that form an active pore across the membrane where substrates pass through. When a molecule enters the transporter, both TMDs domains change their conformation allowing the binding of ATP to NBDs (10) (Fig. 3).

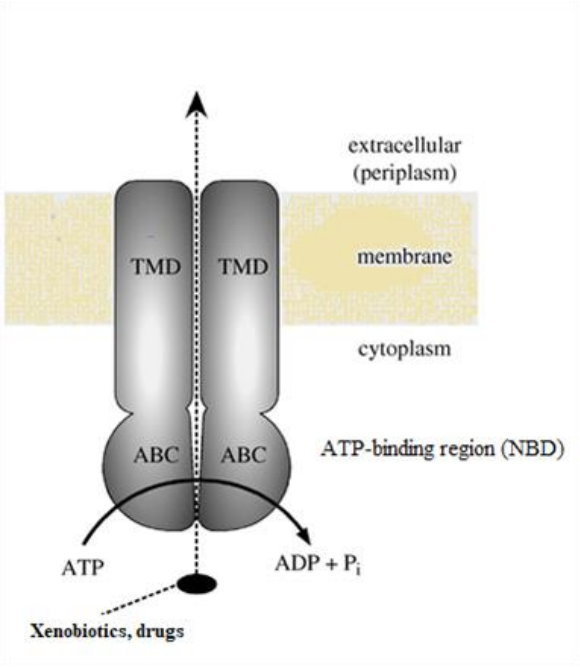

Figure 3: Structure of ABCB1 efflux pumps. Most ATP-binding cassette (ABC) proteins are transporters comprising four structural domains: two transmembrane domains (TMD) and two cytosolic nucleotide-binding domains (NBD). TMDs form the membrane channel and contain the substrate binding sites. NBD bind the adenosine-triphosphate (ATP) molecules. The resulting hydrolysis of ATP provides the energy necessary for the conformational changes required for the translocation of substrate molecules across the plasma membrane, with subsequent production of adenosine diphosphate (ADP) and inorganic phosphate (Pi). Adapted from Locher et al. (27).

The classification of ABC transporters is done using the structure and protein sequence of the NBDs. A minimal ABC functional unit of an ABC transporter consists of a consensus Walker A (binding loop or P-loop) and Walker B motifs, which determine the 3-D structural fold of the nucleotide binding site, Q-loop (conserved glutamine), H-motif (switch region), A-loop and D-loop and the consensus ABC signature motif (LSGGQ),

located between the two walker domains which interacts with ATP and the TMDs domain (alpha helices TM domains, TMD1 to TMD12) (Fig. 4) (28).

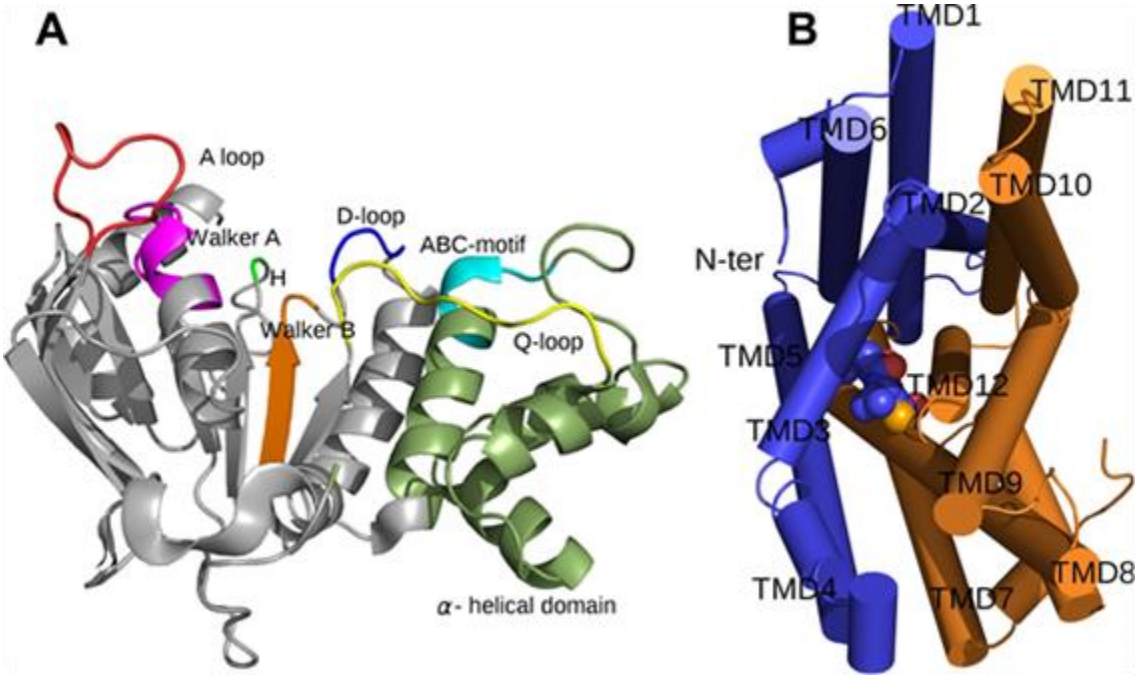

Figure 4: Structure of a Nucleotide Binding Domain (NBD) and a Transmembrane Domain (TMD) of ABCB1 (PDB code: 4M2T). A. Structure of NBD: domains and highly conserved sequence motifs are color-coded: Green, α-helical domain; Gray, regulatory C-terminal domain; Red, A-loop; Magenta, Walker A; Orange, Walker B; Blue, D-loop; Green, H-loop; Cyan, ABC motif; Yellow, Q-loop. B: Structure of ABCB1 TMD dimer, view along the two-fold symmetry axis from the inward side (the NBD domain is not represented): the two TMDs of an ABC transporter are colored in blue and orange. α-helices are numbered TMD1-12. Reprinted with permission of Genovese et al. (29).

ABCB1 is a full transporter with two identical NBDs and two TMDs forming a TMD1-NBD1-TMD2-NBD2 single polypeptide chain (30) (Fig. 5). ABCB1 is post-translationally modified by N-glycosylation (at the first extracellular loop) and phosphorylation (31, 32).

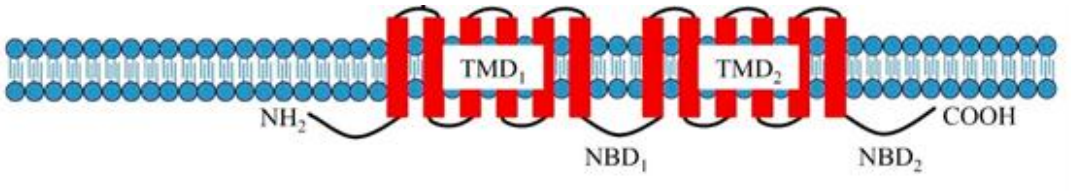

Figure 5: Secondary structure model of a ABCB1 drug efflux transporter. TMD–transmembrane domain; NBD– nucleotide-binding domain, reprinted with permission of Chen Z. et al.(33).

The molecular mechanism behind ABCB1 transport activity is not fully understood. In fact, several models to explain ABCB1 interactions with substrates have been proposed and are being debated (27, 34). However, it is known that substrate binding sites are located throughout the TMDs, where some amino acids are involved in the formation of a binding pocket. This binding pocket formed by the two TMDs determines substrate specificity (35). Some residues lining in the open chamber (residues of TM2, TM5 and TM6) play an important role in substrate recognition (30). ABCB1 transports both neutral and positively charged hydrophobic unmodified compounds which interact with amino acids residues of the transmembrane helices that line the transmembrane pore (binding pocket) (10).

Because of the wide range of compounds that are known to interact with ABCB1 protein, there is evidence that ABCB1 has multiple drug binding sites. Briefly, H-site due to specificity for binding Hoechst 33342 (and also colchicine and quercitine); the R-site, as it binds preferentially rhodamine 123 and anthracyclines; the M-site (modulator site), as it binds to non-transported modulators (interacting with other sites in an allosteric manner); the P-site for progesterone and prazosine; and the ATP1 and ATP2 binding sites (36-40). There is also the verapamil binding site which interacts with amino acids from both H and M sites (41). The mode and/or strength of ABCB1 interaction may differ among ABCB1 substrates. These findings are more evident when known inhibitors of ABCB1 like verapamil, have stronger effect in sensitizing ABCB1 expressing cells to paclitaxel and vincristine than to doxorubicin. These discrepancy may point to differences in the composition of the cell membrane that may influence transporter activity (42). In

addition, differences in ABCB1 sequence and/or structure between cell lines or species may also contribute to this phenomenon (38).

The ABCB1 efflux pump is mainly expressed in the plasma membrane of epithelial and endothelial cells of blood tissue barriers and elimination organs, where they have protective and excretory functions. In sensitive organs such as the brain, testis, placenta, kidney, liver, pancreas, cerebrospinal fluid and in human hematopoietic stem cells, they have an important role in limiting the permeability of drugs and other toxic xenobiotics. They also have an important role in the secretion of metabolites and xenobiotics into bile, urine, lumen of the gastrointestinal tract, hormones from the uterine epithelium and the adrenal gland. Because of their distribution and localization, ABCB1 efflux pumps play an important role in drug pharmacokinetics. The co-administration of drugs with ABCB1 inhibitors are of important relevance in clinical settings and can be either beneficial or deleterious.

The cytotoxic drugs associated with ABCB1 mediated MDR phenotype are anthracylines (doxorubicin, daunorubicin), Epipodophyllotoxins (etoposide and teniposide), Taxanes (paclitaxel), Vinca alkaloids (vinblastine, vincristine), Anthracenes (bisantrene and mitoxantrone) and Camptothecins (topotecan) (43, 44).

In addition, several other exogenous lipophilic and amphipathic compounds can also interact with ABCB1 as substrates or as inhibitors including colchicine-site binding agents, natural products, calcium-channel blockers (e.g. verapamil), calmodulin antagonists, cyclic peptides, antibiotics (erythromycin), loperamide, digoxin and fluorescent dyes (Rhodamine 123, Calcein AM and $DiOC_2$). Among them, the fluorescent dyes are used to evaluate the impact of inhibitors on the transfer function of these transporters, by measuring the capacity of cells to extrude the dye from their compartments. This is the most relevant method to assess clinical MDR in eukaryotic cells (45).

1.3.1.2. Regulation of ABCB1 efflux pumps in cancer cell drug resistance

As described before, MDR can develop in several different ways, with the predominant mechanism being the overexpression of ABCB1 on the plasma membrane of tumor cells.

ABCB1 expression is controlled by several genetic, epigenetic, and environmental factors, being the result of the activation of one or more signal transduction pathways or transcription factors that directly or indirectly influence the activity of ABCB1.

Beside the important research lines around the development of novel drugs able to overcome drug resistance (e.g. efflux inhibitors), there is also a need to understand the regulation of the expression and function of ABCB1 drug efflux pumps, to overcome clinical drug resistance and ABCB1-interactions in the host. MDR can be either intrinsic, when cells naturally express high levels of ABCB1, or acquired after positive response to an initial treatment. Identifying the mechanisms leading to intrinsic or acquired MDR is important for the developing of more effective therapies.

ABCB1 overexpression can occur by a variety of mechanisms, including gene amplification (pre-transcriptional) (46-48), epigenetic transcriptional regulation of ABCB1 gene (DNA methylation and histone H3 acetylation) (49), and post-transcriptional regulation of target genes and protein expression. Phosphorylation and N-glycosylation are believed to be the main posttranscriptional mechanisms by which cells regulate the activity of ABCB1 (50).

There are many transcriptional regulators governing the expression of ABCB1 transporters, including nuclear factor κB (NF-κB), forkhead box-containing protein O1 subfamily transcription factors (FOXO1) and O3a, AP-1, pregnane-X-receptor (PXR), Notch1, and heat-shock transcription factor 1 (HSF1) whose transcriptional factor-binding sites were identified in the promoter region of *ABCB1* gene (51, 52).

Recently there has been accumulating evidence that demonstrate that miRNAs also play a key regulatory role in MDR through modulating various drug resistant mechanisms mentioned above (53) (Fig. 6).

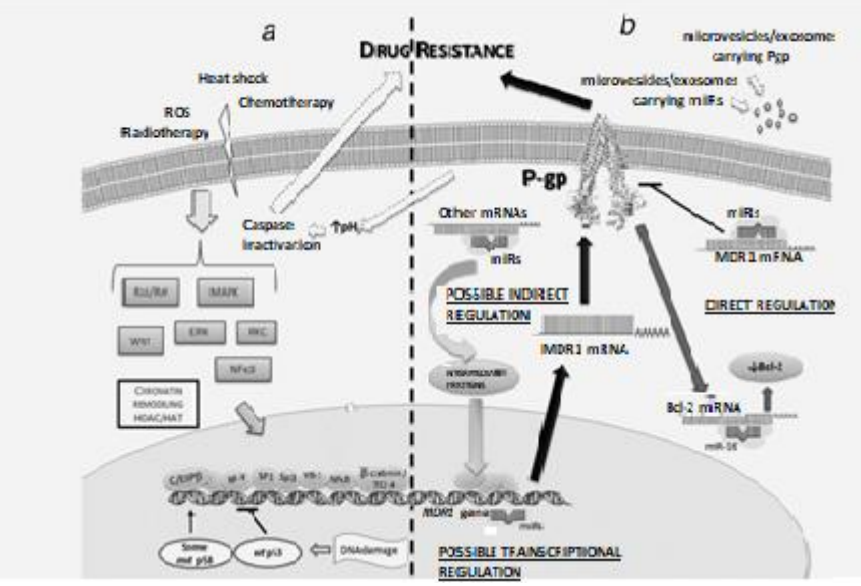

Figure 6: Complex interaction between P-gp (ABCB1), miRs and other cellular proteins to reinforce MDR. (a) Different stimuli (such as chemotherapy) may induce different signalling pathways which regulate the expression of proteins involved in *MDR1* gene transcription and drug resistance. The effect of P-gp on the intracellular pH levels has been suggested to affect apoptosis and drug resistance. (b) MDR1 mRNA levels may be regulated by miRs (directly, indirectly or at the transcriptional level), which will regulate P-gp protein levels and drug resistance. In addition, P-gp may regulate the expression of one miR, which regulates apoptosis and drug resistance. Both P-gp and miRs may be transported to other cells by microvesicles or exosomes. GCS: Glucosylceramide synthase; Glc-Cer: Glucosylceramide; HAT: Histone Acetyltransferases; HDAC: Histone Deacetylase Inhibitors. Figure adapted from Lopes-Rodrigues et al. (54).

1.3.2. **ABC transporters in parasitic diseases**

Changes in structure or expression levels of ABC transporters are also associated with reduced drug susceptibility in parasitic helminths, including schistosomes. In fact, orthologues of human ABC transporters are found in *Schistosoma* and are implicated in reduced susceptibility to praziquantel, the only drug available to treat schistosomiasis (55). Furthermore, the involvement of ABC transporters like P-glycoprotein homologue 1 (Pgh1), that is structurally similar to human ABCB1, has been associated to *P. falciparum* resistance to chloroquine and mefloquine (56). The mechanisms by which *Leishmania* ABC transporters confer resistance, seems to be different from the mechanisms found in mammalian cells, where drugs are actively extruded. Miltefosine, an anti-tumour drug, is the only oral drug available for the treatment of both cutaneous

and visceral leishmaniasis. Studies conducted with cancer cell lines have demonstrated that an overexpression of human ABC transporters reduced sensitivity to miltefosine (57). Therefore, ABC transporters in both parasite and host cell seam to play a key role in reducing antileishmania drug accumulation and thus, avoiding parasite killing.

1.4. Strategies to overcome multidrug resistance due to overexpression of efflux pumps

The recognition that efflux play an important role in drug resistance with a proven clinical impact for many human infectious diseases and cancer, has led to the development of strategies to overcome efflux-mediated resistance. Efflux activity can be impaired either directly or indirectly, by interfering on the mechanisms that regulate the expression and function of ABCB1 efflux pumps or by the use of molecules known as efflux inhibitors or modulators.

Understanding the mechanisms behind the development of MDR by overexpression of drug efflux pumps, understanding how these pumps are regulated, identifying the kind of resistance, can provide researchers and clinicians with new strategies, whenever possible, that may overcome the barrier of MDR that is responsible for treatment failure.

This can be achieved by: i) Chemotherapy through competitive and allosteric modulators; ii) chemotherapy mediated by nanoparticle targeting; iii) targeting transcriptional regulation of ABC transporters; iv) microRNA therapeutics; v) targeting signaling pathways involved in the regulation of ABC transporters; vi) and combinational targeting with chemotherapeutic agents and transporter modulating drugs or dual targeting with a single agent.

1.4.1. **ABCB1 efflux modulators**

Agents which inhibit the efflux pumps activity of bacteria and protozoan microorganisms have shown similar activity against efflux pumps of drug-resistant cancer cells (58, 59). Thus, both eukaryotic (e.g. cancer cell lines, protozoans) and prokaryotic (e.g. bacteria) cell models where overexpression of efflux pumps is the primary mechanism of MDR can be used *in vitro* for the search of new modulators that can reverse the MDR phenotype. These different cells have identical responses when exposed to xenobiotics, overexpressing the efflux pump thereby preventing access to intended targets. However, the mechanisms that control the over-expression of ABC transporters are not fully understood. Moreover, the overexpression of ABC transporters seems to be transient and not permanent, indicating that other mechanisms of drug resistance take over at different moments (60). Furthermore, the effects of continuous or prolonged exposure to efflux inhibitors are not well known, in particular, the effects on gene expression and epigenetic regulation (DNA methylation) of ABC transporters.

A clinical strategy to overcome resistance and reverse or prevent MDR is the short-term administration of inhibitors that can interfere with overexpressed ABCB1 activity (61). *In vitro* studies with inhibitors showed that resistance conferred by the over expression of ABCB1 can de modulated. On the contrary, clinical trial results have been very disappointing because of the wide distribution of efflux pumps in healthy tissues, and their (low) specificity to MDR transporters that requires higher plasma concentrations to reverse multidrug resistance, being associated to unacceptable toxic side effects (61, 62).

So far, four generations of compounds have been identified and developed as ABCB1 inhibitors/modulators. The main mechanisms how the inhibitors can impair activity of ABC efflux pumps is by either, competitive, noncompetitive or allosterically blocking the substrate binding site, by changing the plasma membrane integrity or by interfering with ATP hydrolysis and consequently the transport function (63).

The first generation of ABCB1 inhibitors were initially developed to have other pharmacological properties. These drugs, which interact with ABCB1 efflux pumps, are

not selective, requiring high plasma concentrations to inhibit ABCB1. This can lead to undesirable adverse effects (62). The best known first-generation ABCB1 modulators are verapamil, tamoxifen and cyclosporine A. Verapamil is a calcium channel blocker that also competitively inhibits the function of ABCB1 transporter (64).

The second generation of ABCB1 inhibitors are a class of molecules with a greater affinity to the ABCB1 pump. They can be divided in two categories, those that are analogues of the first generation, i.e. dexverapamil (R-isomer of verapamil without any cardiac activity) (64) and those with new chemical structures. Most of these MDR chemosensitizers are substrates for ABC transporter family.

The clinical failure of the first and second generation of ABCB1 inhibitors, led to the discovery of the third generation of compounds, with the goal to overcome the toxicity of the previous generations and to improve the pharmacokinetic interaction of the compounds. They are not metabolized by cytochrome P450 3A4 and they do not alter the plasma pharmacokinetics of anticancer drugs, being more specific and less toxic (65).

These more potent inhibitors have high affinity to ABCB1 at nanomolar concentrations. An example is elacridar (61). Most of the compounds included here are nitrogenous compounds (66). Some of these third-generation of inhibitors have reached phase III clinical trials (67, 68). Despite the ongoing clinical trials with these promising inhibitors, none of them passed to phase IV and gave satisfactory results. Alternatives approaches are still under study.

Efforts to identify ABCB1 inhibitors have led to numerous candidates. Human clinical trials with first, second or even third generation drugs did not show any satisfactory outcomes, evidencing adverse severe side effects, inhibition of cytochrome P-450 monooxygenases and limited clinical benefits (69, 70).

As an alternative to conventional drug therapy, natural compounds could be less cytotoxic and with fewer side effects, representing the fourth generation of multidrug resistance reversal agents (71). They exert their action through modulation of transcription factors, growth factors, tumor cells survival factors, inflammatory pathways, invasion, and angiogenesis (70, 72-75), which leads to inhibition or reversing of early stages of carcinogenesis as shown in experimental models (72). Some of these molecules of natural

origin have reached the level of human clinical trials, such as marine-derived anticancer drugs (76) or compounds of plant origin (phytochemicals).

Studies conducted by Bailey et al. (77), of the interaction of several drugs with grape fruit, gave the first evidence of herbal applications in ABCB1 inhibition. Later, several plant constituents were identified as strong inhibitors of ABCB1 (78, 79).

Most of the studies conducted with phytochemicals investigated polyphenols (e.g. curcumin, genistein, quercetin, resveratrol, EGCG) as described in recent reviews (72, 80-82). Human clinical trials carried out to test polyphenols had some positive results in patients with colorectal and prostate cancer (59, 81, 82). The activity of polyphenols was not as potent or as effective as for synthetic drugs, but some polyphenols have been shown to be safe and to increase the efficacy of the drug when used in co-treatments or in chemoprevention through dietary interventions, improving chemotherapy efficacy and decreasing side effects (72, 80, 83). Regarding their use as ABCB1 inhibitors, besides being an attractive strategy for overcoming multidrug resistance, blocking the transport function of ABCB1 and thus increasing intracellular concentrations of anticancer drugs, as far as we know, there are no ongoing clinical trials. Natural compounds as ABCB1 modulators have been described in vitro and in vivo (69), alone or in co-treatments to overcome resistance. They can interact with doxorubicin (84, 85), epirubicin (86) as well as other ABCB1 substrates (82).

Anticancer agents of natural origin have an advantage over all the ABCB1 inhibitors tested because they do not have a “single target” feature, as most drugs used in cancer treatment, but they can modulate multiple pathways as outlined earlier (70, 75). Genistein, curcumin (83) or quercetin (86) are some of the phytochemicals described to reverse MDR by increasing the sensitivity of cancer cells to classical chemotherapeutics drugs. Therefore, the search for natural ABCB1 modulators that are safe and non-toxic to overcome resistance can be a promising strategy in anticancer chemotherapy and for this purpose the development of robust methods to assess the permeability and drug transport kinetics by the main eukaryotic membrane transporters is essential.

1.4.2. **Natural compound 6-gingerol**

6-gingerol, a diarylheptanoid phytochemical (Fig. 7), is the most abundant bioactive pungent constituent of two food plants that belong to the family of Zingiberaceaes, the Rhizome of *Zingiber officinale Roscoe* (ginger) and the seeds of *Aframomum melegueta* (87). Both plants have been widely used in the world as spices and in traditional medicine (88). Ginger has been generally recognized as a safe food additive by the U.S. Food and Drug Administration (FDA).

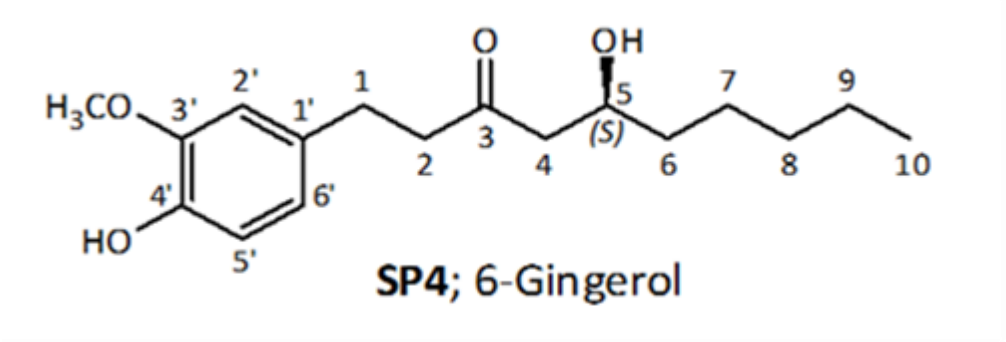

Figure 7: Chemical structure of 6-gingerol, adapted from Gröblacher B. et al. (89).

Seeds of *Aframomum melegueta* (Roscoe) K. Schum. (Zingiberaceae), commonly known as grains of paradise, Guinea grains, alligator pepper, melegueta pepper, or Guinea pepper, are mainly used in traditional West African medicine. Extracts of the seeds are employed as a remedy against various ailments including inflammatory disorders, stomachic diseases, diarrhea, measles, hemorrhage, and leprosy, as well as tuberculosis and snakebites (89).

6-gingerol is chemically related to capsaicin and piperine, two compounds that gives chili peppers and black pepper their respective spiciness. Capsaicin has been associated to carcinogenesis and to have also anticancer properties in different experimental models (90), while 6-gingerol has been described to have anti-tumor activity in different cancers (91) and it has never been reported to be carcinogenic, although its mechanism of action

is not well understood. Recently, it was reported that 6-gingerol and capsaicin can act synergistically against urethane induced lung carcinogenesis (92) and that capsaicin and piperidine synergistically enhanced the cytotoxicity of doxorubicin in cancer cell lines that overexpressed ABCB1 (93). Thus, 6-gingerol appears to be a safe and potent chemotherapeutic/chemopreventive compound, inducing cell stress in cancer cells, by acting through cell cycle arrest and induction of apoptosis, for example in human oral and cervical tumor cells (94, 95) and by presenting antioxidant and anti-inflammatory activities (96). 6-gingerol was shown to significantly inhibit the production of nitric oxide, a highly reactive nitrogen molecule that quickly forms a very damaging free radical called peroxynitrite (91).

The effect of natural compounds like capsaicin, 6-gingerol, curcumin, resveratrol has also shown to have inhibitory effects on human ABCB1 efflux pumps, in a concentration-dependent manner (82, 97). Recently, it was demonstrated that 6-gingerol inhibited ABCB1-mediated digoxin transport in L-MDR1 and Caco-2 cells. These natural compounds seem to be less toxic than the available synthetic inhibitors and therefore have the potential to be used as ABCB1 modulators (98).

1.5. **Thesis Objectives**

Efflux systems play a crucial role in cell survival, but also play an important role in drug resistance. Among the several mechanisms of drug resistance, efflux of drugs from cells by membrane transporters is the most predominant and mutual mechanism of drug-resistance among all organisms. ATP-binding cassette (ABC) mediated efflux is the mechanism most frequently and widely associated with multidrug-resistance.

Therefore, the present study aimed to investigate the function, modulation and regulation of ABC transporters in drug resistance and infection, using eukaryotic parasites, protozoa-infected cells, and cells altered by malignancy as models.

To accomplish the main objective of this study two specific goals were identified. Since available methods to predict and assess the modulator activity of ABC inhibitors were unable to visualize its effectiveness in a real-time basis, the first goal was to establish suitable methodologies to evaluate the activity of ABCB1 efflux systems in real-time. The second specific goal was to evaluate the modulatory activity of efflux inhibitors in different biological models:

- Multicellular parasites (praziquantel-resistant adult worms of *Schistosoma mansoni*) to evaluate the role of ABCB1-like transporters,
- Eukaryotic cells modified by an intracellular infection (*Leishmania infantum*-infected macrophages) to assess the effect of a phytochemical, ouabain and synthetic EIs on immunity and efflux pumps,
- Drug-resistant malignant cells (mouse lymphoma-transfected cells and resistant human breast cancer cells) to decipher the dual role of 6-gingerol and verapamil on cell redox homeostasis and on drug extrusion by interfering in efflux pumps and function,
- Drug-resistant human breast cancer cells to explore the possible regulatory role of miRNA (miR-200c and miR-203a) in ABCB1 pump expression and functionality.

2. Methodologies used to evaluate potential modulators of ABC transporters in eukaryotic cell models.

The cell-membrane ABCB1 (P-gp; MDR1) belongs to the ATP-binding cassette (ABC) family of transporters, is an energy dependent efflux pump, which has been associated with drug resistance in eukaryotic cells. Multidrug resistance (MDR) is related to an increased expression and function of the ABCB1 efflux pump that often causes chemotherapeutic failure in cancer and antimicrobial resistance in parasites. Modulators of this efflux pump, such as the calcium-channel blocker verapamil (VP) and cyclosporine A (CypA) can reverse the MDR phenotype but *in vivo* studies have revealed disappointing results due to adverse side effects. Currently available methods for evaluation of the modulation activity are unable to visualize and assess in a real-time basis the effectiveness of ABCB1 inhibitors on the uptake and efflux of ABCB1 substrates. However, predicting and testing ABCB1 modulation activity using living cells during drug development is crucial. The use of mouse lymphoma *ABCB1*-transfected cell lines to study the uptake/efflux of fluorescent probes like ethidium bromide (EB), rhodamine 123 (Rh123) and $DiOC_2$, in the presence and absence of potential inhibitors, is currently used in our laboratories to evaluate the ability of a drug to inhibit ABCB1-mediated drug accumulation and efflux.

2.1. **Monitoring ABCB1-mediated drug transport of fluorescent compounds**

Characterization of ABCB1 transport properties *in vivo* is challenging because ABCB1 transport properties are difficult to characterize in intact cellular systems. In this chapter we describe three techniques redesigned and optimized during this thesis, currently used in our laboratories for *in vitro* evaluation of the activity of putative modulator compounds of ABCB1, using a cell line that overexpresses the ABCB1 transporter (mouse T-lymphoma cells transfected with the human *ABCB1* gene) and its parental cell line. This cell-based model revealed to be very useful for the evaluation of agents which can modulate the activity of the ABCB1 transporter because these cells grow easily *in vitro* and it is possible to carry out quantitative measurements of efflux by following the intra- and extracellular amount of different fluorescent substrates, in the presence and absence of ABCB1 modulators. These eukaryotic cell lines also have low expression of other endogenous drug transporters that can make the interpretation of experimental data more difficult, especially when the reporter fluorescent substrate used for the evaluation of ABCB1 modulators is a common substrate of other efflux pumps. Noteworthy, these techniques can also be optimized for other specific cell lines that overexpress ABC transporters, using specific fluorescent substrates.

Several compounds have been used to study drug transport due to their inherent fluorescence, such as anthracyclines, acridines, Calcein-AM®, Rhodamine 123 (Rh123), and DNA-binding fluorochromes such as Hoechst 33342 and Ethidium bromide (EB) (99). These fluorescent substrates have different intracellular and extracellular fluorescence, which occurs due to their interaction with cellular components. In the three techniques presented in this chapter, Rh123, $DiOC_2$ and EB are used as reporter ABCB1 substrates to evaluate the binding activity of new compounds, by monitoring the fluorescent dye transport across the cells (efflux pump activity). Rh123 and $DIOC_2$ bind specifically to mitochondria of living cells and both can be used to evaluate the ABCB1 pump activity. EB is a broad range substrate of efflux pumps being recognized by bacterial efflux pumps and ABC transporters of eukaryotic cells. EB is highly fluorescent when it goes across the cell membrane and starts to intercalate with nucleic acids inside

the cells, even in very small concentrations. In aqueous solution, outside the cell, it loses almost completely its fluorescence affording the advantage that can be easily quantified by fluorometry, on a real-time basis (100, 101).

The semi-automated fluorometric method is an easy and accurate method that evaluates EB efflux by ABC transporters of lymphoma cell lines providing quantitative assessment of the efflux activity of this transporter in cell suspensions. The method is carried out by using a new application of the thermocycler Rotor-Gene^{TM} 3000 (Corbett Research, Sidney, Australia) that monitors the accumulation and extrusion of EB on a real-time basis (101, 102). This assay is conducted for a specific period of time with a non-toxic concentration of EB that does not cause its accumulation inside the cells. The slope of EB accumulation over time (number of units of fluorescence per minute) provides an assessment of baseline efflux and possible alterations of this slope induced by efflux inhibitors allows the identification of compounds that act as efflux inhibitors, since more EB is retained inside the cells in suspension and fluorescence increases accordingly. The fluorescence emitted by the accumulation of EB inside all the cells in suspension is followed by real-time fluorometry at 25 ºC (for optimizing conditions of maximum EB accumulation) in the Rotor-GeneTM 3000 (Corbett Research), using 530 nm band-pass and 585 nm high-pass filters as excitation and emission wavelengths, respectively.

Flow cytometry is another powerful equipment that can also be used to monitor the transport of fluorescent compounds in sensitive and multidrug resistant tumour cells and provides information about the physical and biological characteristics of individual cells as well as about subpopulations in a heterogeneous cell population. In flow cytometry, laser light is usually applied to excite the fluorochromes used in the functional assays monitoring the efflux activity of the cells. These lasers produce light in the UV and/or visible range and fluorochromes are selected based on their ability to fluoresce with the wavelengths of light emitted by the lasers.

Nowadays, the fluorescence flow cytometers can measure small-angle or forward light scatter, which is related to the size of the cells and large-angle or side scatter, providing information about internal granularity, roughness of the cell surface and particular characteristics, allowing single-cell identification (103). Flow cytometry is an ideal technique to measure fluorescent drug retention in tumour cells. Furthermore it can

provide information about compounds enhancing the intracellular drug retention and the chemosensitivity of cancer cells by modulating their efflux activity (104).

Lastly, fluorescent live cell imaging assays, using a fluorescence microscope, is also an effective and efficient method to screen ABCB1 efflux inhibitors using the previously described approach of monitoring the transport of fluorescent dyes. The efflux blocking activity of tested compounds is measured by cellular fluorochrome drug retention profiles (e.g. Rh 123 or $DiOC_2$) given by the presence and absence of the tested compound. All results are compared with a positive control, namely the fluorescence retention profile of the cells in the presence of verapamil or cyclosporine A, which are well-known inhibitors of the ABCB1 (positive controls). The fluorescence profile given by verapamil or cyclosporin A represents 100 % inhibition in the well characterized mouse T-lymphoma cell line overexpressing the ABCB1 protein (100 % accumulation). Negative control is given by the untreated cells incubated with the same fluorescent dye (0% accumulation).

The semi-automated fluorometric assay using EB as a fluorescent substrate is a simple, rapid and sensitive method for screening of large number of samples and the positive samples and/or suitable candidates detected should be further analyzed by single-cell flow cytometry or fluorescent microscopy. These two techniques allow the visualization of intracellular distribution of fluorescent probes in individual living cells (population of cells) and the assessment of cell viability before and after treatment allowing the screening and identification of putative ABCB1 modulators as well as the evaluation of the cytotoxicity of the tested compounds.

This chapter describes general optimized protocols for the evaluation of cell viability and for the evaluation of the permeability, transport kinetics of fluorescence substrates, and inhibition of the ABCB1 efflux pumps by drugs of chemical synthesis or extracted from natural sources, using model cancer cell lines overexpressing this transporter, namely:

(i) Cell viability by Trypan blue
(ii) Cell viability assay by MTT (tetrazolium salt)
(iii) Ethidium bromide accumulation assay by a semi-automated fluorometric method
(iv) Rhodamine-123 and $DiOC_2$ cell accumulation in the presence of EPIs by fluorescent microscopy
(v) Fluorescent substrate accumulation by Flow cytometry

2.2. General procedures

2.2.1. Trypan blue viability assay

This assay is based on the principle that live cells possess intact cell membrane that exclude certain dyes such as trypan blue. Viable cells have a clear cytoplasm whereas non-viable cells appear with a blue cytoplasm. After centrifugation, cell pellet is resuspended in a 1 ml of medium. Twenty microliters of cell suspension are mixed with 20 µl of 0.4 % trypan blue (Sigma-Aldrich). The trypan blue/cell mixture is applied into a hemocytometer and cells are observed under a light microscope. The viable and non-viable cells are counted and the percentage of viable cells is calculated accordantly to the formula:

$$\text{Viability (\%)} = \frac{\text{viable cells per ml}}{\text{total number of cells per ml}} \times 100$$

2.2.2. Colorimetric assay for determination of cell viability

This assay allows to access the influence of ABC modulator compounds on cell proliferation. The cytotoxic effects of increasing concentrations of the compounds are studied using the MTT test. The MTT assay is based on a redox potential reaction, where viable cells (with active mitochondria) convert the water-soluble MTT into an insoluble purple formazan (crystals). The formazan crystals formed are then solubilized and the purple color formed in the wells can be easily measured by optical density. The protocol described was optimized for cells that grow in suspension.

After harvesting cells from an exponential phase of growth by centrifugation, cells were counted by the use of a hemocytometer and cell viability was determined by trypan blue exclusion method. 1-5 × 10^4 of cells in 100 µl of complete medium were plated onto 96-well plates coated with Poly-D-lysine (Sigma-Aldrich), and incubated at 37 ºC. After 24 h, medium was replaced by 100 µl of fresh medium containing various concentrations of the compound to be tested was added to each well and incubated for 48 to 72 h. All plates mas contain control wells: blank without cells (only medium), control with cells plus DMSO. At the end of the treatment period, the medium is removed and 0.5 $mg.ml^{-1}$ of MTT dissolved in culture medium is added. Cells were incubated for an additional period of 3 h. Media is discard and 200 µl of DMSO was added to each well to dissolve the formazan crystals. After homogenization, plates were read at the absorbance of 595 nm using a microplate reader. All cytotoxicity data represents the means of at least three independent experiments. Inhibition of the cell growth is determined by calculating the ID50 according to the formula:

$$ID50=100-\left[\frac{OD_{sample}-OD_{medium\ control}}{OD_{cell\ control}-OD_{\ medium\ control}}\right]\times 100$$

ID50 is defined as the inhibitory dose that reduces the growth of the compound-exposed cells by 50% (105).

2.2.3. Ethidium bromide accumulation assay by a semi-automated fluorimetric method

This simple method has been developed to assess the real-time accumulation and extrusion of the fluorochrome EB on a real-time basis from the bulk of cells in suspension in an Eppendorf tube, a technique initially developed for monitoring the efflux activity of

bacteria (102). This assay employs a new application of the thermocycler, Rotor-Gene™ 3000, which delivers real-time data on transport kinetics of the fluorochrome substrate, reflecting the balance between accumulation of EB via passive diffusion (through membrane permeability) and extrusion via efflux. EB is widely used to quantify the transport across the membrane of the cells, because it generates an easily measurable and quantifiable signal between EB inside and outside the cell. This assay is conducted for a specific period of time with a nontoxic concentration of EB that does not cause its accumulation inside the cells due to its extrusion by an active efflux pump system of the cell. The slope of EB accumulation over time (number of units of fluorescence per minute) provides an assessment of baseline efflux and alterations to this slope, by the use of compounds that promote EB retention inside the cells (fluorescence increases accordingly), being an easy and high-throughput screening procedure (up to 32 tubes and different experimental conditions can be assessed simultaneously in one assay using this protocol) for the identification of compounds that act as efflux inhibitors, initially described in our laboratory by Spengler et al. (101).

The fluorescence emitted by the accumulation of EB inside cells due to the presence of the efflux inhibitor is monitored by real-time fluorometry, collecting data each 60 s at 37 °C for 1 h, and the relative final fluorescence activity ratio (RFF) is calculated as the relation of the determined relative fluorescence (RF) at the last point (30 or 60 min) of the EB retention curve of the cells treated with the inhibitor and the RF at the last point of the EB retention curve of the untreated cells (containing the equal volume of the solvent used to solubilize the drug to be tested — solvent control), divided by the RF of the untreated cells. The activity of the compound in test will be quantified according to the following formula:

$$\text{Relative final fluorescence (RFF)} = \frac{RF_{treated} - RF_{untreated}}{RF_{untreated}}$$

RFFs higher than 1 represent retention of the fluorochrome that is proportional to the inhibitory activity of the tested compound.

Cells were adjusted to a density of 2×10^6 cells.ml^{-1}, centrifuged at 2000×g for 2 minutes and re-suspended in phosphate-buffered saline (PBS) at pH 7.4. The cell suspension was

distributed in 90 µl aliquots into 0.2 ml tubes. The tested compounds were individually added at different concentrations in 5 µl volumes of their stock solutions and the samples incubated for 20 minutes at room temperature. After this incubation, 5 µl (0.5 $\mu g.ml^{-1}$ for MDR cells and 0.25 $\mu g.ml^{-1}$ for PAR cells as final concentrations) of EB were added to the samples, the tubes were placed into a Rotor-Gene™ 3000 thermocycler (Corbett Research, Sydney, Australia) and the fluorescence monitored on a real-time basis. Prior to the assay, the instrument was programmed for temperature (37 °C), the appropriate excitation and emission wavelengths of EB (530 nm band-pass and 585 nm high-pass filters, respectively), and the time and number of cycles for the recording of the fluorescence. The results were evaluated by Rotor-Gene Analysis Software 6.1 (Build 93) provided by Corbett Research. A complete and detailed description of the optimized and improved method was presented in detail by Armada et al. (106).

The cytotoxicity of EB and the EPI is determined previously by trypan blue exclusion method or by MTT viability assay to quantify cell viability and guarantee that the concentrations used in the subsequent assays will not affect cell viability. The lowest EB concentration that reflects the natural and intrinsic balance between accumulation and efflux is calculated previously (EB final concentrations of 0.25, 0.5, 1 and 2 $\mu g.ml^{-1}$). The optimum concentration of EB for studying accumulation in L5178 PAR and MDR mouse T-lymphoma cells was 0.25 $\mu g.ml^{-1}$ and 0.5 $\mu g.ml^{-1}$.

2.2.4. **Fluorescence microscopy efflux assay**

This methodology is used to confirm the preliminary analysis of the data obtained with the semi-automated fluorometric method and as an alternative technique to flow cytometry for evaluation of the EPI activity as putative ABCB1protein inhibitors in MDR cancer cells, using as substrate Rhodamine 123 (or $DiOC_2$ depending on the available microscope filters). With this method it is not possible to quantify precisely the fluorescence but it is a useful technique to visualize the retention of the fluorochrome on

an individual cell basis and confirm the levels of retention/inhibition observed at the end of the semi-automated fluorometric accumulation assays.

Cells were counted (ex. PAR and MDR mouse T-lymphoma cells or other cells), centrifuged and the cell number were adjusted to 2x 10^6 cell.ml^{-1} (final concentration in McCoy's 5A culture medium without colchicine). One milliliter of the cell suspension is seeded into each well of a 24-well tissue culture plates. EPI agent or control solution was added to each well. Incubate the plates at 37 ºC for 30 min. Rh123 (at 5.2 µM final concentration) or $DiOC_2$ (at 1 µg.ml^{-1} final concentration) dissolved in complete medium without colchicine, was added to each well and plates were incubated for another period of 60 min at 37 °C.

Cells were harvested by centrifugation at 2000 × g for 5 min, culture medium was aspirated and cells washed twice with ice cold PBS; The pellet of cells is resuspended in 1 ml of fresh medium without fluorescent probe (with or without inhibitors), transfer to a new plate and incubate for 1 h (efflux). Cells are harvested by centrifugation and each pellet is resuspended in 20 µl cold PBS with inhibitor/without inhibitor (control).

At the end, cells are examined by fluorescence microscopy at 485 nm excitation laser and 530/30 nm emission filter for green fluorescence ($DiOC_2$).

Cells were grown in sterile glass-slides in 24-well plates with or without efflux modulator (VP 10 µM as positive control) for 30 min and then exposed to fluorescent probes dissolved in RPMI medium (Sigma-Aldrich) for another period of 30 min at 37 °C followed by washing the cells 3 times with PBS. Cells were examined by epifluorescence microscopy at both 546 and 485 nm excitation.

2.2.5. Fluorescent substrate efflux assay by flow Cytometry

This methodology is used to corroborate the analysis of the data obtained with the semi-automated fluorometric method and microscopy for evaluation and quantification of the modulation activity of putative inhibitors of ABC transporters in MDR Cells using the non-toxic ABCB1 (MDR1) substrate Rhodamine 123 (Rh123) or $DiOC_2$. This assay has been fully described previously (106). The cells are adjusted to a density of 2×10^6 cells.ml^{-1}, resuspended in serum-free McCoy's 5A medium and distributed in 0.5 ml aliquots into Eppendorf centrifuge tubes. The tested compounds were added at a final concentration that showed accumulation in previous assays, and the samples were incubated for 1 hour at room temperature. Ten microliters (5.2 µM final concentration) of the indicator Rh123 (Sigma-Aldrich) or $DiOC_2$ (1 µg.ml^{-1} final concentration) was added to the samples and the cells were further incubated for another 45 min at 37 ºC, washed twice and resuspended in 0.5 ml phosphate-buffered saline (PBS) for analysis. The fluorescence of the cell population is measured with Attune flow cytometer or CytoFlex (Beckman Coulter). VP was used a positive control in the Rh123 exclusion experiments. The percentage mean fluorescence intensity was calculated for the treated MDR and parental cell lines as compared with the untreated cells. The fluorescence activity ratio (FAR) is calculated via the following equation, on the basis of the measured fluorescence values[1]:

$$\mathrm{FAR} = \left(\frac{\mathrm{MDR_{treated}}}{\mathrm{MDR_{untreated}}}\right) \times 100$$

[1] Partial text and figures were extracted from the original manuscript: Armada A, Martins C, Spengler G, Molnar J, Amaral L, Rodrigues AS, Viveiros M. Fluorimetric methods for analysis of permeability, drug transport kinetics and inhibition of the ABCB1 membrane transporter. Cancer Drug Resistance' book- series Springer 'Methods in Molecular Biology'. 2016; 1395:87-103.

3. Selection of compounds with inhibitor effect on drug transporters

3.1. Biological model #1: Adult worms of *Shistosoma*

3.1.1. Introduction

Schistosomiasis is a neglected tropical disease that affects approximately 249 million people worldwide, 97% of which are located on the African continent. Schistosomiasis treatment relies almost exclusively on the anthelminthic praziquantel (PZQ), however this drug does not prevent reinfection and, with large-scale control programs promoting the extensive use of PZQ for more than 20 years in some African nations, concern regarding the selection of drug resistant parasites has been raised. It is imperative to understand the mechanism underlying this resistance phenomenon to identify new strategies to combat this parasite. In this chapter, two different strains of *Schistosoma mansoni* (one susceptible and one resistant to PZQ) were used to demonstrate if the over expression of *SmMDR2* gene (encoding for SMDR2, a *S. mansoni* ABCB1-like protein) leads to an increased activity of ABCB1-like efflux pumps on male adult worms, and their involvement in resistance to PZQ.

We evaluated the role of efflux pumps in *Schistosoma mansoni* resistance to PZQ, by comparing the efflux pumps activity in susceptible and resistant strains. The evaluation of the efflux activity was performed by the EB accumulation assay in the presence and absence of VP using an adaptation of the methodology described in chapter 2 (2.2.3). The role of efflux pumps in resistance to PZQ was further investigated comparing the response of susceptible and resistant parasites in the absence and presence of different doses of VP, in an *ex vivo* assay.

3.1.2. Material and Methods

3.1.2.1. Reagents

Verapamil (VP), Ethidium Bromide (EB) were purchased from Sigma-Aldrich (St. Louis, MO, USA). Praziquantel (PZQ) was purchased from Merck & Co. (Kenilworth, NJ, USA) and dissolved in Dimethyl Sulfoxide (DMSO) from Sigma-Aldrich, used for stock solutions, which were subsequently diluted to an appropriate concentration in culture media. All solutions were prepared in distilled, sterile water, on the day of the experiments.

3.1.2.2. Adult worms of *Schistosoma mansoni*

In this study two parasite strains were used, a *S. mansoni* BH strain from Belo Horizonte, Minas Gerais, Brazil, susceptible to PZQ, and a stable PZQ-resistant strain (IHMT-LISBON) which was obtained from the BH strain as described by Pinto-Almeida et al. (22, 107). Adult worms were collected through liver-perfusion (8-10 weeks' post-infection), as previously described by Pinto-Almeida et al. (22), washed and maintained in saline solution for the EB efflux assay or in RPMI medium (Sigma-Aldrich) for the *ex vivo* PZQ susceptibility assays. By RT-qPCR, PZQ-resistant males showed, in the absence of PZQ, that the expression levels of *SmMDR2* was 32 times higher than PZQ-susceptible males ($p < 0.05$) (22).

3.1.2.3. **Ethidium bromide efflux assay**

EB efflux assay was performed with the objective of comparing the efflux pumps activity between adult male worms of both PZQ-susceptible and PZQ-resistant parasite strains as described by Armada et al. (106), adapted in this study for the assessment of parasite efflux activity. VP (2.2 µM and 4.4 µM), known as a broad range inhibitor of ABCB1 (Pgp) efflux pump activity was used to inhibit EB efflux at concentrations that did not compromise the viability of the worms. EB concentration was previously optimized for each strain of adult worms in order to determine the lowest concentration which reflects the balance between EB accumulation by influx (passive diffusion) and extrusion by active efflux during the 35 min of the assay (EB influx-efflux steady-state whose accumulation (fluorescent signal) inside the worms is above the lowest signal detectable by the fluorescence microscope). This ensures that the observed increase of accumulation of EB during the 35 min of the assay is due to inhibition of efflux pumps that promotes increased accumulation of the fluorophore inside the worms (108). To measure the time-curve of increased EB accumulation promoted by the inhibitor VP, our EB control group were worms incubated with the same concentration of EB in the absence of VP. All experiments were carried out in triplicate with three worms each (n=9). For quantification of fluorescence, three areas, of each worm, of the same size, of the worm central section (below the cecum ramification), as shown in Fig. 8, were defined and fluorescence intensity was measured and quantified using ImageJ software (imagej.nih.gov) and background intensity was subtracted. Thus, each time-point of relative fluorescence in each assay corresponds to the mean of EB fluorescence (n=9) that remains accumulated per unit of time that we compare to the EB control group (no inhibitor) (108).

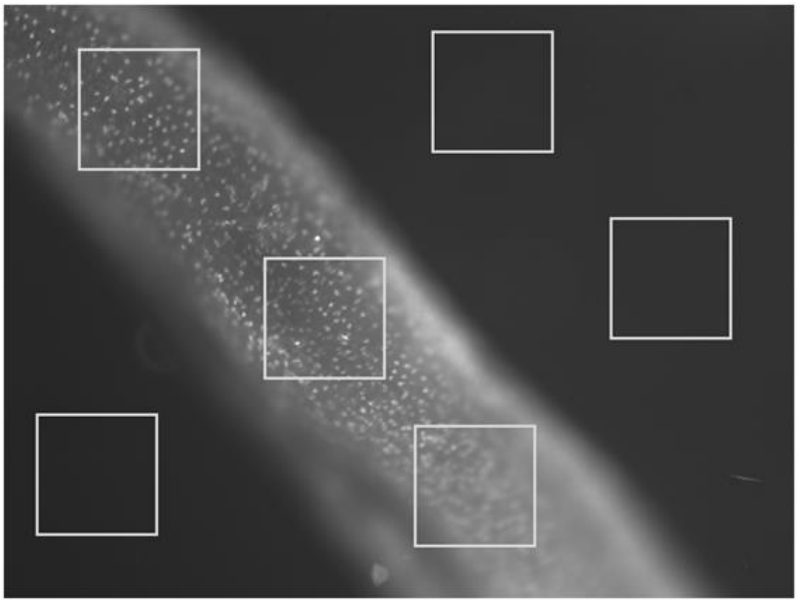

Figure 8: Schematic representation of the worm areas analysed by ImageJ. Fluorescence quantification was made in three defined regions, of the same size, corresponding to the worm central section (below the cecum ramification), of each worm and fluorescence intensity within each region was quantified using ImageJ software (imagej.nih.gov) and background intensity was subtracted. Figure adapted from Pinto-Almeida et al. (22).

24-well culture plates were prepared using RPMI-1640 culture medium, 200 mM L-glutamine, 10 mM HEPES (4-(2-hydroxyethyl)-1-piperazineethanesulfonic acid), 24 mM de $NaHCO_3$, 10000 UI of penicillin and 10 $mg.ml^{-1}$ of streptomycin (Sigma-Aldrich), pH 7 and supplemented with 15% fetal bovine serum (FBS) and three parasites were added on each well for each studied group. Parasites were incubated overnight at 37 ºC in a 5% CO_2 atmosphere to recover from stress caused by liver perfusion. After this period, the worms were washed twice with saline solution to clean any traces of culture medium. The worms were then exposed to the inhibitor for one hour in the previously-mentioned concentrations, after which EB was added (0.6 µM) and parasites were observed under fluorescence microscopy (Zeiss, Axioskop HBO50) for a maximum of 35 min and pictures were taken every 2 min. All worms were at the same exact position, magnification and fluorescence intensity for overall analysis of the assays. Three control

groups were used: 1 - Without VP, 2 - Without EB and 3 - Without both VP and EB (negative control). Fluorescence was quantified using the ImageJ software (imagej.nih.gov) and compared between different groups.

3.1.2.4. *Ex vivo* PZQ susceptibility assay

An *ex vivo* assay was devised to assess the susceptibility of adult worms of *S. mansoni* from both PZQ-susceptible and PZQ-resistant parasite strains, in the presence and absence of VP, to ascertain the involvement of ABCB1-like efflux pumps in the PZQ resistance phenotype.

Parasites were collected as previously described and separated by sex. 24-well culture plates were prepared as described in the previous section and various concentrations of PZQ and VP were used in this susceptibility assay (Table 2), five worms were kept in each well and the same concentration of drug and inhibitor was used in two wells of the same plate. The experiment was done in triplicate, with at least 30 worms used for each concentration of drug and inhibitor. After adding VP and/or PZQ, parasites were incubated for another 24 h at 37 ºC in a 5% CO_2 atmosphere after which the medium was switched for a drug free medium and kept for another 48 h. Parasites were observed every 12 h and the culture medium was changed after each observation. Parasites that did not present any movement after being observed at the microscope for a period of 2 min were considered dead. Lethal dosages were calculated using the software SPSS20® for Windows using Probit regression model with a 95% confidence. The lethal dosages obtained were used for graphical construction design, using GraphPad Prism software.

Table 2: Praziquantel (PZQ) and verapamil concentrations used for the *ex vivo* PZQ susceptibility assay, adapted from Pinto-Almeida et al. (22).

Parasite strains	Verapamil (uM)	PZQ (uM)
Susceptible	0.0	0-25.6
	0.2	0-25.6
	1.1	0-25.6
Resistant	0.0	0-128.0
	1.1	0-64.0
	2.2	0-48.0
	4.4	0-48-0
	8.8	0-32.0

3.1.2.5. Statistical Analysis

Data were expressed as mean ± standard deviation (SD), and tested for statistical significance using either ANOVA or unpaired t-tests. Probit regression model with a 95% confidence was used to calculate the lethal dosages, and the graphic construction was performed using GraphPad Prism 6.0 software.

3.1.2.6. Ethics statement

This research project was reviewed and approved by the Ethics Committee and Animal Welfare (CEBEA), Faculty of Veterinary Medicine, UTL (Ref. 0421/2013). Animals were maintained and handled in accordance with National and European legislation (DL 276/2001 and DL 314/2003; 2010/63/EU adopted on 22 September 2010), with regard to the protection and animal welfare, and all procedures were performed according to National and European legislation.

3.1.3. Results

3.1.3.1. Ethidium bromide efflux assay

Efflux pump activity was compared between PZQ-resistant and PZQ-susceptible adult males through fluorescence microscopy observation. EB is a common substrate to all efflux pumps, when outside the cells the signal is low, but when inside, the signal is amplified, and can be detected and quantified by time-course fluorescence spectroscopy (109). Intracellular accumulation of EB after efflux inhibition by VP was assessed by the increase in fluorescence intensity, using Image J software. As shown in Figure 9 in the susceptible variant strain after exposure to 2.2 μM of VP, the efflux of EB was inhibited resulting in a clear increase of fluorescence. The control groups without EB showed viability and no intrinsic fluorescence was observed thus it is not represented. These findings are of importance considering that ABCB1 and MRPs (ABCC) are members of the "traffic ATPase" superfamily, which use the energy of ATP hydrolysis for maintaining their membrane transport function.

In the PZQ-resistant parasite strain, after exposure to 2.2 μM of VP, there was an initial increase in fluorescence that later stabilized, showing EB accumulation levels lower than the PZQ-susceptible strain. Only by exposing the PZQ-resistant strain to 4.4 μM of VP, fluorescence levels reached levels similar to the susceptible parasites (Fig 9).

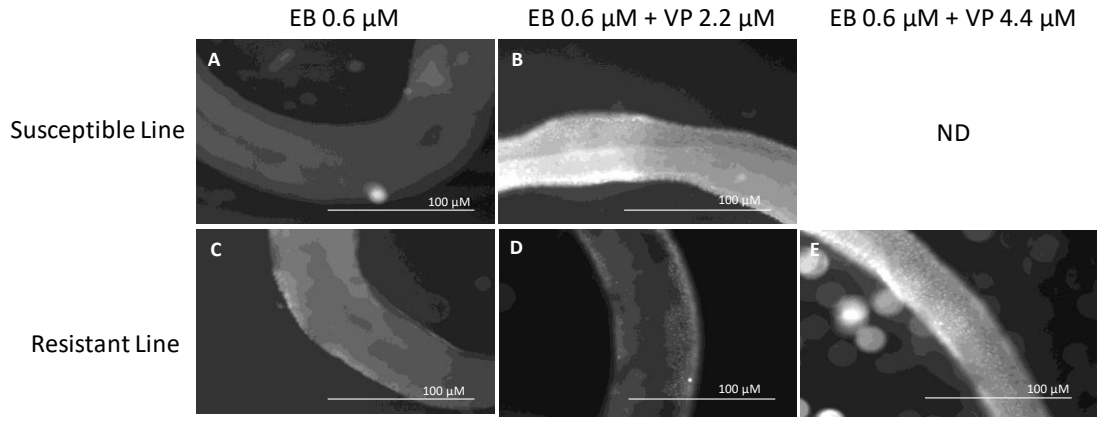

Figure 9: Ethidium bromide (EB) efflux assay in adult males of *S. mansoni* PZQ-susceptible strain (A, B) and *S. mansoni* PZQ-resistant strain (C, D): A and C: Control group - worms exposed to 0.6 µM of EB (20 min); B and D:worms exposed to 2.2 µM of VP (20 min); E: worms exposed to 4.4 µM of VP (20 min). Figures were adapted from Pinto-Almeida et al. (22), ND (not determined). Figures were adapted from Pinto-Almeida et al. (22). PZQ: praziquantel; VP: verapamil.

As described in the Material and Methods section (3.1.2.3), throughout the efflux assays, fluorescence microscopy images were taken every 2 min for 35 min. Fluorescence was quantified in each picture in three areas of the worm central section (below the cecum ramification), as shown in Fig. 8, and background fluorescence was subtracted for each parasite (n=9) at each time-points. The average was calculated and real-time efflux graphics were created to obtain an EB accumulation time course in presence and absence of VP in both variant strains (Fig. 10 and Fig. 11). In the PZQ-susceptible parasite strain with the worms exposed to 2.2 µM of VP, it was possible to observe a steady increase in the fluorescence over time, reaching approximately twice the mean relative fluorescence levels after 20 min, once compared to parasites not exposed to VP (Fig. 10A).

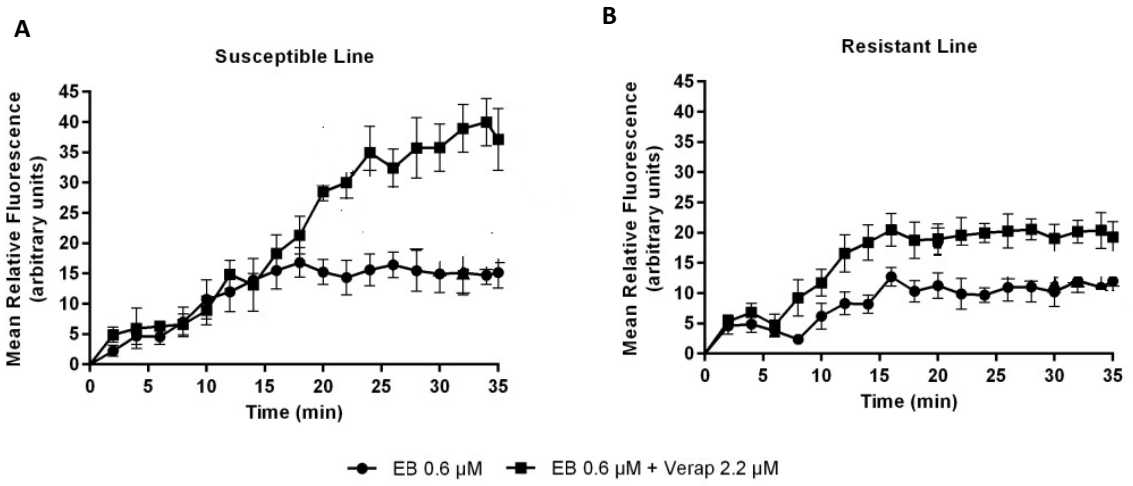

Figure 10: Variation in ethidium bromide (EB) accumulation (Mean relative fluorescence) in the presence and absence of verapamil (Verap) in *S. mansoni* PZQ-susceptible adult males (A) and *S. mansoni* PZQ-resistant adult males (B). Three worms were used for each group and the experiment was performed three times. Quantification measurements were made in three areas of the worm central section (below the cecum ramification) and background fluorescence was subtracted for each parasite at each time-point. The average measurement was calculated for each time-point. Data are expressed as mean fluorescence of the EB accumulated intracellularly over time. Figures were adapted from Pinto-Almeida et al. (22). PZQ: praziquantel.

In the PZQ-resistant strain, for the parasites exposed to 2.2 µM of VP, there was an increase in fluorescence in the first 16 min, then maintaining a constant fluorescence over time at lower levels than the susceptible strain (Fig. 10B). Once exposed to 4.4 µM of VP, the parasites showed a steady increase in the mean fluorescence over time (Fig. 11). The PZQ-resistant parasite strain only showed fluorescence accumulation levels similar to the PZQ-susceptible strain when exposed to twice the concentration of VP.

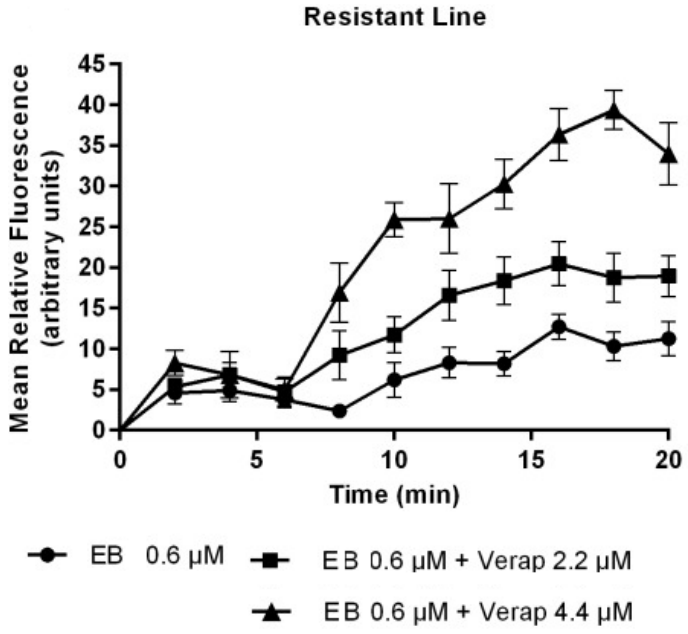

Figure 11: Variation in ethidium bromide (EB) accumulation (Mean relative fluorescence) in the absence and presence of 2.2 µM and 4.4 µM of verapamil (Verap) in *S. mansoni* PZQ-resistant adult males. Three worms were used for each group and the experiment was performed three times. Quantification measurements were made in three areas of the worm central section (below the cecum ramification) and background fluorescence was subtracted for each parasite at each time-point. The average measurement was calculated for each time-point. Data are expressed as mean fluorescence of EB accumulated intracellularly over time. Adapted from Pinto-Almeida et al. (22). PZQ: praziquantel.

3.1.3.2. *Ex vivo* PZQ susceptibility assay

- **PZQ-susceptible male worms**

In the absence of VP, adult males of the PZQ-susceptible strain achieved a 50% lethal dose (LD50) when exposed to 17.8 µM of PZQ; a lethal dose of 90% (LD90) when exposed to 24.2 µM of PZQ and a lethal dose of 99% (LD99) when exposed to 31.0 µM of PZQ.

In the presence of VP, it was possible to observe a reduction in the amount of PZQ required to achieve the lethal dosages mentioned above. In the presence of 0.2 µM and 1.1 µM of VP the LD50 was 15.1 µM and 12.5 µM of PZQ, respectively. LD90 was 20.6 µM and 16.9 µM of PZQ, and LD99 was 26.4 µM and 21.7 µM of PZQ, respectively (Table 3). LD50 are represented in graph bars (Fig. 12).

Table 3: Lethal doses of praziquantel (PZQ) calculated using Probit regression model with a 95% confidence, for *S. mansoni* PZQ-susceptible males in the presence of different concentrations of verapamil.

	Mortality (%)						
Verapamil (µM)	**1**	**10**	**30**	**50**	**70**	**90**	**99**
	PZQ (µM)						
0	10.2	13.1	15.7	17.8	20.2	24.2	31.0
0.2	8.7	11.1	13.4	15.1	17.2	20.6	26.4
1.1	7.2	9.2	11.0	12.5	14.1	16.9	21.7

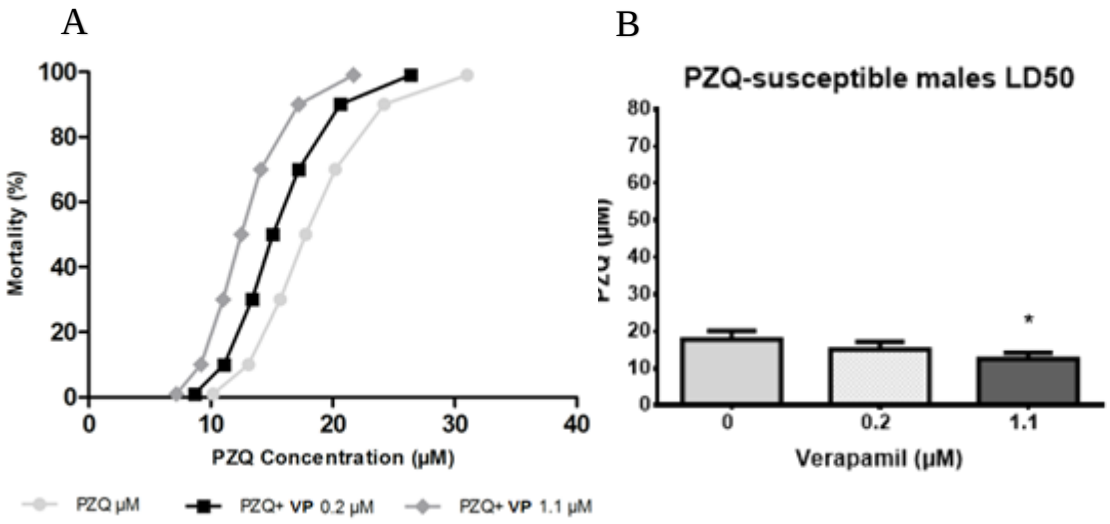

Figure 12: Mortality trends and LD50 of *S. mansoni* adult males PZQ-susceptible exposed to praziquantel (PZQ) in the presence of verapamil (VP). The mortality levels to increase concentrations of VP (0.2 and 1.1 µM) are represented by survival curves (A) and lethal doses of 50% (LD50) (B). Additionally, the survival curve and LD50 of parasites unexposed to VP is also represented. The Probit regression model was used with a 95% of confidence. Figure A was adapted from Pinto-Almeida et al. (22).

3.1.3.3. **PZQ-resistant male worms**

In the absence of VP, male worms of the PZQ-resistant strain achieved the LD50 when exposed to 65.2 µM of PZQ, LD90 when exposed to 98.1 µM and the LD99 when exposed to 137.0 µM of PZQ.

When exposed to a non-toxic concentration of VP, it was possible to observe a reduction in the amount of PZQ required to achieve the lethal dosages mentioned above. In the

presence of four different concentrations of VP (1.1 µM, 2.2 µM, 4.4 µM, and 8.8 µM), the PZQ lethal dose decreased significantly: LD50 concentrations of PZQ was 33.9 µM, 19.7 µM, 5.1 µM and 3.6 µM, LD90 was 52.4 µM, 37.5 µM, 19.8 µM and 12.8 µM and the LD99 was 74.7 µM, 63.2 µM, 59.8 µM and 35.9 µM, for each of the four concentrations of inhibitor used (Table 4).

Table 4: Lethal doses of praziquantel (PZQ) calculated using Probit regression model with a 95% confidence, for *S. mansoni* PZQ-resistant parasite strain males in the presence of various concentrations of verapamil.

	Mortality (%)						
Verapamil (µM)	**1**	**10**	**30**	**50**	**70**	**90**	**99**
	PZQ (µM)						
0	30.98	43.27	55.11	65.16	77.05	98.14	137.03
1.1	15.39	21.95	28.38	33.92	40.53	52.41	74.74
2.2	6.16	10.38	15.17	19.72	25.64	37.46	63.20
4.4	0.44	1.33	2.95	5.13	8.92	19.85	59.81
8.8	0.36	1.01	2.15	3.60	6.05	12.79	35.94

The lethal PZQ dose values for PZQ-resistant males when exposed to different concentrations of VP were plotted in a mortality dose dependent curve (Fig.13A) and LD50 bars (Fig. 13B) showing the effect of VP on the susceptibility to PZQ in this variant strain. Once again, in the presence of VP, a decrease in the PZQ concentration required to achieve the same level of mortality was observed, compared to parasites not exposed to this inhibitor. In the presence of 1.1 µM of VP, the lowest concentration tested in this strain, the PZQ lethal concentrations were twice as low compared to the ones obtained for the group not exposed to the inhibitor. Overall, it was demonstrated that the drug-resistant strain reduces or reverts its resistance to PZQ in the presence of VP obtaining LD values close to or even lower than those obtained for the susceptible variant strain.

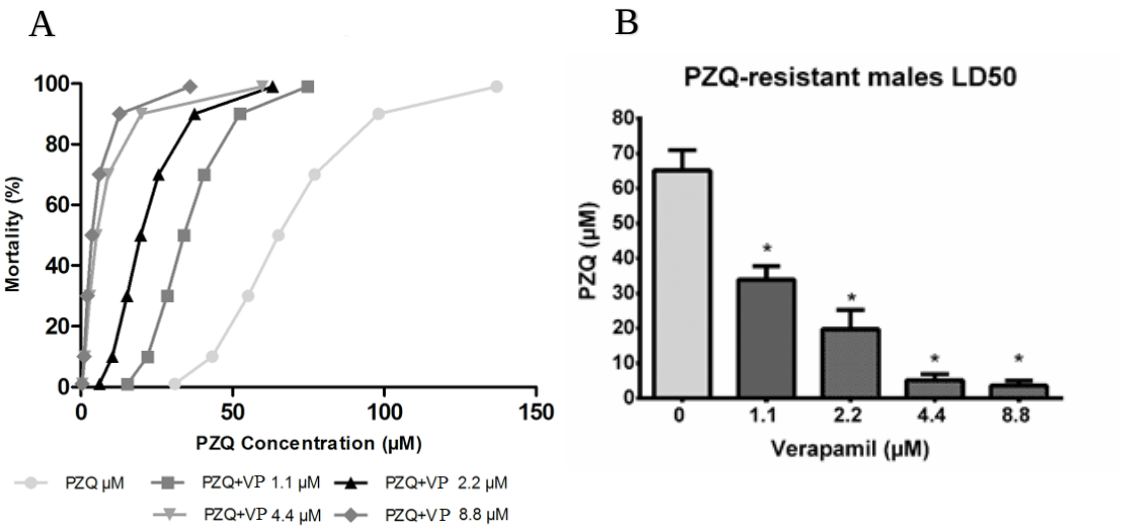

Figure 13: Mortality trends and LD50 of *S. mansoni* adult males PZQ-resistant exposed to PZQ in the presence of VP. The mortality levels to increase concentrations of VP (1.1 – 8.8 μM) are represented by survival curves (A) and LD50 (B). Additionally, the survival curve and LD50 of parasites unexposed to VP is also represented. The Probit regression model was used with 95% confidence level. Figure A was adapted from Pinto-Almeida et al (22). VP: verapamil; PZQ: praziquantel; LD50: Lethal dose of 50%.

3.1.4. **Discussion**

PZQ resistant parasite strain was used to analyze the involvement of efflux pumps in the induced PZQ-drug resistance phenotype. Efflux pump activity of *S. mansoni* adult male worms, was observed and monitored by fluorescence microscopy using for the first time an adaptation of the semi-automated fluorometric methodology described by Armada A. et al. (106). EB was used as a universal fluorescent substrate in the presence and absence of an efflux inhibitor – VP - thus the emission of the accumulated fluorescence was monitored throughout sequential photographs, taken every 2 min, during a maximum period of 35 min.

In PZQ-susceptible adult males, the exposure to 2.2 μM of VP led to a substantial increase in accumulated fluorescence suggesting that VP is able to inhibit EB efflux in *S. mansoni* males of the susceptible strain.

In PZQ-resistant adult male's EB accumulation was up to 2 times lower than the PZQ-sensitive males, when exposed to 2.2 µM of VP. Only when PZQ-resistant adult males were exposed to 4.4 µM of VP the intracellular accumulation of EB was similar to the susceptible variant strain. This suggests that males of the resistant strain have a higher number of transporters responsible for the EB efflux, which was further demonstrated by the quantitative RT-PCR results on the SmMDR2 RNA expression level. Other authors have also shown an increased expression level of the SmMDR2 RNA in PZQ resistant clinical isolates of *S. mansoni* (110-114). Here in this study an increase of ABCB1-like efflux pumps activity in male worms from resistant strains was demonstrated, which was in agreement with our RT-PCR previous results (22), where parasites that were exposed to sub lethal concentrations of PZQ have shown to have reduced susceptibility to PZQ.

The greatest advantage of this experimental model over other PZQ resistant parasites described in the literature is the fact that they are isogenic allowing a comparison of the influence of efflux pumps in PZQ resistant phenotype within the same genetic background. Therefore, it was possible to observe that the *S. mansoni* adult male's variant resistant to PZQ presented an increased efflux pump activity suggesting that Pgp-like efflux pumps play an important role in PZQ-drug resistance in *S. mansoni*. In the EB efflux assay, when observing both PZQ-susceptible and PZQ-resistant adult males, fluorescence levels in the absence of VP, resistant strain males showed lower levels of fluorescence. This could be explained by a higher number of EB efflux pumps in the resistant strain, which, was reinforced by the assessment of the expression of SmMDR2 RNA, through RT-PCR, where a significant difference in *SmMDR2* expression was observed (22). To further put in evidence that over-expression of efflux pumps is involved in PZQ acquired drug-resistance, an *ex vivo* assay, using both *S. mansoni* strains, was performed to assess the degree of susceptibility of the adult parasites to PZQ, in the presence and absence of VP. When adult males of the susceptible strain were exposed to VP the PZQ concentration required to reach lethal dosages was lower than those observed in the absence of the inhibitor. Other authors have already reported that blocking the activity of the ABCB1 and MRPs transporters by VP increases the pharmacological susceptibility of helminths such as *Caenorhabditis elegans*, *Haemonchus contortus*, and *Cooperia oncophora* to various anthelminthic drugs (115, 116). For male worms of PZQ-resistant strain, in the presence of this efflux inhibitor, a lower PZQ concentration was

required to achieve the same level of mortality compared to the same parasites not exposed to the inhibitor. In the presence of the lowest concentration of VP tested in the resistant strain, PZQ lethal concentrations were twice as low as the ones obtained for the group not exposed to the inhibitor.

Overall, it was possible to observe that PZQ susceptibility of the PZQ-resistant strain, in the presence of VP, has LD values close to or even lower than those obtained for the PZQ-susceptible strain. Ardelli and Prichard also showed that a *C. elegans* ivermectin-resistant strain in the presence of VP, presented an increased susceptibility to ivermectin, suggesting an involvement of ABCB1-like efflux pumps on this ivermectin drug resistance phenotype (115). These results also suggest that, just as in the resistant strain of *C. elegans*, the adult males of this resistant strain have ABCB1-like pumps involved in the drug resistance phenotype as demonstrated by the SmMDR2 expression level analysis.

Collateral sensitivity (CS) of drug-resistant cancer cells to VP (117) has been reported, a phenomenon that might have occurred in this *ex vivo* PZQ susceptibility assay in PZQ-resistant worms by a mechanism possibly linked to the expression of SmMDR2. This susceptibility, observed by PZQ LD50 obtained from resistant worms in the presence of increasing concentrations of VP, can circumvent potential problems that might be associated with adjuvant therapy using EPIs during standard therapy with PZQ, where the main objective is to treat patients by killing all the worms (susceptible and resistant worms) without causing side effects. Also, CS opens a new approach for the identification of new re-sensitizing compounds in the management of PZQ resistance and to elucidate the mechanisms involved.

Previous studies regarding drug resistance have already presented evidence of an increased tolerance to PZQ in male worms (110-114, 118). It should be noted that when using *in vivo* and *ex vivo* assays the interaction between the effects caused by the drug and those caused by the host immune system on the parasite are not taken in consideration (119-121).

In conclusion, this work describes for the first time, the application of a successful methodology previously applied in bacteria and cancer cells, using the broad range efflux pump substrate EB, for the evaluation of drug transporter systems on *S. mansoni* adult

worms as a multicellular cell model using an *ex vivo* assay. The methodology used demonstrated the involvement of adult male *Schistosomes* ABCB1-like transporters SmMDR2 in PZQ drug resistance phenotype, evidenced by the fact that lower doses of VP successfully reverted PZQ drug resistance when using sub lethal concentrations of PZQ. The World Health Organization warns about the possible emergence of *Schistosoma* spp. populations that are resistant to PZQ thus recommending continued vigilance(122). Therefore, studies on genetic resistance mechanisms against PZQ are of extreme importance to understand the potential mechanism(s) of resistance/increase tolerance to PZQ, contributing to the development of new drugs and the delineation of new strategies for schistosomiasis control[2].

[2] Partial text was extracted from the original manuscript: Pinto-Almeida A, Mendes T, Armada A, Belo S, Carrilho E, Viveiros M, Afonso A. The role of efflux pumps in *Schistosoma mansoni* praziquantel resistant phenotype. PLoS One. 2015; 10: e0140147. doi:10.1371/journal.pone.0140147.

3.2. **Biological model #2: Macrophage intracellular infection**

3.2.1. **Introduction**

Macrophages (MØ) are the major effector cells able to phagocyte and destroy pathogens, playing a crucial role in the innate immune systems. These cells harbor microbicide mechanisms such as the acidification of phagolysosomes and the production of reactive oxygen (ROS) and nitrogen species (RNS).

There are intracellular pathogens, like *Mycobacterium*, *Staphylococcus* and *Leishmania*, responsible for human and animal diseases, that target MØs. These microorganisms are able to counteract MØs antimicrobial activities, being able to survive in the intracellular compartments. The intracellular environment is also used for the acquisition of nutrients necessary for the replication of intracellular pathogens.

Leishmaniasis is a vector born disease that comprises a variety of clinical syndromes caused by more than 20 different *Leishmania* species. It is spread through the bite of infected female phlebotomine sandflies. *Leishmania* parasites are obligate, intracellular protozoa of the genus *Leishmania* (family Trypanosomatidae) which, depending on the parasite species and the immune response of the mammalian host, causes several types of clinical manifestations of the disease. The most common forms are cutaneous (CL) and visceral leishmaniasis (VL). VL is caused by *L. donovani* or *L. infantum* and, the most severe form of the disease is almost fatal if untreated. Man and dogs are the most commonly affected hosts, and they can also be potential reservoirs (123).

Worldwide there are 350 million people in 88 countries at risk of getting infected and approximately two million new cases each year, affecting tropical and sub-tropical regions (World Health Organization Regional Office for Africa, 2017). Treatment currently relies on few chemotherapeutic options, antimonial drugs, including sodium stibogluconate and meglumine antimoniate, being the first-line treatment in most affected countries. The second line drugs include amphotericin B, pentamidine and the oral agent miltefosine. Miltefosine, which was originally developed as an antineoplastic agent, was

the first oral drug available to treat leishmaniasis (LC and LV), including antimony-resistance infections (124).

However, conventional antileishmanial drugs are far from satisfactory and do not achieve a parasitological cure. In fact, in addition to important side effects, treatment does not completely eliminate the parasite allowing relapses to occur. The emergence of resistance has limited even further the few available therapeutic options. Therefore, new alternatives for the treatment of leishmaniasis are greatly needed. According to the WHO, plants are the best and largest source of drugs for humanity and there are a number of plants with anti-*Leishmania* activity that have been described in the literature (125, 126). Most of the anti-leishmanial activity of plants has been attributed to the presence of compounds such as alkaloids, chalcones, triterpenoids, naphthoquinones, quinones, terpenes, steroids, lignans, saponins, and flavonoids (127, 128).

Leishmania is a heteroxenic protozoan parasite with a digenetic life cycle: the elongated and flagellated promastigotes (extracellular form) localized in the insect vector and the round nonmotile intracellular amastigote present in the mammalian host. During the blood meal, the insect vector deposits metacyclic promastigotes in the skin of the host. After infection, promastigotes are taken up by host dendritic cells and by MØs where they differentiate into amastigotes, replicate and persist within the acidic phagolysosome. MØs are the definitive host cells of *Leishmania* parasites.

Thus, understanding the complex interactions between *Leishmania*, and the mammalian host at a molecular level is crucial to design new therapeutic approaches and establish effective control measures (129).

The sensitivity of eukaryotic cells to therapeutic agents may be intrinsic or induced by the drug used. Both forms of sensitivity are due to overexpression of membrane proteins that recognize the agent and extrude it from cells before reaching the intended target (130). Membrane ABC transporters, like ABCB1 coded by *MDR1* gene, are involved in recognizing and extruding several substrates (131-133). Inhibition of extrusion results in the build-up of cytoplasmic concentration of drugs that could reach levels able to inhibit cell replication (132, 133). The key to successful therapy of intracellular infections involve adjuvants able to inhibit ABC transporters without harming host cells. Unfortunately, of the known agents that inhibit ABC pumps, none have proven to be

successful at clinical concentrations. The study of *Leishmania* ABC transporters has been on-going for many years (131-133) and much is known about the range of substrates recognized and extruded and the methods used for their assessment.

Tamoxifen, an estrogen receptor antagonist, and also an inhibitor of ABCB1 efflux pumps, currently used in the treatment of breast cancer, has demonstrated to have great activity against intracellular amastigotes *in vitro* studies and was also able to cure *Leishmania* infection in laboratory mice (134) (Nagle 2014). It has been also demonstrated that this drug is able to shift the pH of parasitophorous vacuoles from acid to neutral, which in turn heightens the drug effect on amastigotes (135).

The mechanism by which efflux-pump inhibitors enhance the cure of intracellular infections without causing injury to MØs has been suggested by many authors (136-139). The activation of MØs hydrolases is dependent on K^+ and Ca^{2+} ions (140, 141) and the role of inhibitors of K^+ transport, like ouabain, on destruction of MØ intracellular parasites has already been described (137). Inhibitors of Ca^{2+} and K^+ transport, like phenothiazines and verapamil, has been reported to be as effective as ouabain in enhancing MØ killing activity. Verapamil is also known as an efflux modulator of *Leishmania* ABC transporters (142).

However, to survive in the acidic environment of phagolysosomes, *Leishmania* actively transport protons by efflux pumps keeping a H^+ gradient that guarantees nutrient uptake (143). Tricyclic compounds and phenothiazines have antileishmanial activity by reducing H^+ efflux (144, 145). Impaired proton extrusion leads to intracellular acidification of amastigote, limiting amastigotes replication and dispersion. Stimulating MØ mechanisms in order to destroy pathogens is a new concept for intracellular infection therapy. This concept targets MØs rather than the parasite itself. However, compounds can also have a direct effect on the parasite, having a dual effect.

Three different classes of ABC transporters have been described in *Leishmania*. The first group is homologous of human multidrug resistance protein (ABCC1) subfamily, MRPA, responsible for thiol efflux (146) and reduction of antimony active form (147). The second class is constituted by transporters with higher similarity to mammalian P-glycoproteins (MDR). *Leishmania* ABCB1 (PRP1) is related to pentamidine resistance and antimony cross-resistance. The third group has high homology with mammalian ABC

superfamily (148). Resistant parasites strongly increase expression of ABCB1-like and MRP1 on infected MØs, resulting in impairment of drug accumulation, indicating that parasite antigens can upregulate these transporters.

The unravelling ion channel blockers action mechanisms, as is the case of verapamil, thioridazine, chlorpromazine or ouabain, points the use of those compounds as antiparasitic agents, efflux inhibitors and enhancers of MØ killing activity against *Leishmania* parasites, providing new insights about their potential as future adjuvants on the treatment of Leishmaniasis conventional treatment.

Therefore, looking for strategies that could promote the use of low doses of conventional drugs, minimizing side effects and maximizing the cure this study aims to evaluate the effect of efflux inhibitors (EI) and the natural compound 6-gingerol (6G) in macrophages infected with *L. infantum* by studying the potential of these compounds to enhance the killing activity by the dual activity mentioned above and the MØ inflammatory response.

3.2.2. Material and Methods

3.2.2.1. Reagents

Verapamil (VP), ouabain (OUAB), chlorpromazine (CPZ), thioridazine (TZ) and ethidium bromide (EB) were purchased from Sigma Aldrich Química SA (Madrid, Spain). All solutions were prepared in deionized, sterile water on the day of the experiment and kept protected from light. 6-gingerol (6G), isolated from the seeds of *Aframomum melegueta*, (89) and kindly provided by Prof. Franz Bucar (University Graz, Austria) was dissolved in dimethyl sulfoxide (DMSO). By NMR Spectroscopic data 6G was characterized to be exclusively (5S)-6G with a MW of 294.16 and 99 % purity, described as compound number 4 in Gröblacher et al. (89).

Lipopolysaccharide (LPS, 100 $ng.ml^{-1}$) from *E. coli* (Sigma-Aldrich) was used as a cell inflammatory control.

Acridine orange (AO) (Molecular Probes, Eugene, OR) stock solution was diluted in water (1 mg.ml^{-1}) and stored at 4 ºC, and LysoTracker® Red DND-99 (LTR, Molecular Probes) was dissolved in PBS (50 nM) and stored at 4 ºC. Dihydrorhodamine 123 (DHR) was dissolved in DMSO (10 mM).

3.2.2.2. Cell culture and parasites

The murine MØ-like cell line RAW 264.7 (*Mus musculus* MØs) was established from the ascites caused by a tumour induced in a male mouse by intraperitoneal injection of Abselon Leukaemia Virus (A-MuLV) (ATCC ® TIB-71 ™). RAW 264.7 cells were cultured in RPMI 1640 supplemented with 10% fetal bovine sera (FBS, Gibco), 2 mM L-glutamine, 10 mM HEPES (hydroxyehyl piperazineethanesulfonic acid, Sigma-Aldrich) and 100 units.ml^{-1} of penicillin and 100 µg.ml^{-1} of streptomycin (Sigma).

L. infantum virulent promastigotes strain (MCAN/PT/2012/IMT0005SG) isolated from a canine leishmaniasis case, were cultured in Schneider's Drosophila medium (SCHN, Sigma-Aldrich) supplemented with 10% (v/v) of heat-inactivated bovine sera (FBS, Gibco) and penicillin-streptomycin at 100 U.ml^{-1} and 100 µg.ml^{-1} respectively (complete SCHN medium), at 24 ºC under normal atmospheric conditions. The concentration of promastigote suspension was determined in a Neubauer-improved chamber (Sigma-Aldrich) in an optical microscope.

All assays were conducted with stationary growth phase promastigotes. Viable parasites were centrifuged at 1800 g for 10 min and resuspended in RPMI medium (Sigma) (1:2) with 40 % glycerol.

L. infantum (MHOM / MA / 67 / ITMAP-263) expressing a green fluorescent protein (GFP) was kindly provided by Professor Ana Tomás of the Institute of Molecular and Cell Biology. *L. infantum* GFP-promastigotes were cultured in SCHN medium, as described above, with 0.1 mg.ml^{-1} of geneticin (G418 disulphate saline solution, Sigma-Aldrich).

3.2.2.3. Cell viability assays

RAW 264.7 cells were plated at a density of 2.5×10^5 cells per well in a 96-well microplate and incubated at 37 °C for 24 h until being adherent. The effects of compounds on cell growth was tested using the MTT (3-[4,5-dimethylthiazol-2-yl]-2,5-diphenyl tetrazolium bromide) assay, according to the protocol previously described in chapter 2 (2.2.2). Briefly, cells were exposed to increasing concentrations of VP (10-1280 µM), OUAB (0.125-16 µM), 6G (6.8-870 µM), TZ (0.8-100 µM) and CPZ (0.8-100 µM). After 48 h incubation, the medium was removed and MTT dye was added to a final concentration of 0.5 $mg.ml^{-1.}$ Cells were incubated for 1 h at 37 ºC and MTT solution was removed. DMSO was added and cell viability was determined by measuring the optical density (OD) at 570 nm with an ELx808 ™ Absorbance Microplate Reader (BioTek®) with Microplate manager software 5.2.1. The results were analyzed in GraphPad Prism software version 5.00. Cytotoxic concentrations of CC10, which ensure cell viability (90 % viability), were estimated and used in the following assays.

Calcein AM® (Molecular Probes) was used as a control of cell viability. Calcein AM is a non-fluorescent hydrophobic compound that easily permeates viable cells. Calcein AM is hydrolyzed by intracellular esterases and converted to a strongly green-fluorescent calcein, a hydrophilic compound that is well-retained in the cytoplasm. After treatment, cells were incubated with 1 µM Calcein AM in PBS for 30 min at 37 ºC. Cells were visualized under a fluorescence microscope (Nikon eclipse 80i and camera Nikon DS-Ri1) with excitation/emission of 590/520 nm (green). Images were acquired using the NIS-Elements BR 3.2 imaging software.

Also, cell viability and concentration were determined by the Trypan blue (Sigma-Aldrich) exclusion dye assay in a Neubauer's chamber as previously described (chapter 2, 2.2.1).

3.2.2.4. Accumulation assay

Intracellular accumulation assay, for the assessment and extrusion of the fluorochrome ethidium bromide, was done as described in chapter 2 (2.2.3) with minor modifications,

by real-time fluorometry assay. The EB concentration at which influx and efflux reached an equilibrium was determined by using increasing concentrations of EB that ranged from 0.125 to 2 µg.ml^{-1}. The relative fluorescence (RF) value for treated and non-treated (solvent control) cells exposed to EB was calculated by the mean value of the fluorescence arbitrary units measured after 60 min in addition to the value of the standard deviation (SD) ($RF_{treated\ cells}$ and $RF_{non\text{-}treated\ cells}$). The RF of treated cells is the RF at the last point of the EB retention curve in the presence of an inhibitor and the $RF_{non\text{-}treated}$ is the relative fluorescence at the last point of the EB accumulation of the untreated control having the same solvent control. The effect of TZ (5-40 µM), CPZ (5-40 µM), VP (25-200 µM), OUAB (0.025-0.2 µM) and 6G (30-240 µM) on the accumulation of EB at 37 °C was determined as previously described (chapter 2, 2.2.3). The fluorescence was expressed in terms of relative final fluorescence (RFF) according to the formula:

$$RFF = \frac{RF_{treated} - RF_{non\text{-}treated}}{RF_{non\text{-}treated}}$$

Results are expressed by the mean and SD of three independent assays and triplicates per sample (±SD).

3.2.2.5. *L. infantum* infected macrophages

Stationary phase promastigotes were added to Raw 264.7 MØs at a proportion of three parasites per cell. Microplates were incubated for 5 h at 37 ºC in a humidified atmosphere with 5% CO_2. Thereafter extracellular *Leishmania* promatigotes were removed by washing with warm RPMI medium and fresh culture medium (RPMI-10% FBS) was added to the wells. Then slides of each well, Infection index was calculated by optical microscopy (OM) after methanol fixing and staining with Giemsa. Frequency of infected cells (i.e. number of infected cells per 100 MØ) and intensity of infection (i.e. number of amastigotes per infected cells) were determined by light microscopy at ×1000 magnification by counting at least 100 cells per well.

3.2.2.6. Immunolocalization of ABCB1 efflux pumps

An indirect fluorescent antibody test was performed for the detection of ABCB1 on the surface of infected macrophages, as an adaptation of the method described by Armada A. et al. (149). Briefly, cells were seeded in sterile cover-slips ($5x10^5$ cells/coverslip) inside 12-well plates filled with the RPMI 10% FBS. MØs were incubated for 24 h at 37 ºC in an atmosphere of 5% CO_2 and 95% humidity in order to adhere. Medium was removed, cells were first fixed in ice-cold acetone for 10 min. Cover slips were blocked with 2% BSA in PBS and 0.05% Triton X-100 and incubated with mouse monoclonal anti human ABCB1 (Mdr-1 (D-11): sc-55510, Santa Cruz Biotechnology) diluted 1: 200 in RPMI 10% FBS for 3 h at room temperature. Slides were washed 3 times in PBS and incubated for 1 h with FITC-conjugated goat Anti-Mouse IgG diluted (Sigma) 1:200 in RPMI 10% FBS for 1 h. After three washes in PBS and a 3 min incubation with 1 $\mu g.ml^{-1}$ DAPI (4',6-diamidino-2-phenylindole dihydrochloride) nuclear stain (Vector), followed by a final wash, slides were mounted in Fluorprep antifade reagent (Biomérieux Laboratories) and examined under a fluorescence microscope.

3.2.2.7. Evaluation of intracellular pH

Changes in intracellular pH were evaluated by using pH-sensitive fluorescent AO and LTR, which emit red fluorescence proportional to the degree of acidity.

Cells were grown on round coverslips ($5x10^5$ cells/coverslip) inside 12-well plates filled with the RPMI 10% FCS. MØs were incubated for 24 h at 37 ºC in an atmosphere of 5% CO_2 and 95% humidity in order to adhere. Medium was removed and parasites (*L. infantum* promastigotes and GFP-promastigotes) were added. After 5 h MØs were treated with VP, TZ, CPZ, OUAB and 6G at non-toxic concentrations (CC10) for 4 h and 24 h. In parallel resting-MØs and LPS-stimulated MØs were treated with VP, TZ, CPZ, OUAB and 6G. For LPS-stimulated MØs, LPS (100 $ng.ml^{-1}$) was added to RPMI 10% FCS and left in contact with the cells for 4 h. Cells were visualized by fluorescence microscopy and images were acquired.

The fluorescence intensity observed was rating using a five-point grading scale: negative (-) if no fluorescence was observed, low (±), weak (+), middle level (++) and high level (+++) of fluorescence.

- **Acridine orange staining**

Acridine Orange (AO) is a basic molecule that easily crosses cell membranes. In acidic conditions, the AO protonated form can constitute aggregates (a H-type aggregate) that when excited emits red fluorescence (~ 630 nm). The protonated AO monomer emits green fluorescence (~ 530 nm). Fluorescent emission at 630 nm corresponds to a highly acidic region or the lysosomes, making possible to localize lysosome vesicles inside the cell.

AO was added to the cells at a final concentration of 2.6 µM in PBS and incubated for further 30 min at 37 ºC. Cells were visualized by fluorescence microscopy with excitation/emission of 502/525 nm (green) and 460/650 nm (red) and images were acquired.

- **LysoTracker Red staining**

LysoTracker® probes are fluorophores, linked to a weak base, that freely permeate membranes of living cells, being highly selective for acidic organelles.

MØs grown on coverslips were then washed with PBS and incubated with 25 nM LTR for 30 min (at 37 °C and 5% CO_2) accordingly to the manufacture's recommendation. Cells were observed under a fluorescence microscopy with excitation/emission of 577/590 nm and images were acquired.

3.2.2.8. Determination of *Leishmania* survival

L. infantum infected MØs ($2x10^7.ml^{-1}$) free of extracellular parasites and treated with non-toxic concentrations (CC10) of VP, TZ, CPZ, OUAB and 6G were incubated at 37 ºC in a humidified atmosphere with 5% CO_2 for 24 h, 48 h and 72 h. To allow parasite release from MØs and conversion of intracellular amastigotes into extracellular promastigotes,

at each time point, cells were transferred to complete SCH medium and plates were incubated at 24 ºC. After seven days of incubation, the amount of viable *L. infantum* was estimated by counting extracellular motile promastigotes (viable parasites) using a Neubauer haemocytometer chamber (reversion). In parallel, non-treated MØ exposed to parasites were also used as controls (24 h, 48 h and 72 h) (Fig. 14). The number of viable parasites recovered from treated cells at each time point was normalized by the mean of promastigotes (prom) released from non-treated MØ that were exposed for 5 h to parasites, after seven days of incubation at 24 ºC (T0), according to the following formula:

$$Viable\ prom\ fold\ changes = \frac{Mean\ motile\ prom\ recovered\ from\ treated\ MØs)}{Mean\ motile\ prom\ recovered\ from\ T0\ MØs}$$

Each sample was evaluated in triplicate and the results were shown as mean values of three independent experiments.

Statistical analyses were performed using the GraphPad Prism 6 (GraphPad Software, Inc.). *P* values ≤ 0.05 were considered statistically significant.

3.2.2.9. *Leishmania* proliferation assay

Promastigotes released from treated-MØs on the 7th day and also from non-treated MØs were left for growth for more 2 days (8th and 9th days) at 24 ºC. In order to evaluate the capacity of *L. infantum* parasites to replicate after being under efflux modulator (EIs) pressure, motile parasites were quantified at day eight and nine of incubation (Fig. 14) as previously described.

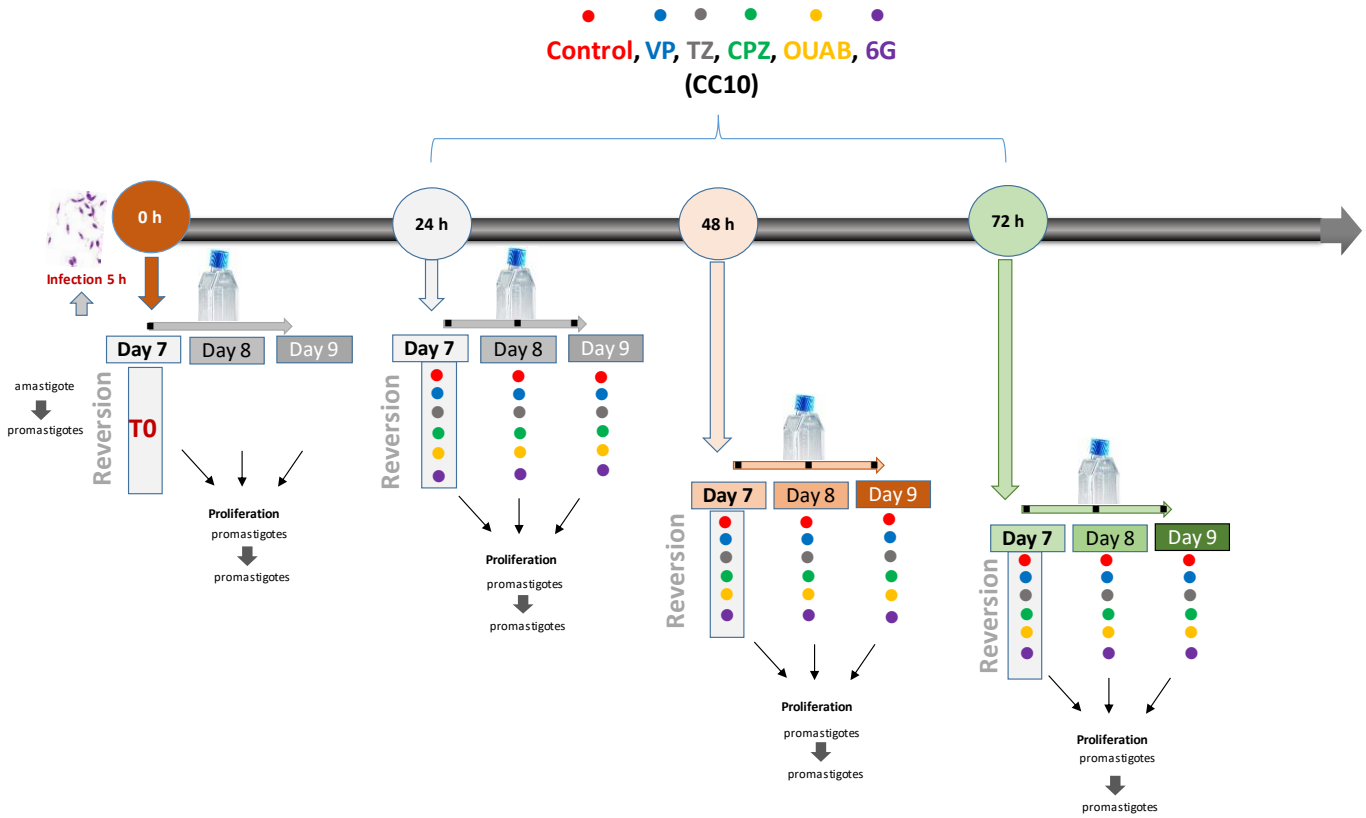

Figure 14: Survival ability and proliferation capability of *L. infantum* parasites after being under efflux inhibitors pressure. *L. infantum* infected MØ treated with verapamil (VP), thioridazine (TZ), chlorpromazine (CPZ), ouabain (OUAB) and 6-gingerol (6G) for 24 h, 48 h and 72 h were moved for EIs-free Schneider medium and intracellular amastigotes were allowed to transform into extracellular motile promastigotes for 7 days (reversion). Survival promastigotes were then left to replicate for more 2 days (proliferation). Infected non-treated MØ were used in parallel as controls. T0: time zero; EIs: efflux inhibitors.

3.2.2.10. **Assessment of ROS formation**

The cell permeant fluorogenic dye Dihydrorhodamine 123 (DHR) was used for the detection of reactive oxygen species (ROS) by fluorescence microscopy. After being uptake by cells, non-fluorescent DHR is oxidized by ROS (such as peroxide and peroxynitrite) and converted to the green fluorescent Rh123 that accumulates in the mitochondria.

Cells were seeded on sterile glass coverslips placed into 12-well culture plates. Adherent cells were loaded with 3 µM DHR (Molecular Probes) in complete RPMI medium for 30 min at 37 ºC accordantly to the method described by Brito MA and colleagues (150), with minor modifications. After removing medium with DHR, cells were incubated in RPMI medium with EPIs at CC10 concentration. To assure that cells were in functional conditions a positive control of inflammation was included. Lipopolysaccharide (LPS) is a major constituent of the cell wall of most gram negative bacteria. It is a highly immunogenic antigen with the ability to enhance the immune response. LPS-RPMI (100 $ng.ml^{-1}$) was added to cells for 4 h and resting-MØs were used as a negative control. Cells were incubated for 24 h at 37 ºC in a humidified atmosphere with 5% CO_2. Supernatants were periodically collected (3 h and 24 h) and kept at -70 ºC until further use. At the end of the incubation period, cells were washed with PBS and observed under a fluorescence microscope with filters of 500/525 nm. In order to validate the methodology, 2 µM hydrogen peroxide (H_2O_2) was added to the resting-MØs for 1 h and these cells were used as indicative of maximal fluorescence.

The fluorescence intensity was rated using a five-point grading scale: negative (-) if no fluorescence was observed, very low (±), weak (+), middle level (++) and high level (+++) of fluorescence (MØ plus H_2O_2).

3.2.2.11. **Determination of nitric oxide**

Nitric oxide (NO) is generated by the inducible nitric oxide synthase (iNOS), an enzyme that catalyzes the oxidation of L-arginine in NO and L-citrulline. Secondary nitrogenous reactants, such as nitrite and nitrate are produced from NO.

Total nitrite production was measured in cell culture supernatants of resting-MØs, LPS-stimulated MØs, *L. infantum*-infected MØs, *L. infantum*-infected MØs treated with EIs for 3 h and 24 h by using the colourimetric Griess reaction (method adapted from the protocol described in Technical Bulletin #TB229 of Promega). Briefly, 50 µl of supernatant and 50 µl of Griess reagent (Sigma-Aldrich) was added to a 96-well plate. Plates were incubated at room temperature in the dark for 10 min. A standard curve was built to estimate the concentration of the metabolites in the sample, by reading the absorbance of known sodium nitrite ($NaNO_3$) amounts (final concentrations between 1.56 µM and 100 µM). Absorbance was measured at 550 nm using a microplate reader (Anthos 2010, Austria). Triplicates for sample of three independent experiments were performed.

3.2.2.12. **Statistical analysis**

Significant differences were determined using the non-parametric Wilcoxon test for two paired samples (GraphPad Prism 6.0, GraphPad Software, Inc, USA). A significance level of 5% ($p < 0.05$) was used to evaluate statistical significance. Results from three independent experiments and samples in triplicate are represented by graph bars (as mean and standard error).

3.2.3. Results

3.2.3.1. Macrophages efflux system is inhibited by ion-channel blockers and 6-gingerol

Macrophages are the definitive host cell for *Leishmania* parasites. MØ efflux pumps can interfere with drug pharmacokinetics at the intracellular level or even with the normal function of the cells.

To confirm the ability of the EIs and 6G to interfere, on a real-time basis, with the efflux activity of murine MØs (RAW 264.7), EB (a universal efflux substrate) efflux was evaluated by a fluorometric assay (chapter 2, 2.2.3) (106, 151).

The equilibrium between EB influx and efflux was achieved at an EB concentration of 0.5 $mg.ml^{-1}$. This equilibrium was modified by EIs at a concentration dependent manner (except for VP) as can be seen in Table 5.

Considering that all RFF values higher than zero is indicative of increasing intracellular accumulation of EB in consequence of the inhibition of cell pump efflux activity, it was shown that ion channel blockers and the phytochemical were able to promote EB accumulation. CPZ and TZ were responsible for the highest increase in EB accumulation followed by OUAB, VP and 6G (Table 5).

Table 5: Accumulation of ethidium bromide (EB) by RAW MØs exposed to efflux inhibitors. MØs treated with different concentrations of verapamil, thioridazine, chlorpromazine, ouabain and the phytochemical 6-gingerol were evaluated by real-time fluorometry and the relative final fluorescence (RFF) was determined for each compound. Bold values indicate enhanced accumulation of EB in the presence of efflux inhibitors.

		EI (μM)	RF ± SD	RFF
Compounds (EPIs)	**Verapamil**	**200**	9.4 ± 1.0	**0.4**
		100	7.1 ± 0.6	0.1
		50	14.1 ± 0.9	**1.1**
		25	6.9 ± 1.0	0.0
	Thioridazine	**40**	18.3 ± 0.3	**1.7**
		20	9.6 ± 0.8	**0.3**
		10	8.8 ± 0.8	**0.3**
		5	6.8 ± 0.5	0.0
	Chlorpromazine	**40**	17.8 ± 1.0	**1.6**
		20	16.5 ± 0.6	**1.4**
		10	6.3 ± 0.7	0.1
		5	6.8 ± 0.7	0.1
	Ouabain	**0.2**	16.1 ± 0.7	**1.4**
		0.1	7.2 ± 0.6	0.1
		0.05	8.2 ± 1.0	0.2
		0.025	8.3 ± 0.9	0.2
Phytochemical	**6-gingerol**	**240**	12.8 ± 0.4	**0.9**
		120	8.6 ± 0.4	**0.3**
		60	8.4 ± 0.7	0.2
		30	7.0 ± 1.0	0.0
Base line values	**cells**	**-**	6.74±0.44	-

EI: efflux inhibitor; EPI: efflux pumps inhibitors; EB: ethidium bromide

3.2.3.2. Cytotoxicity of efflux inhibitors and 6-gingerol on macrophages

EPIs cytotoxicity on RAW 264.7 MØs was evaluated 48 h after treatment by using the MTT colorimetric assay and the cytotoxic values CC10 and CC50 (non-toxic concentrations for at least 50% of the MØ population) were estimated (Table 6). The inhibitors TZ and CPZ were the ones that have shown higher toxicity, followed by VP, OUAB and 6G.

Table 6: Cytotoxic concentrations (CC) of compounds against non-treated RAW 264.7 MØs.

	Cytotoxic concentrations (µM)	
Compound	**CC10**	**CC50**
Verapamil	11.0	99.2
Thioridazine	1.0	8.8
Chlorpromazine	1.5	13.8
Ouabain	>16	> 0.154
6-gingerol	29.9	268.0

Taken into account the cytotoxicity of these compounds over MØs non-exposed to parasites, none of them have the potential to be used as an inhibitor of efflux pumps in prolonged assays at concentrations that are non-toxic to cells. Thus, in the following assays, inhibitors were used at non-toxic concentrations for at least 90% of the MØ population (CC10) that guaranties the survival of at least 90 % of the MØ population.

3.2.3.3. *Leishmania* parasites upregulate the expression of ABCB1 efflux pumps in mouse macrophages

The percentage of MØs infected with *L. infantum* parasites was determined by morphological evaluation through OM (Fig. 15C).

The observation of MØs exposed to *L. infantum* promastigotes under OM revealed that in the majority of infected cells the parasite was found in the amastigote-like form (Fig. 15C). Taken into account all the assays made, MØ infection rates ranged between 10% and 45%.

After evaluating the efflux pump's activity in MØs, using specific ion-channel inhibitors, which included verapamil, a known inhibitor of ABCB1, and in order to investigate if ABCB1 membrane transporter plays a role during MØ infection, ABCB1 proteins were detected by immunofluorescence. The expression of ABCB1 pumps in MØs exposed to *L. infantum* parasites was confirmed (Fig. 15B). Although using this methodology, it was not possible to detect ABCB1 pumps in non-infected MØs (Fig. 15A). These results suggest that parasites induce the upregulation of ABCB1 pumps in mouse MØs.

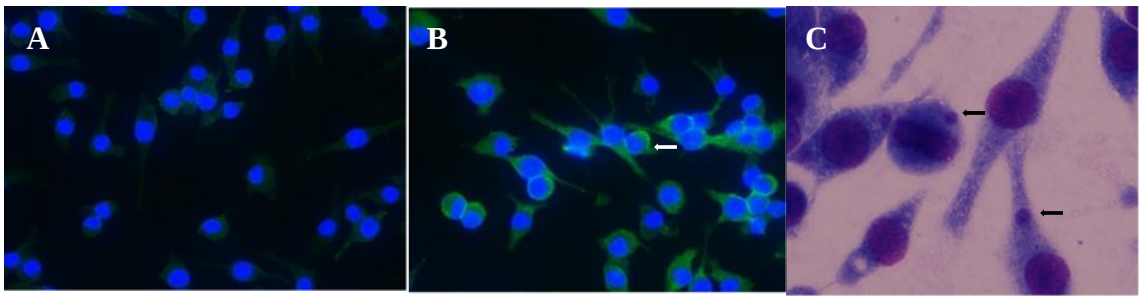

Figure 15: ABCB1 pumps in *L. infantum* – infected MØs. Cells exposed to *L. infantum* promastigotes for 5 h were stained with Giemsa and ABCB1 surface pumps were marked by C219 monoclonal antibody (B-green) and DNA nuclear staining by DAPI (blue). Cells were observed by optical (C) and fluorescence microscopy (A and B) and images were acquired. In parallel, resting MØ were also observed by fluorescence microscopy (A). Intracellular amastigote-like (arrows) forms can be observed inside macrophages (× 1000 magnification).

3.2.3.4. Immunomodulatory effect of ion channel blockers and 6-gingerol

EIs and 6G were evaluated for their immunomodulatory effects on MØ microbicide functions, by detecting intracellular ROS and by measuring the release of nitric oxide.

- **Verapamil consistently induces ROS production**

Non-fluorescent DHR dye and LysoTracker Red was used with the aim of investigating the intracellular generation of reactive oxygen species (ROS) in MØs treated with TZ, CPZ VP, OUAB, and 6G at non-toxic concentrations (CC10) for 24 h.

DHR passively diffuse across cell membranes and is oxidized by the presence of ROS and peroxidases into a green fluorescent compound (Rhodamine 123. Lysotracker red was used to stain endocytic acidic compartments (lysosomes).

Resting-MØs (non-treated negative control) and *L. infantum*-exposed MØs showed no fluorescence (-), pointing towards a blunted ROS production (Table 7, Fig. 16) while MØs plus H_2O_2 (DHR positive control) emitted a high level of fluorescence (+++). TZ- and CPZ-treated MØs (+), LPS-stimulated MØs, CPZ- and OUAB-treated MØs stimulated by LPS and TZ-treated *L. infantum*-exposed MØs showed a weak fluorescence (+), indicating ROS generation. However, resting-MØs, LPS-stimulated MØs and *L. infantum*-exposed MØs emitted middle levels of fluorescence when treated with VP (++). On the other hand, cells treated with 6G did not emit fluorescence (-). These results indicate that VP is a ROS inductor and 6G, on the contrary, avoid ROS production.

To investigate in detail whether VP (DHR middle positive) and 6G (DHR negative) interfere with the pH of MØs endocytic compartments, treated-MØs were stained with DHR and LTR and observed by fluorescence microscopy.

MØs plus H_2O_2 DHR stained (positive control) showed, a bright-green punctuated pattern, resting-MØs (negative control) presented no fluorescence, and LPS-stimulated MØs exhibited a low fluorescent pattern (Fig. 16A). MØs treated with VP at CC10 concentration (10 µM) and at a higher concentration (20 µM) stained with DHR evidenced a similar middle fluorescence and 6G-treated MØs did not emit fluorescence.

Table 7: Effect of compounds and phytochemical in ROS production by mouse MØs. After VP, TZ, CPZ, OUAB and 6G treatment of resting-MØs, *L. infantum*-exposed MØs and LPS-stimulated MØs were stained with DHR and observed under a fluorescence microscope. Fluorescence emission was rating using a four-point grading scale (- to +++). In parallel, fluorescence emission of non-treated MØs (MØ), LPS-stimulated MØs (MØ + LPS) and parasite-exposed MØs (MØ + *L. infantum*), and of MØs plus H_2O_2 were also rated.

		MØ	MØ + LPS	MØ + *L. infantum*
	Non-treated	-	+	-
	H_2O_2	+++	ND	ND
Compounds	**VP**	++	++	++
	TZ	+	-	+
	CPZ	+	+	-
	OUAB	-	+	-
Phytochemical	**6G**	-	-	-

ND-Not determined

VP: verapamil; TZ: thioridazine; CPZ: chorpromazine; OUAB: ouabain; 6G: 6-gingerol; LPS: lipopolysaccharide.

Cells plus H_2O_2 stained with DHR (green) and LysoTracker Red showed a predominant green fluorescence rarely punctuated by red fluorescence. On the contrary, LPS-stimulated MØs emitted red fluorescence interrupted by a few green fluorescence dots. Overlay of red and green fluorescence was highly observed in MØs treated with a high concentration of VP (20 μM) and also in MØs treated with VP at CC10 (10 μM) concentration, although at lower extent. Resting-MØs and 6G-treated MØs presented a faint red fluorescence (Fig. 16). These results indicated that VP induces MØs to produce ROS that mainly localizes in the acidic endocytic compartments in a dose-dependent manner. On the other hand, 6G does not seem to present a notable direct effect on cell activity.

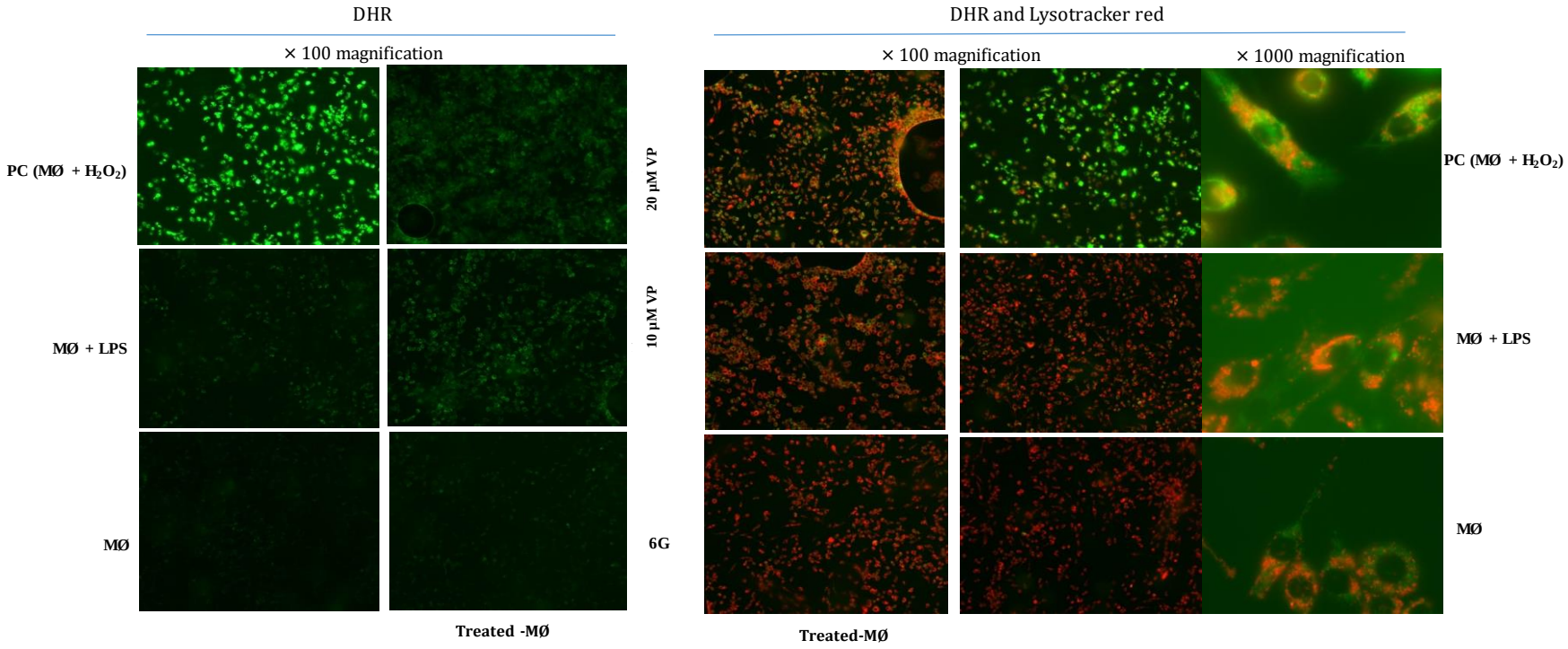

Figure 16: Effect of verapamil (VP) and 6-gingerol (6G) in ROS production and in the acidification of MØ endocytic compartments. Resting-MØs, LPS-stimulated MØs and MØs treated for 24 h with 6G at CC10 concentration and with VP at two concentrations (10 µM and 20 µM) were stained with LysoTracker® Red DND-99 (LTR) and dihydrorhodamine 123 (DHR). MØs plus H_2O_2 (MØ + H_2O_2) were used as a ROS positive control. Cells were observed by fluorescence microscopy and images of DHR (green, ×100 magnification) and DHR-LTR overlay (green and red, ×100 and ×1000 magnification) were acquired. PC: Positive control (MØ+H_2O_2); ROS: Reactive oxygen species; LPS: Lipopolysaccharide; MØ: Macrophage.

- **EIs promote minimal oxidative stress in *L. infantum* exposed macrophages**

Nitric oxide (NO) is produced by immune activated MØs and is recognized as a potent leishmanicidal agent. In this study, we evaluated the effect of EIs and 6G in NO production by MØs by a colorimetric assay.

The ability of EIs and 6G to modulate NO production was evaluated in MØs exposed to *Leishmania* parasites, in LPS-stimulated MØs (positive control) and in resting-MØs (negative control). As expected, LPS induced NO production, and the treatment with the compounds or with the phytochemical at CC10 concentration did not seem to interfere with cell activity. TZ and OUAB induce MØs to release NO, although not significantly different from resting-MØs. VP induces parasite-exposed MØs to release NO although at low levels and CPZ induced a significantly higher production of NO (Fig. 17). No trace of NO production was detected in MØs treated with 6G, indicating that this phytochemical does not interfere with oxidative burst pathway.

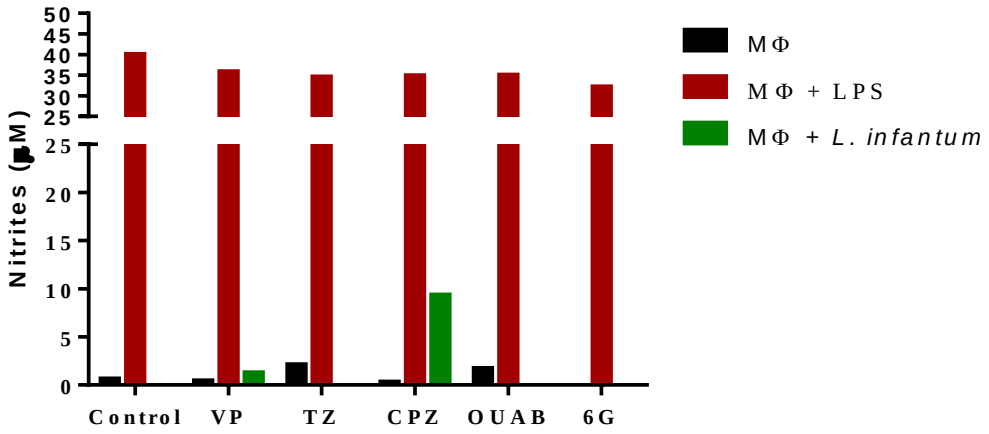

Figure 17: Effect of compounds and phytochemical on NO production by MØs. Supernatant of resting-MØs (MØs), LPS-stimulated MØs (MØs + LPS) and, *L. infantum*- exposed MØs (MØs + *L. infantum*) treated for 24 h with VP, TZ, CPZ, OUAB, and 6G (CC10) were used for the indirect evaluation of NO production. In parallel, non-treated cells were used as control. Results of three independent experiments and triplicate samples are represented by mean and SEM. The non-parametric Wilcoxon test was used for statistical comparisons ($p < 0.05$). * represents statistical significance values when comparing non-treated cells (control) vs treated cells. VP: verapamil; TZ: thioridazine; CPZ: chorpromazine; OUAB: ouabain; 6G: 6-gingerol; LPS: Lipopolysaccharide.

3.2.3.5. Ion channel blockers enhances the acidification of endocytic vesicles

The fluorescent dyes AO and LTR were used to trace acidic vesicles in living MØs treated with VP, TZ, CP, OUAB and 6G for 4 h and 24 h.

However, VP-, TZ-, CPZ- and OUAB-treated MØs also showed cytoplasm dots emitting brighter green fluorescence, pointing towards the presence of vesicles with higher pH (Table 8). After 24 h of treatment, higher green fluorescence (monomeric AO) intensity was observed in all cases, even in non-treated cells. VP- and TZ-treated cells showed larger fluorescent dots and 6G treated cells showed bright dots. The red component of AO fluorescence was undetectable (-) in resting cells.

LPS-stimulated MØs did not present AO red fluorescence except when treated with VP for 4 h. In this case, cells emitted low fluorescence (+). When treated with VP, TZ, CPZ and OUAB for 4 h, LPS-stimulated MØs emitted a faint green fluorescence (+). Only VP treatment led to a bright green fluorescence (++) (Table 8), of a pH increase.

Table 8: Effect of ion channel blockers and of 6G in MØ intracellular pH. Resting MØs (MØ), LPS-stimulated MØs (MØs + LPS), *L. infantum*-exposed MØs (MØs + *L. infantum*) treated with VP, TZ, CPZ, OUAB and 6G for 4 h were stained with AO. Red and green fluorescence were observed by fluorescence microscopy and fluorescence intensity was rating using a five-point grading scale (- to +++). In parallel, fluorescence emission of non-treated MØs (Control) were also registered.

		MØ		MØ + LPS		Ø + *L. infantum*	
		Green	Red	Green	Red	Green	Red
Compounds	Non-treated	-	-	+	-	+	+
	VP	+	-	++	+	+	++
	TZ	+	-	+	-	+	+
	CPZ	+	-	+	-	+	++
	OUAB	+	-	+	-	+	+
Phytochemical	6G	-	-	-	-	+	-

VP: verapamil; TZ: thioridazine; CPZ: chorpromazine; OUAB: ouabain; 6G: 6-gingerol; LPS: lipopolysaccharide; MØ and Ø: macrophages

VP-, TZ-, CPZ- and OUAB-short treatment (4 h, Table 8) promoted the acidification of endocytic compartments of parasite-exposed MØs. This acidification was visualized by the presence of red endocytic vesicles (AO aggregated) (Fig. 18). In parasite-exposed

MØs treated with 6G, occasionally a red spot was seen. Larger acidic vesicles were observed in cells that were under a VP longer treatment (24 h). A faint green fluorescence was observed in the cytoplasm of non-treated parasite exposed MØs and also in parasite-exposed MØs after 4 h of treatment with VP, TZ, CPZ and OUAB, indicating a less acidic to neutral pH.

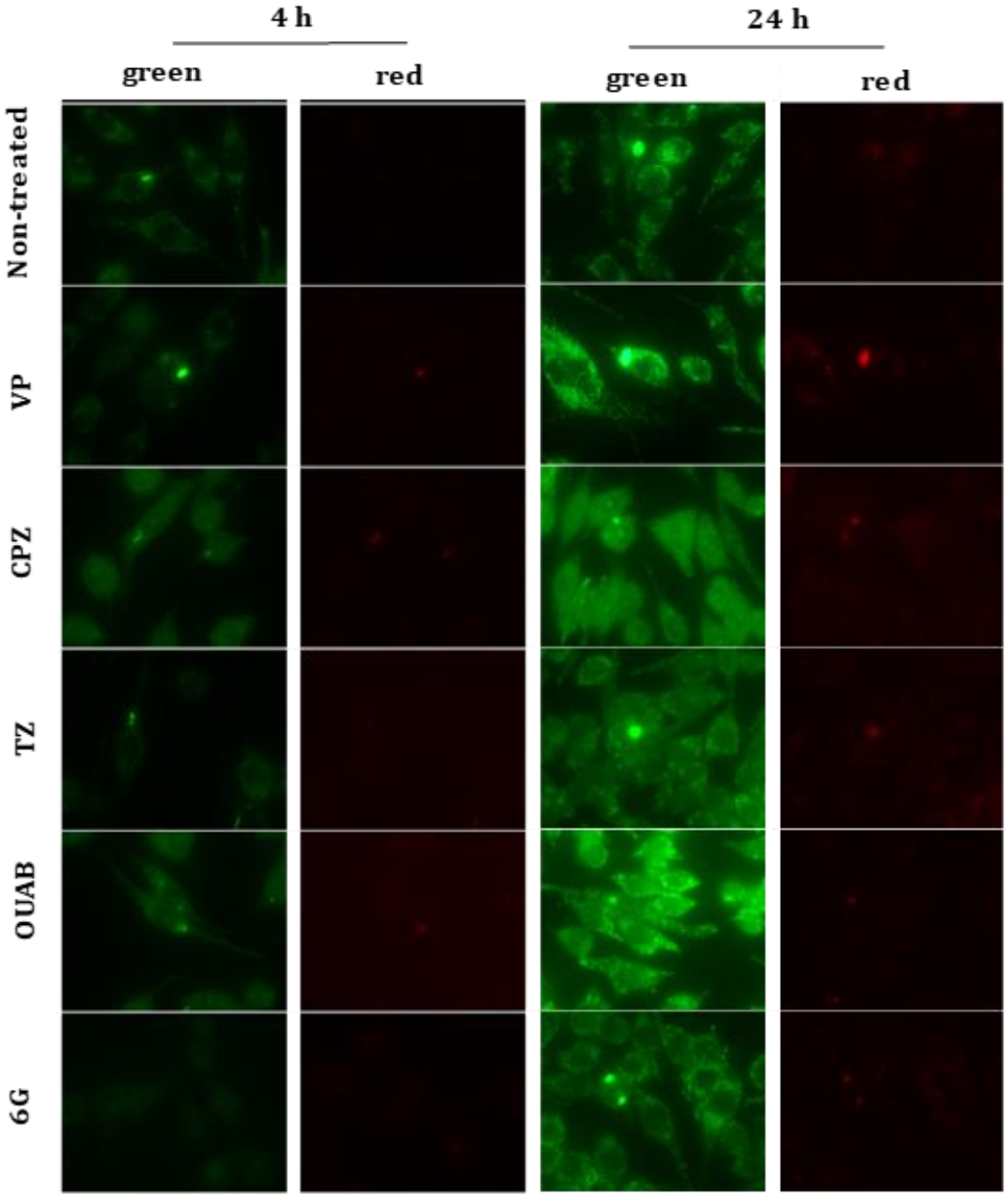

Figure 18: Intracellular acidification of *L. infantum*-exposed MØs treated with VP. Non-treated MØs and MØs treated with VP, TZ, CPZ, OUAB and 6G during 4 h and 24 h were stained with acridine orange. Cells were observed under a fluorescence microscope and images were acquired (× 1000 magnification). Emission of green fluorescence is indicative of intracellular acidification with a higher pH and red fluorescence are indicative of vesicles with higher intracellular acidification (low pH).

In order to evaluate whether lysosomes were involved in the acidification process, 24 h-treated MØs were stained with LysoTracker Red.

Resting-MØs (negative control) showed reduced fluorescence (-), pointing towards a blunted acidification. TZ-, OUAB-, and 6G-treated MØs exhibited low fluorescent levels (+), indicating the generation of some acidic vesicles although at low levels. However, CPZ-treated MØs emitted fluorescence similar to non-treated MØs (-), showing that this compound does not induce MØs acidification. On the other hand, VP treated MØs evidenced the emission of middle fluorescent levels, pointing towards cell acidification. LPS-stimulated MØs treated with VP and 6G also emitted middle fluorescent levels (++). Non-treated LPS-stimulated MØs and TZ-, CPZ-, and OUAB-treated LPS-stimulated MØs showed low fluorescence (+). These results suggest that during inflammation, VP and 6G increase cell acidification, which is represented by an increase of acidic vesicles (Table 9) *L. infantum*-exposed MØs treated with VP (++) emitted middle fluorescence whereas TZ, CPZ and 6G (+) showed low fluorescence. Non-treated parasite-exposed MØs exhibited very low fluorescence (±) and OUAB presented a reduced fluorescence emission (-) reflected by the low number of endocytic fluorescent vesicles (Table 9, Fig. 19). These results indicate that VP increases the acidification of parasite-exposed MØs.

Table 9: Verapamil (VP) induces macrophages (MØ) acidification. *L. infantum*-exposed MØs and LPS-stimulated MØs were treated with VP, TZ, CPZ, OUAB and 6G for 24 h and stained with LTR. Cells were observed under a fluorescence microscope and fluorescent emission was rating using a five-point grading scale (- and ± to +++). In parallel, fluorescent emission of non-treated MØs (MØ), LPS-stimulated MØs (MØ + LPS), and parasite-exposed MØs (MØ + *L. infantum*) were also rated.

		MØ	MØ + LPS	MØ + *L. infantum*
	Non-treated	-	+	±
Compounds	**VP**	++	++	++
	TZ	+	+	+
	CPZ	-	+	+
	OUAB	+	+	-
Phytochemical	**6G**	+	++	+

VP: verapamil; TZ: thioridazine; CPZ: chorpromazine; OUAB: ouabain; 6G: 6-gingerol; LPS: lipopolysaccharide.

When compared with non-treated MØs, the emission of red fluorescence increased in treated MØs, especially by VP (Fig. 20) and TZ (not shown), suggesting that treatment with EIs induced an increase of the number of acidic endosomal vesicles and also promoted vesicles enlargement in the parasite-exposed MØs (Fig. 19).

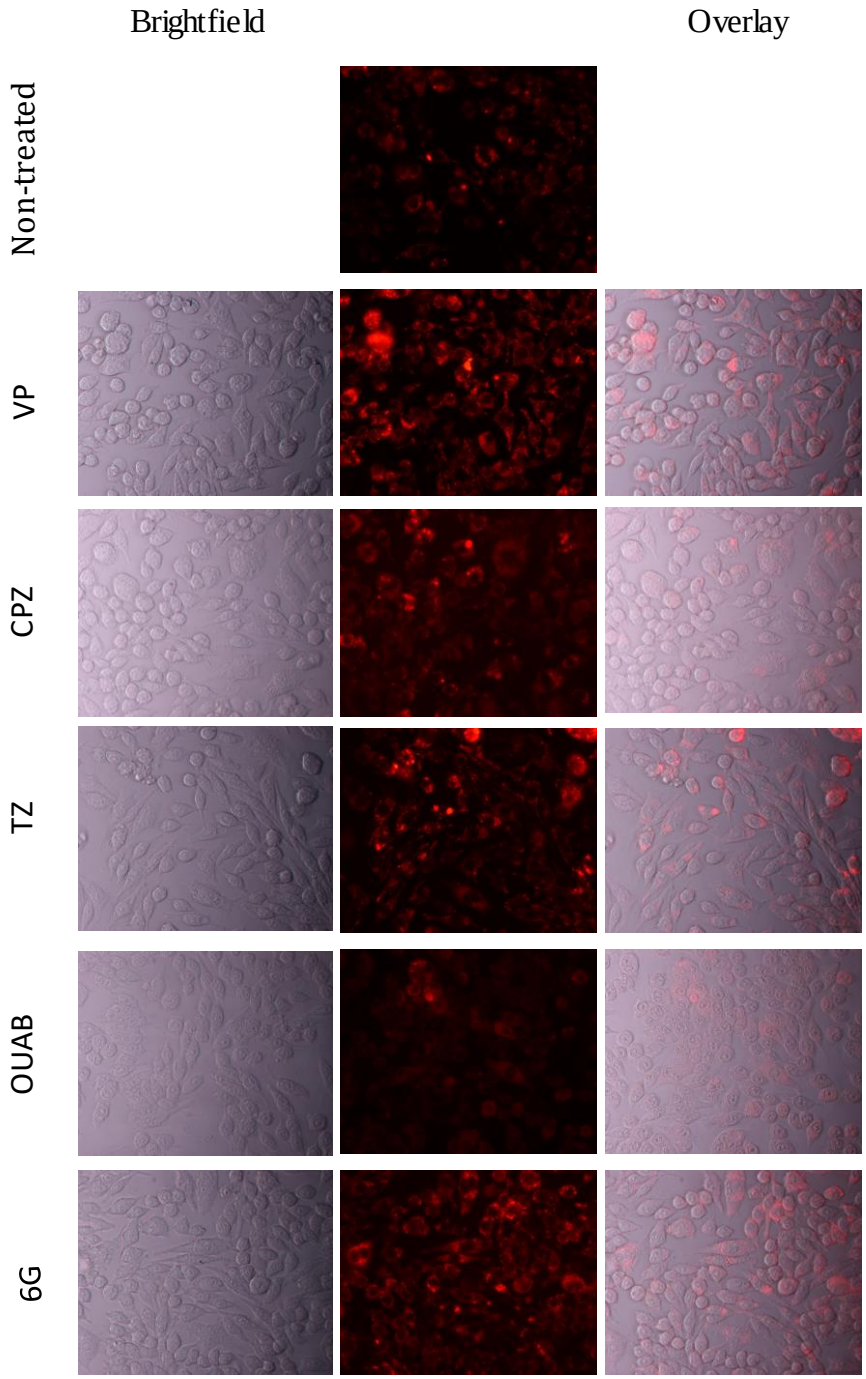

Figure 19: Intracellular acidification of *L. infantum*-exposed MØs treated with verapamil (VP) as a consequence of lysosomes. Parasite-exposed MØs were treated with VP, TZ, CPZ, OUAB and 6G during 24 h and stained with LysoTraker red. Cells were observed under a fluorescence microscope and images were acquired (× 400 magnification). In parallel, non-treated parasite-exposed MØs were also observed. Emission of red fluorescence indicates the presence of acidic endocytic compartments. MØ: macrophages; VP: verapamil; TZ: thioridazine; CPZ: chorpromazine; OUAB: ouabain; 6G: 6-gingerol; LPS: lipopolysaccharide.

In addition, it was possible to observe the co-localization of GFP-*Leishmania* with the increased intensity of LysoTracker Red signal in parasite-exposed MØs treated with VP (Fig. 20). However, in non-treated parasite-exposed MØs, the majority of the parasites were not co-localized with the acidic vesicles as well as in parasite-exposed MØs treated with other EIs.

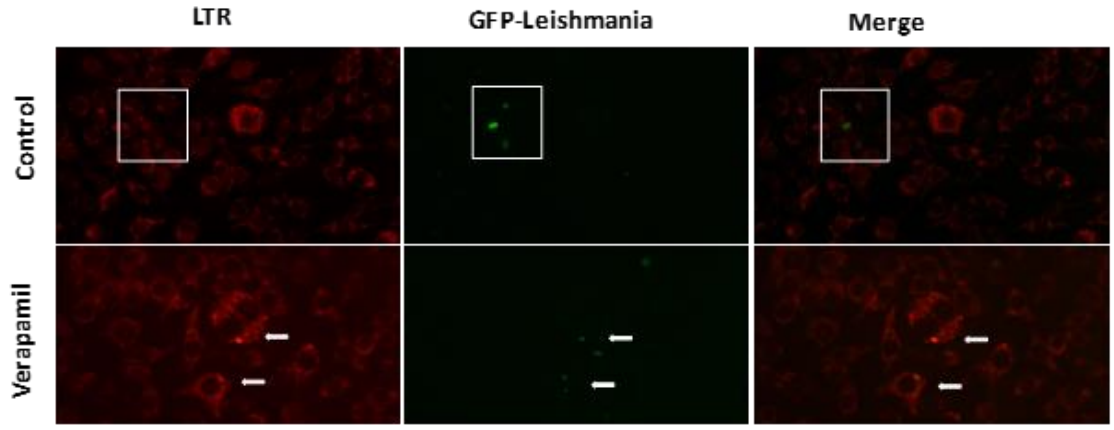

Figure 20: Co-localization of intracellular acidic compartments with GPF-*L. infantum*. MØs exposed to GFP-parasites were treated with VP during 24 h and stained with LysoTracker Red (LTR). Non-treated parasite-exposed MØs were also stained (Control). Cells were observed under a fluorescence microscope (× 400 magnification) and images were acquired. Green fluorescence – GFP-*L. infantum* amastigote; Square –non acidic area (LTR negative) plus GFP-*L.infantum*; arrows – Indicate the parasite co-localized with acidic organelles (LTR positive).

Calcein AM was used to confirm cell viability during the microscopy assays. Parasite-exposed MØs treated with EPIs for 24 h were labelled with calcein and stained with LTR. MØs and amastigote exhibited a green fluorescence, indicating that both cells and parasite were viable. Furthermore, red fluorescence pointing towards the presence of acidic vesicles that co-localize with the amastigote form (Fig. 21).

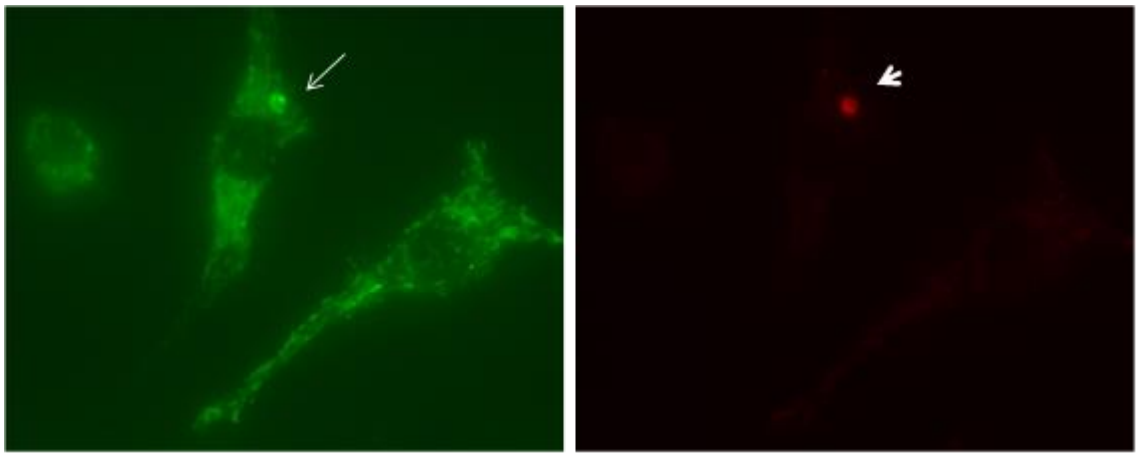

Figure 21: Image representative of viable amastigote co-localized with an acidic vesicle in a viable MØ. Parasite-exposed MØs treated with chlorpromazine (CPZ) for 24 h were labelled with calcein and stained with LysoTracker Red (LTR). Cells were evaluated by fluorescence microscopy and images were acquired (×1000 magnification). Calcein green fluorescence reflects the viability of cells and parasite (arrow) and LTR retention marks an acidic endocytic compartment (arrowhead) that co-localizes with the amastigote.

3.2.3.6. EIs and 6G reduce *L. infantum* survival and parasite growth

The effect of 6G and EIs at CC10 on the viability *L. infantum* amastigotes internalized by MØs was assessed by counting the surviving parasites after being released from MØs and differentiated in the motile promastigote forms (reversion) normalized to promastigotes from non-treated MØs with 5 h of infection (T0).

After 7 days of incubation at 24 ºC, the number of viable *Leishmania* promastigotes recovered from non-treated infected MØs and from infected MØ treated with VP, CPZ, TZ, OUAB and 6G for 24h were highly reduced (Fig. 22) although not significantly different from control, pointing towards a predominant leishmanicidal activity of MØs.

After 48 h of treatment, the number of viable parasites recovered from MØs exposed to 6G ($P = 0.0132$) and OUAB ($P = 0.0006$) was significantly lower when compared to non-treated MØs. However, the number of viable parasites recovered after 72 h of treatment with VP ($P = 0.0006$), TZ ($P = 0.0442$) and CPZ ($P = 0.0061$) were significantly reduced when compared to non-treated MØs (Fig. 22).

Taken together, these results suggest that OUAB and 6G had a maximal effect on intracellular parasites after 48 h treatment and that VP, TZ and CPZ need a longer treatment (72 h) to reduce parasite survival.

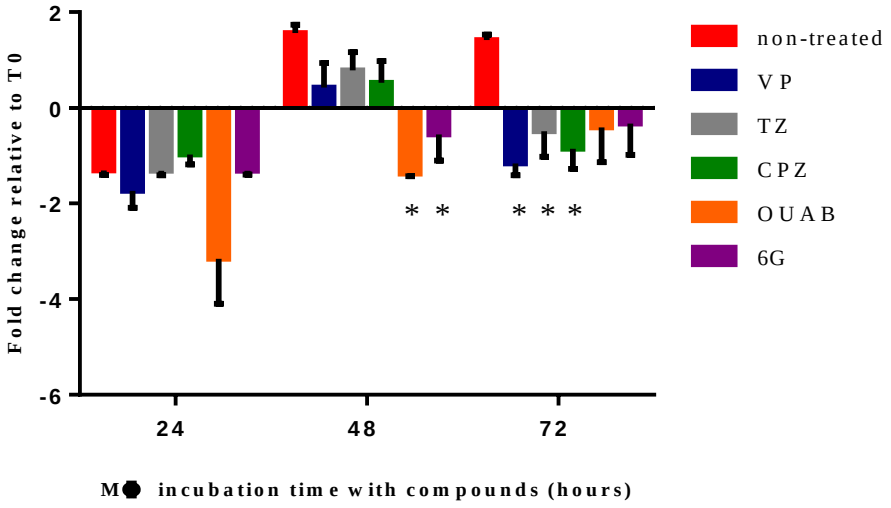

Figure 22: Survival of *L. infantum* parasites after treatment of infected MØs treated with VP, TZ, CPZ, OUAB and 6G. Infected MØs treated for 24 h, 48 h and 72 h were incubated in Schneider complete medium for 7 days at 24 ºC and motile promastigotes forms were quantified at optical microscopy. Data were normalized by the number of parasites recovered from non-treated MØs with 5 h of infection (T0). In parallel, non-treated infected MØs were used as positive controls. Results are represented by mean and SEM of three independent experiments and three replicates per sample. * ($P < 0.05$) indicates statistically significant differences when comparing treated vs non-treated cells. MØ: macrophages; VP: verapamil; TZ: thioridazine; CPZ: chlorpromazine; OUAB: ouabain; 6G: 6-gingerol.

The ability of *L. infantum* parasites that had survived to EIs treatment to replicate in the extracellular environment was subsequently evaluated (proliferation).

As expected, promastigotes recovered from non-treated MØs with 5 h of infection (T0) continued to grow (Fig. 23A). Promastigotes recovered from MØ treated with OUAB and 6G during 24 h (Fig. 23B), 48 h (Fig. 23C) and 72 h (Fig. 23D) showed a reduction in the number of parasites over time. At the 9th day of growth, promastigotes showed a significant reduction (P OUAB 24h <0.0001, p OUAB 48h = 0.0022, p OUAB 72h = 0.0029, P6G 24h = 0.0013, p 6G 48h = 0.0009, p 6G 72h = 0.008) when compared with non-treated infected MØ (control). Promastigotes recovered from MØ treated with TZ

and CPZ during 24 h showed a stable population (Fig. 23B). However, promastigotes that were under CPZ treatment showed a significant reduction of parasite load at 9th day of culture (P = 0.0416). After 48 h (P TZ $^{9th\ day}$ = 0.0039), P CPZ $^{9th\ day}$ = 0.0110) (Fig. 23C) and 72 h (P TZ$^{9th\ day}$ = 0.0356, P CPZ $^{9th\ day}$ = 0.0115) of treatment a significant reduction in parasite replication (Fig. 23D) was observed. VP showed their effect on parasite growth after 24 h (P $^{9th\ day}$ = 0.0328) and 72 h (P $^{9th\ day}$ = 0.0453) of treatment, which was reflected by a continued decrease in parasite numbers (Fig. 23D).

Taken into account MØ leishmanicidal effect and the exhaustion of medium nutrients evidenced at 72 h by decreased promastigote population that were not under EIs pressure (non-treated infected MØs - control), these findings suggest that VP, TZ, CPZ, OUAB and 6G negatively interfere with parasite replication, significantly reducing the parasitemia in a permanent and non-transient way (Fig. 22)

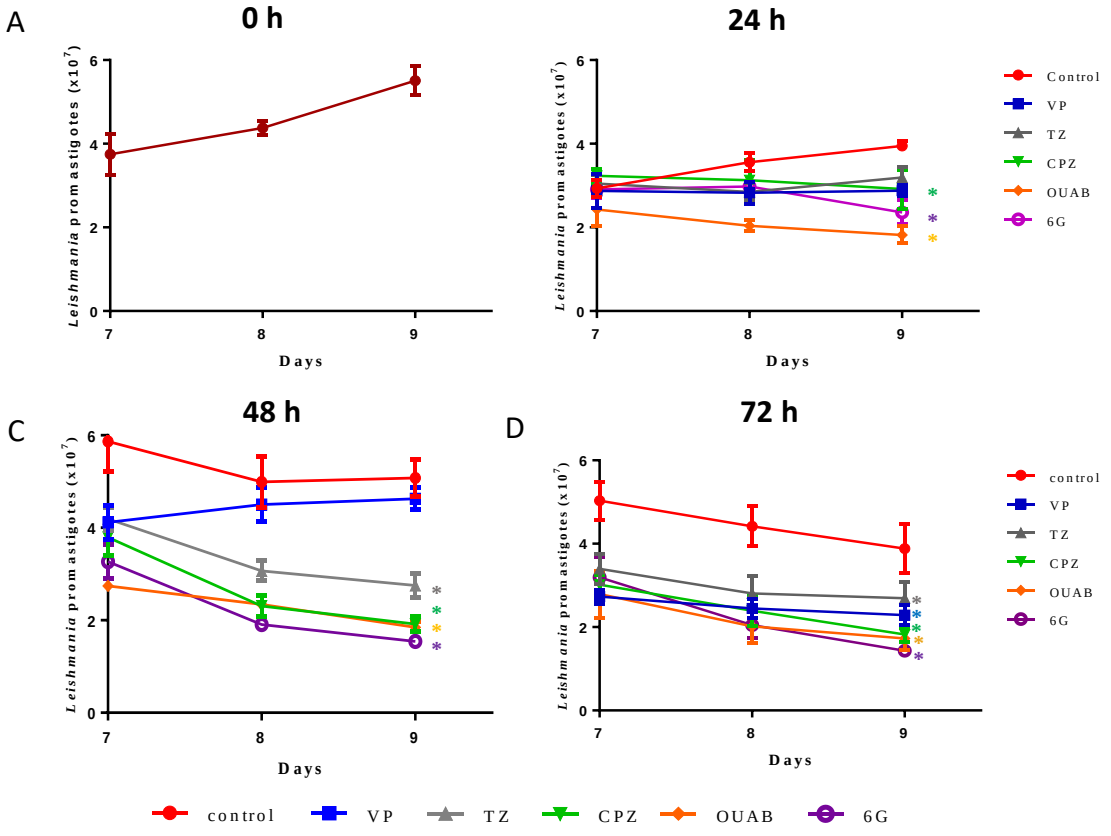

Figure 23: Growth of *L. infantum* parasites after treatment of infected MØs with VP, TZ, CPZ, OUAB and 6G. *L. infantum*-infected MØs treated for 24 h (B), 48 h (C) and 72 h (D) with VP, TZ, CPZ, OUAB and 6G were allowed to differentiate promastigote forms and parasite growth was followed during three days. In parallel, the growth of promastigotes recovered from non-treated MØs (control) with 5 h of infection (T0) (A) and non-treated MØs (control) was also evaluated at 24 h (B), 48 h (C) and 72 h (D). Results are represented by line charts indicating mean and SEM of three independent experiments and three replicates per sample. * ($P < 0.05$), indicates statistically significant differences when comparing treated vs non-treated cells (control). MØ: macrophages; VP: verapamil; TZ: thioridazine; CPZ: chorpromazine; OUAB: ouabain; 6G: 6-gingerol.

3.2.4. **Discussion and conclusions**

Macrophages represent an important first line of defense against disease, playing a crucial role in infection resolution. They have great functional diversity and, depending on the surrounding environment can adopt different phenotypes. Their important function as professional phagocytes can be exploited by certain parasites as an important route for parasite entry. Inside the host cell, these microorganisms can hide and multiply, being

protected from other elements of the host immune system. However, to survive, these intracellular pathogens must deploy numerous mechanisms able to counterattack the microbicide mechanisms of MØs, such as, inhibiting the phagosome-lysosome fusion, block phagosome acidification and avoid the production of reactive oxygen and nitrogen species.

After entry into the host cell *Leishmania* promastigotes differentiate within the parasitophorous vacuole into the amastigote life form and replicate. This differentiation is triggered by stress signals, including a rapid increase in temperature, ROS and an acidic environment. Amastigotes harbor a broad spectrum of protective mechanisms against host defenses, making of phagolysosome a perfect environment for parasite replication. *Leishmania* parasites are one of the few intracellular pathogens that can live and replicate in the harsh environment of a mature phagolysosome.

The ability of *Leishmania* parasites to manipulate the host cell machinery, has already been described and in this study, we demonstrated that intracellular *L. infantum* parasites can promote upregulation of ABCB1 transporters of MØs. These findings are in agreement with Basu and collaborators (146), which demonstrated that *L. donovani* infection or even soluble leishmanial antigens induce the over-expression of two important drug efflux pumps, MRP1 and ABCB1. Curiously, both these efflux pumps are associated with cancer MDR (146).

In the present study, we have demonstrated the existence of active efflux systems in non-infected MØs and all the EI compounds tested have shown relevant inhibitory effects on MØs efflux systems. However, the phytochemical 6G was the compound that presented less toxicity, followed by OUAB, VP, CPZ and TZ. These findings have shown for the first time the potential role of 6G as a low toxic modulator of efflux systems in eukaryotic cells.

Taking into account that activated MØs acquire a different phenotype, especially after infection, and that well-known inhibitors of ABCB1 efflux pumps, like VP can only be applied at concentrations above their inhibitory effect (CC10 is lower than the concentration necessary to reach an inhibitory effect), the present work focused on their efflux modulator ability to change the MØ intracellular environment and consequently interfering in parasite survival and parasite growth.

The ability of ion-channel blockers to drive MØs to inactivate intracellular microorganisms has already been described for the case of *M. tuberculosis* (152) by mechanisms still to be fully described. However, the inhibition of K^+ and Ca^{2+} transport from the parasitized phagosome to the cytoplasm of murine MØs by efflux inhibitors can promote the conditions that may reduce intracellular parasite survival, taking advantage of the dual-role of these compounds.

Since MØ oxidative stress is one of the most important microbicide weapons against *Leishmania* parasites, to survive these parasites usually modulate MØ activity, reducing oxidative stress. This work demonstrates that calcium-channel blockers, especially VP, were able to trigger infected and non-infected MØ enhancing ROS production. These findings are in agreement with what was previously reported by Meister et al. (153) that VP induces ROS production. 6G, as previously described by others (154), acted as an antioxidant, decreasing ROS production.

However, in the present study low concentrations of pump inhibitors were used and, under such conditions, none of the compounds were able to neutralize the production of NO by LPS-stimulated MØs. Once inside the cell, *Leishmania* parasites completely abolished both ROS and NO production by MØs. In this particular case, only CPZ was able to significantly stimulate NO production by infected MØs, indicating that CPZ contributes to the enhancement of MØ microbicidal function, but this mechanism is not the primordial mechanism of the EI enhanced killing activity noticed.

Phagosome maturation into a functional phagolysosome is accompanied by an acidification of the PV and this acidification is normally modulated by the parasite during differentiation of promastigotes into amastigotes. The findings obtained in the present study indicate that the evaluated compounds could effectively disturb the acidification process causing an imbalance in PVs environment, reducing parasite replication and survival. In fact, AO, a less sensitive dye for the detection of intracellular acidic vesicles, revealed what looks like an acidic PV in treated-infected MØs and allowed to visualize a higher density of acidic endocytic vesicles that possibly corresponds to lysosomes. As expected, resting-MØs have shown a certain amount of acidic vesicles or lysosomes.

Our study demonstrated that VP, TZ and 6G promote an increase of acidic intracellular compartments in MØs exposed to *L. infantum* that probably corresponds to the acidic PV

and other acidic endocytic vesicles. The co-localization of GFP-*Leishmania* with some of these vesicles in the majority of the infected cells indicate that acidic PV can include amastigote forms.

An increase of H^+ leads to hydrolases activation causing the killing of intracellular pathogens (140). However, to survive in the phagolysosome acidic environment *Leishmania* parasites actively transport protons by efflux pumps maintaining the H^+ gradient that guarantees nutrient uptake (143). In the early stage of infection, acidification of PVs is actively regulated during the *Leishmania* promastigote differentiation process towards amastigote forms. Contrary to the intracellular promastigotes, the amastigote form is fully adapted to the acidic pH found in the PVs.

Recent studies with naloxonazine (a μ1-opioid receptor (MOR) antagonist) have demonstrated a host dependent anti-leishmanial activity against intracellular amastigotes, which was associated with upregulation of V-ATPases and an increased volume of intracellular acidic vacuoles, thus delaying phagosome maturation (155), however the mechanisms involved still needs to be investigated. The increased volume of intracellular acidic vacuoles was also observed in this work after treatment of *Leishmania*-exposed MØs with VP, which could be correlated to the fusion of acidic vesicles, in particular with lysosomes, with PV. Targeting phagolysosome acidification as a strategy to fight intracellular pathogens has been demonstrated for *M. tuberculosis* after treatment with imatinib. Imatinib is an inhibitor of Abelson tyrosine kinase used for the treatment of chronic myeloid leukaemia, that impaired the growth of intracellular *M. tuberculosis* by triggering intracellular acidification in monocyte-derived MØs (155, 156). This seems to be the major mechanism of enhanced killing activity promoted by the EIs.

The impact of microbicide mechanisms induced by EIs in parasite survival and growth was examined. After phagocytosis, some intracellular promastigotes are probably killed by MØ leishmanicide mechanism. These findings suggest that parasites, in order to survive, require an additional time to adapt to PV harsh conditions. This observation was confirmed by evaluating these newly released promastigotes' ability to multiply. Only the promastigotes released from the control group were able to multiply after 2 days. It was not possible to demonstrate that a short treatment (24 h) with EIs inactivates parasites, although it was shown that these compounds negatively interfered with parasite

replication. After 48 h of treatment OUAB and 6G are able to impair parasite viability, but phenothiazines (TZ and CPZ) and VP (calcium antagonist) seems not to disturb parasite survival. Furthermore, amastigotes previous contact with TZ, CPZ OUAB and 6G makes extracellular parasite replication difficult. A longer treatment was needed (72 h) for VP, TZ and CPZ to impair parasite survival. In fact, after 72 h less than 50% of the amastigotes that survived were able to differentiate into promastigotes. Promastigotes released from the control group have shown a decrease of parasite replication likely driven by nutrient shortage. Therefore, it was not possible to describe the effect of EIs in parasite replication. However, none of the compounds was able to completely eliminate intracellular parasites.

Despite inhibiting cell efflux pumps, EIs also interfered with different MØ mechanism, affecting intracellular parasites. VP, TZ and CPZ probably induce MØ by increasing PV acidification. Whether this was a direct or indirect role over the parasites must be further clarified. OUAB, a Na^+/K^+ ATPase inhibitor, has probably affected the initial stages of infection by disturbing the K^+ homeostasis of the parasite in the PV, however unexpectedly, OUAB did not induce oxidative stress or a significant decrease of the endocytic vesicles pH, suggesting the existence of other mechanisms.

Of utmost importance, is the fact that 6G controlled parasite infection, inactivating parasites and impeding further parasite growth. However, the mechanism by which this phytochemical negatively interferes with parasite survival needs to be clarified. Its antioxidant capacity, together with its anti-inflammatory activities (157), may have played a decisive role in keeping even infected cells fit. These well-known properties of 6G in association with their capacity to promote an increase of endocytic acidic vesicles were probably the mechanisms responsible for the decrease of parasite survival after longer (48 h and 72 h) treatments.

This is the first time that the effect of ion-channel blockers and 6G on a cell parasitic infection model has been described. By targeting the cell directly, these efflux inhibitors interfere with the activity of *Leishmania*-infected MØ but also with parasite extracellular survival, by losing the capacity to proliferate. Stimulating MØ ability to destroy pathogens is a new concept for intracellular infection therapy. Ion efflux and influx modulation by known ion channel blockers, interferes with the intracellular ion

homeostasis from both MØ and parasite. In this work treatment resulted in a MØ intracellular pH decrease and consequently impaired parasite growth.

6G, one of the major bio-active compounds present in plants (ginger, grains of paradise) that are part of human diet is also reported to account for many of the pharmacological effects of the plant in part associated with their anti-oxidant and anti-inflammatory properties. The importance of ion-channel blockers as adjuvants of anti-*Leishmania* treatment and its contribution to the design of anti-leishmanial modulators, directing the search of new therapeutic options by exploring new drug targets should be taken in consideration. Synergy studies must be conducted in order to improve the therapeutic efficacy and reduce compounds toxicity.

3.3. **Biological model #3: Tumor cells**

The study of 6-gingerol (6G) as a putative modulator of ABCB1 efflux pumps was performed, initiated with the promising results obtained with the protozoa models was further explored using mouse lymphoma cells expressing human MDR1, with the methodologies described in chapter 2. Modulator properties of this natural compound were evaluated in view of the development of nontoxic modulators able to be applied in novel therapeutic approaches directed to overcome cancer multidrug resistance (MDR).

3.3.1. **Mouse lymphoma cell lines**

The cell-membrane P-glycoprotein (MDR1, ABCB1), belongs to the ATP-binding cassette (ABC) family of transporters and is an energy dependent efflux pump (EP) associated to drug resistance in eukaryotic cells, as already discussed.

In eukaryotic cells, MDR is related to the higher expression and increased activity of the ABCB1 efflux pumps that very often causes failure of cancer chemotherapeutic. *In vitro,*

modulators of ABCB1 can reverse this phenotype. Currently, available methods to evaluate the modulation activity of ABCB1 are unable to visualize and assess, on a real-time basis, the effectiveness of these compounds on the uptake and efflux of ABCB1 substrates. As such, predicting and testing ABCB1 modulation activity using living cells during drug development is important and necessary. Here, we evaluate the phytochemical 6G as a putative ABCB1 efflux pump inhibitor using MDR mouse T-cell lymphoma cell line transfected with the human gene that encodes the ABCB1 transporter (MDR1). The expression of human ABCB1 in this cell line is much higher than in human normal cells which makes it a good cell line model to examine the ABCB1-related drug resistance.

3.3.1.1. Material and Methods

- **Reagents**

6-gingerol (6G), a diarylheptanoid, obtained from the n-hexane extract of a commercial sample of seeds of *A. melegueta* (Kottas, Vienna, Austria) (89) that was dissolved in DMSO. Verapamil (VP) was purchased from Sigma-Aldrich, dissolved in water, 0.22 µm filter sterilized and stored in aliquots at -20 ºC. The 3-ethyl-2-[5-(3-ethyl-2(3H)-benzoxazolylidene)-1,3-pentadienyl]- iodide ($DiOC_2$) was obtained from Invitrogen.

- **Cell culture**

The cell lines used in the present study were the L5178v MDR transfected with pHa MDR1/A retroviral vector (MDR1) and parental L5178y mouse T-cell lymphoma (PAR). These cell lines were kindly provided by Professor Michael M. Gottesman (National Cancer Institute, Bethesda, MD, USA). The ABCB1-expressing cell lines were selected by culturing the infected cells with 60 $ng.ml^{-1}$ of colchicine (Sigma-Aldrich) to maintain the MDR phenotype. L5178y mouse T-cell lymphoma cells (parental) and the human ABCB1-gene transfected sub-line were cultured in McCoy's 5A medium (Sigma-Aldrich) supplemented with 10% heat-inactivated horse serum (Sigma-Aldrich), L-

glutamine (Sigma-Aldrich) and antibiotics (penicillin, streptomycin) (Sigma-Aldrich) at 37 ˚C and in an atmosphere with 5% CO_2.

- **Immunolocalization of ABCB1**

Cells were scraped and prepared by Cytospin (StatSpin2 Cytofuge, USA) centrifugation (55×g for 4 min) on glass slides, air dried and fixed with ice cold acetone for 10 min (149). Cover slips were blocked with 2% BSA (bovine serum albumin) in PBS and 0.05% Triton X-100 and incubated with mouse monoclonal anti human ABCB1 (Mdr-1 (D-11): sc-55510, Santa Cruz Biotechnology) for 3 h. Slides were washed 3 times in PBS and incubated for 1 h with FITC-conjugated goat Anti-Mouse IgG diluted (Sigma) diluted 1:200 in PBS. After three washes in PBS and a 3 min incubation with 1 $\mu g.ml^{-1}$ DAPI (fluorescent nuclear stain 4',6-diamidino-2-phenylindole dihydrochloride from Vector Laboratories, USA), followed by a final wash, slides were mounted in Fluorprep antifade reagent (Biomérieux Laboratories) and examined under a fluorescence microscope and imaged using a Nikon DS-Ri1 camera installed a Nikon eclipse 80i microscope using the NIS-Elements BR 3.3 software.

- **Cell viability assay**

Cell viability assays were done to determine the non-toxic concentrations of 6G and VP to be used in the efflux assays. A 96-well plate previously coated with D-lysine were seeded with 1×10^4 cells per well of PAR and MDR1 cells. The effects of increasing drug concentrations on cell growth were tested by MTT assay after 48 h of treatment, according to the protocol described in chapter 2 (2.2.2). In parallel cells with DMSO were used as a vehicle control. The level at which cytotoxicity no longer occurs was evaluated accordingly to the ISO 10993-5:2009 recommendations for medical devices where percentages of cell viability above 80% indicate that drugs can be considered as non-cytotoxicity.

Cell viability was then determined by measuring the optical density (OD) at 550 nm (ref. 630 nm) with a Multiscan EX ELISA reader (Thermo Labsystems, Cheshire, WA, USA). The relative cell viability (%) was expressed as a percentage relative to the untreated

control cells. Half inhibitory concentration (IC50) is defined as the inhibitory dose that reduces the growth of the compound-exposed cells by 50%.

- **Ethidium bromide accumulation assay**

EB accumulation assay was assessed by using the semi-automated fluorometric method (Rotor-gene 3000, Corbett Research) that monitors EB uptake and extrusion by cells on a real-time basis using the, according to general procedures from chapter 2, section 2.2.3.

The activity of the compound, namely the relative final fluorescence index (RFF), was calculated according to the formula described in chapter 2 (2.2.3).

- **$DiOC_2$ efflux analysis by fluorescence microcopy**

Cells in suspension were collected, counted and re-suspended in serum-free McCoy's 5A medium and distributed in 0.5 ml aliquots into Eppendorf centrifuge tubes at a concentration of 2×10^6 cells.ml^{-1}. Efflux modulators (VP 10 µM or 32 µg.ml^{-1} 6G) were added and the samples were incubated for 10 min at room temperature. In parallel, control cells were grown in the absence of efflux modulators. Then, $DiOC_2$ was added for a period of 2 h and cells were incubated in dye-free medium at 37 ºC for further 45 min, following the protocols previously described in chapter 2 (2.2.4). Cells were washed twice with ice-cold phosphate buffered saline (PBS) and resuspended in 100 µl cold PBS. Cells in suspension (10 µl) were deposited on glass slides and examined under a fluorescence microscope, using exciting wavelengths of 546 and 485 nm.

- **Rhodamine efflux analysis by flow cytometry**

Cells in suspension were collected, counted and re-suspended in serum-free McCoy's 5A medium and distributed in 0.5 ml aliquots into Eppendorf centrifuge tubes at a concentration of 2×10^6 cells.ml^{-1}. Efflux modulators (VP 10 µM or 32 µg.ml^{-1} 6G) were added and the samples were incubated for 10 min at room temperature. In parallel, control cells were grown in the absence of efflux modulators. Then PAR and MDR1-overexpressing lymphoma cells were loaded with rhodamine-123, and incubated at 37°C

in the presence or absence of VP (10 µM) and 6G (32 µg.ml^{-1}), washed, incubated in dye-free medium according to the protocol described in chapter 2 (2.2.5).

Cells were washed twice with ice-cold PBS, spin down, and resuspended in 500 µl ice-cold PBS and fluorescence retention was measured by flow cytometry using CytoFlex flow cytometer (Beckman Coulter) at an excitation wavelength of 488 nm BP 525/40 collection and emission recorded in FITC-A channel. Data analysis was performed using FlowJo v10 software (Tree Star, Inc., Ashland, OR).

- **Statistical Analysis**

Statistical analyses were conducted using the Student's t-test. The accepted level of significance was $p<0.05$. The analyses of the dose-response curve were done by using the Software GraphPad Prism 6 (GraphPad Software, Inc).

3.3.1.2. Results

- **MDR1 mouse lymphoma cells presents ABCB1 overexpression**

In this study, the expression of the human ABCB1 transporters was characterized in the transfected cells in order to validate MDR1 transporters in MDR1-T lymphoma cell line. The presence of the human P-glycoprotein in the membrane of MDR and in the corresponding parental cells (PAR) was demonstrated by labeling cells with a monoclonal antibody specific for human ABCB1. Mouse lymphoma cells transfected with human ABCB1 gene expressed higher levels of MDR1 than PAR cells which MDR1 was not detected (Fig. 24).

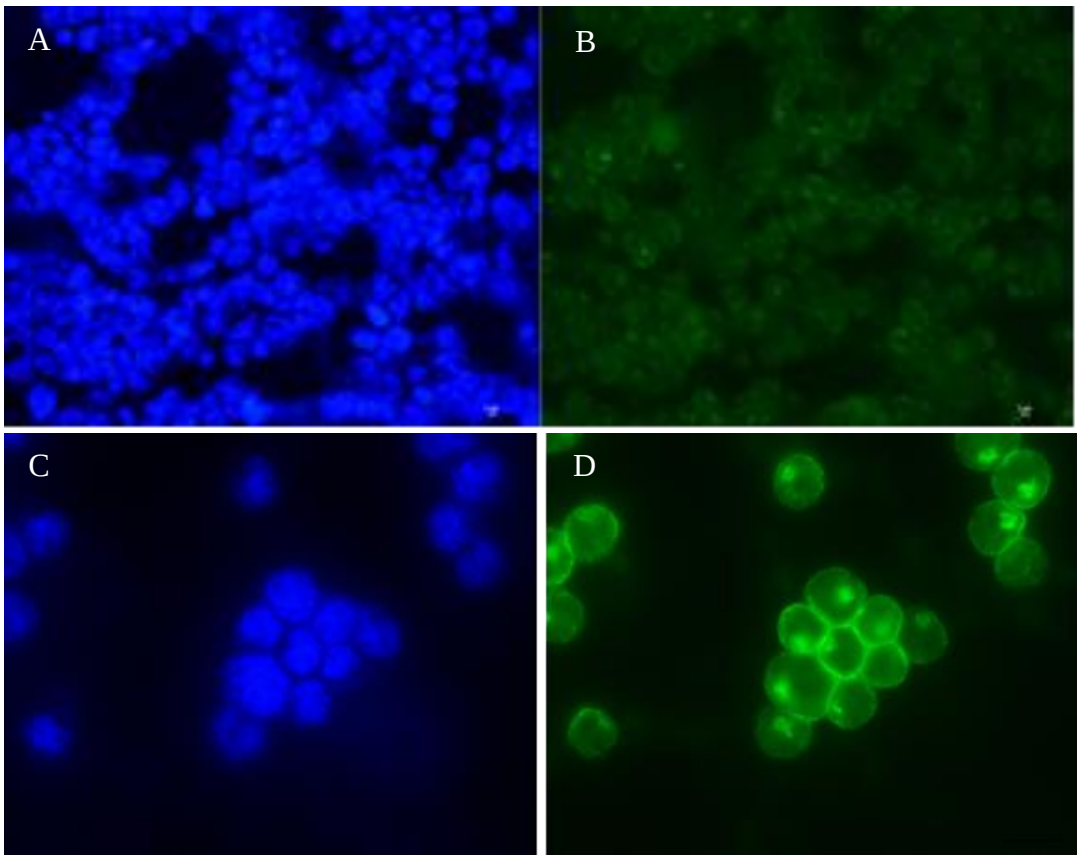

Figure 24. Human ABCB1 immunolocalization in mouse lymphoma cells. ABCB1 immunolocalization in L5178y mouse T-cell lymphoma cells (PAR cells, A and B) and L5178/MDR1 overexpressing human ABCB1 efflux pumps (MDR1 cells, C and D) were observed by fluorescence microscopy and images were acquired. Nuclear DNA staining with DAPI (blue), immunostaining with monoclonal antibody directed against human ABCB1 glycoprotein (green).

- **Viability assay of the diarylheptanoid 6-gingerol and verapamil**

The cytotoxic activity of 6G and VP was evaluated on PAR and MDR1 cells treated for 48 h with 6G and VP concentrations ranging from 4 $\mu g.ml^{-1}$ to 128 $\mu g.ml^{-1}$.

The half inhibitory concentration (IC50) of 6G in PAR and MDR1 cells was 64.74 (214.5 µM) and 72.37 $\mu g.ml^{-1}$ (245.3 µM) respectively. Curiously, 128 $\mu g.ml^{-1}$ (434 µM) of 6G has shown to be more cytotoxic on MDR1 cells than to PAR cells, indirectly indicating that MDR1 cells are highly dependent on ABCB1 overexpression and activity for survival

and is a preliminary indication of the inhibitory activity of 6G against the ABCB1 transporter (Fig. 25).

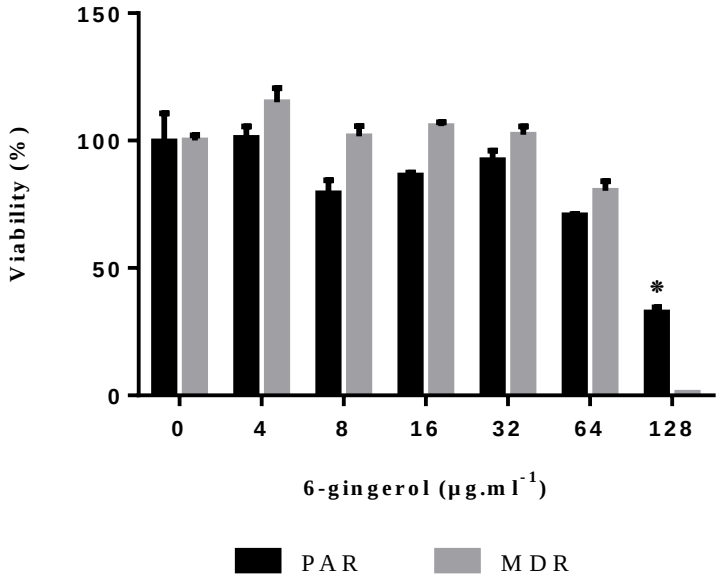

Figure 25: Cytotoxicity of 6G on PAR and MDR1 cell lines. Viability of cells treated for48 h with different 6G concentrations was evaluated using the MTT assay. OD was read at 570 nm in a ELISA plate reader. Cytotoxicity activity was expressed by cell viability (%). Results are represented by mean ± SEM of three independent experiments and three replicates per sample. *P < 0.05 indicate significant differences when comparing PAR-treated cells vs MDR-treated cells.

- **6-gingerol is an inhibitor of ABCB1**

In order to assure cell viability during the EB accumulation and efflux assays, the concentrations of 6G and VP applied in this study were equal or lower than the IC50.

The ability of 6G as a potential ABCB1 modulator was assessed on PAR and MDR cell lines by measuring the accumulation of EB, a broad range fluorescent substrate. The calcium channel blocker VP, a known modulator of ABCB1, was used as a positive control.

Previously, it was calculated the EB minimal concentration that assures the balance between the accumulation of EB that enters the cell by passive diffusion and the EB that is extruded from the cell by active efflux. The lowest EB concentration to be used in the semi-automated EB fluorometric assay was determined to be 1 µg.ml^{-1} for MDR1 cells and 0.5 µg.ml^{-1} for PAR cells.

RFF values higher than one were considered to be indicative of active ABCB1 modulators. Thus, 6G at 64 µg.ml^{-1} (half of the IC50) inhibited the efflux activity of human ABCB1 transporter (Table 10, Fig. 26B) in MDR1 cells. EB intracellular concentration increased in MDR1 cells treated with VP. As expected, in parental cells, the inhibition of ABCB1 efflux pumps by 6G was insignificant when compared to EB accumulation in non-treated cells (DMSO) (Fig. 26A) and similar to VP treated cells.

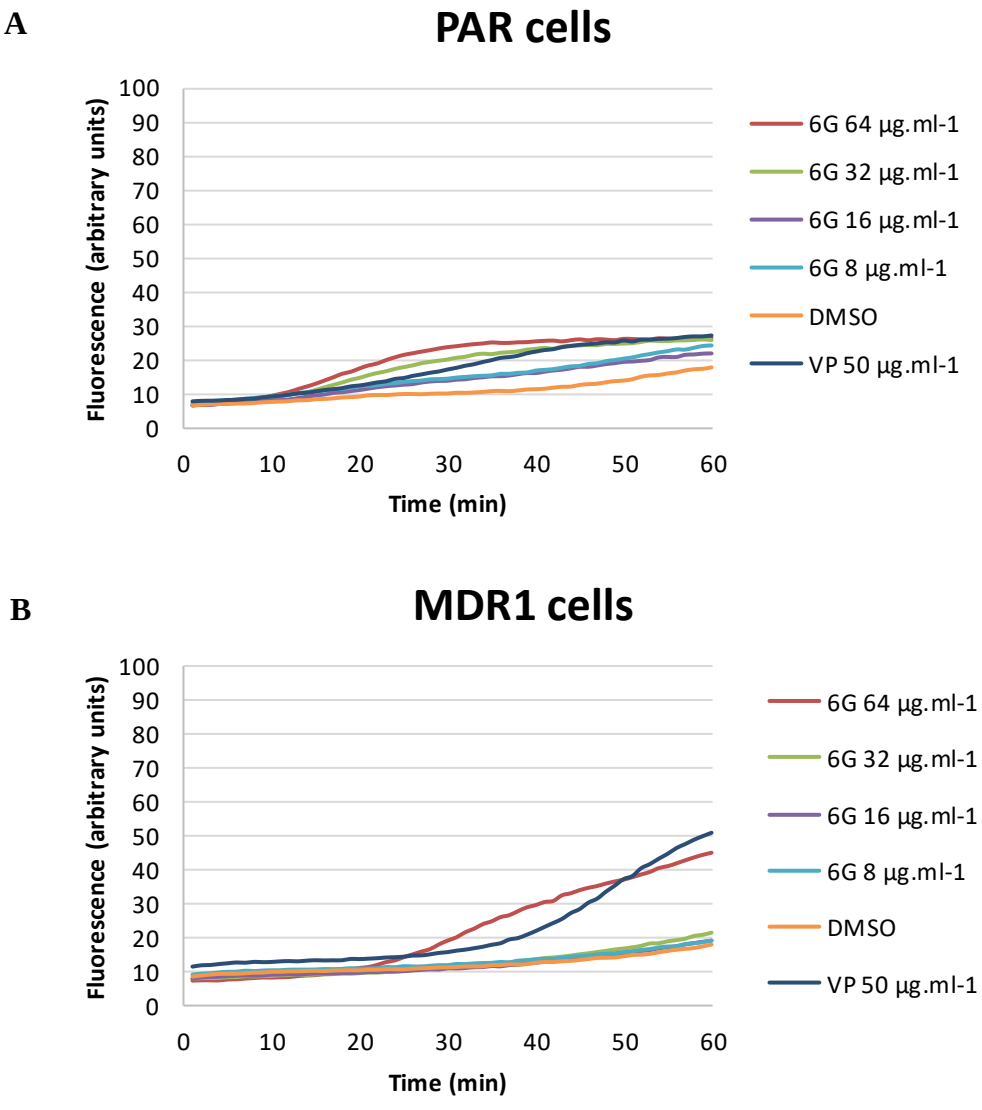

Figure 26: Effect of 6G on EB accumulation by PAR and MDR1 cell line. Intracellular retention of EB (1 µg.ml^{-1}) by PAR (A) and MDR1 (B) cells treated with growing concentrations of 6G were evaluated during 60 min. In parallel, cells treated with 0.5% DMSO (negative control) and 50 µM of VP were also analysed.

Table 10: Effect of 6G and VP on the intracellular accumulation of EB by mouse lymphoma cells transfected with human ABCB1 gene (MDR1 cells) and the respective parental cell line (PAR cells). Treated cells were evaluated by real-time fluorometric method and the relative final fluorescence (RFF) was estimated after 60 min. Bold values indicate enhanced accumulation of EB in the presence of efflux inhibitors.

			RFF	
		EI ($\mu g.ml^{-1}$)	PAR	MDR
Compounds (EPIs)	**Verapamil**	**50**	0.53	**1.85**
		64	0.51	**1.5**
		32	0.46	0.20
Phytochemical	**6-gingerol**	16	0.23	0.07
		8	0.38	0.06
		4	0.23	0

EI- Efflux inhibitor, EPIs – verapamil (VP) and 6-gingerol (6G).

To directly assess the efflux inhibitory activity of 6G and VP on these cell lines by observing drug intracellular retention, cells were loaded with $DiOC_2$ and Rh123 fluorescent probes. Cells were observed by fluorescence microscopy ($DiOC_2$) and quantified by flow cytometry (Rh123) following the protocols previously described in chapter 2.

In the resistant cell line (MDR1), where ABCB1 is overexpressed, emission of Rh123 and $DiOC_2$ fluorescence was lower compared to the PAR cell line (no efflux), ratifying the presence of highly active ABCB1 efflux pumps in the MDR1 cell line (Fig. 27 and Fig. 28). In PAR cells $DiOC_2$ fluorescence was not significantly affected by VP and 6G. Even so, a moderate increase of fluorescence emission of both dyes was noticed on PAR cells after blocking the activity of ABCB1 by VP.

Conversely, the MDR1 cells treated with 6G and VP also showed increased fluorescence when compared with non-treated cells, indicating that VP and 6G inhibited Rh123 efflux.

The fluorescence microcopy and flow cytometry efflux assays confirmed the results obtained by the semi-automated real-time EB assay, confirming the inhibitory properties of 6G.

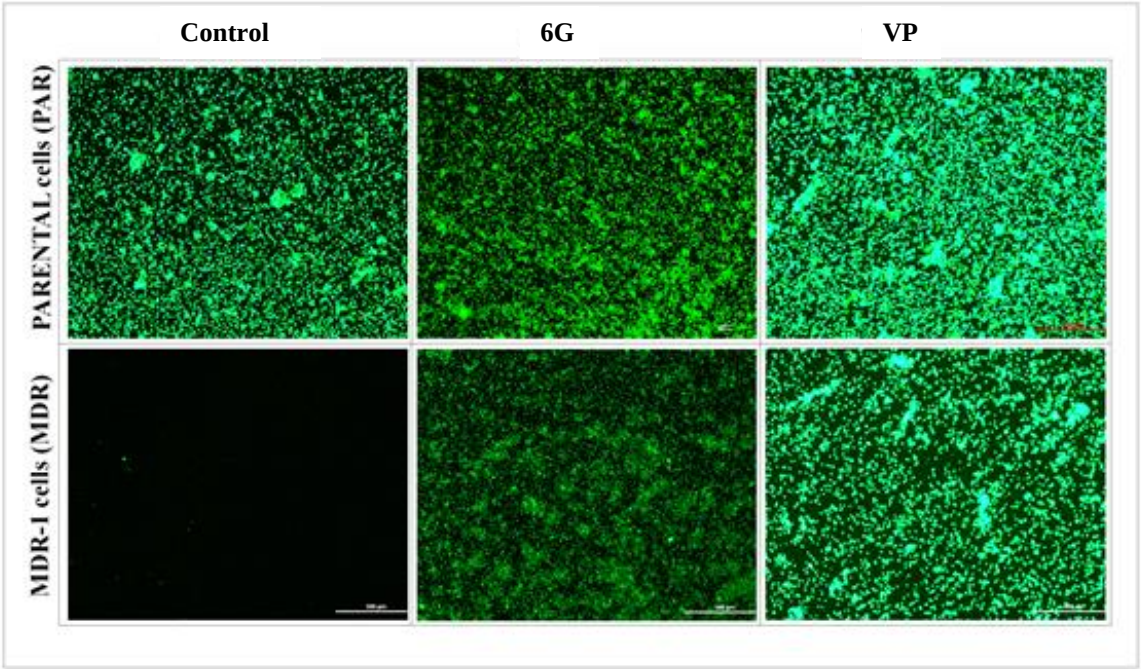

Figure 27: Intracellular accumulation of $DiOC_2$ in PAR and MDR1 cells treated with 6G and VP. Treated cells loaded with $DiOC_2$ (1 µg.ml^{-1}) were observed by fluorescent microscopy and images were acquired (100 × magnification). Non-treated cells (control) were also analysed in parallel.

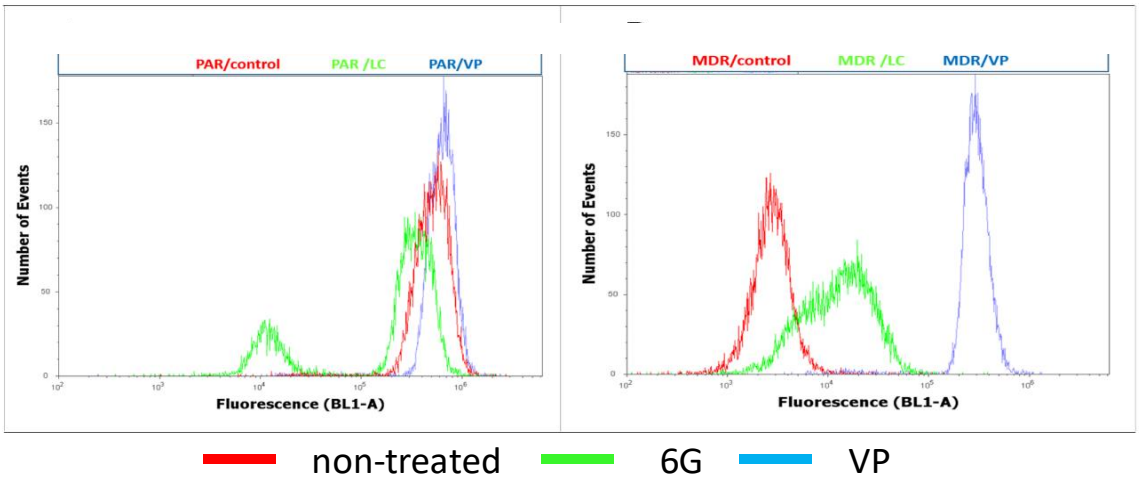

Figure 28: Flow cytometry analysis of Rh123 accumulation within PAR (A) and MDR-1 (B) cells. 6G- and VP-treated cells were loaded with Rh123 and analysed by flow cytometry. Results of cell fluorescent emission is expressed by histograms. Red line - non-treated cells (control); Green line – 6G treated cells and Blue line - VP-treated cells.

3.3.1.3. **Discussion and Conclusions**

In the present study, the potential role of the phytochemical 6G as a modulator of ABCB1 efflux pumps was assessed. For such, a cancer cell line that overexpresses ABCB1 transporter was used as a cell model. The inhibitory effect of 6G in drug efflux was demonstrated by showing intracellular accumulation of three different fluorescent probes using three different methodologies, including the evaluation of drug accumulation in real-time.

All the methodologies were able to detect the accumulation of fluorescent substrates after inhibition of ABCB1 efflux pumps with 6G at concentrations near its IC50. The evaluation of VP inhibitory activity by real-time EB accumulation assay using the semi-automated fluorometric method was shown to be less sensitive than the efflux assays conducted by flow cytometry and fluorescence microscopy since a higher concentration

of VP was needed to achieve EB accumulation, once compared with the efflux inhibitory ability of the compound 6G for these cancer cell lines.

The ABCB1 activity determined by the dye efflux assay was related with the degree of cell surface expression of ABCB1 measured by immunofluorescence.

The search for MDR modulators has been extended to natural products and their derivatives, such as the natural compound 6G, natural source compounds have become the most widely used of fourth-generation ABCB1 inhibitors because they are less toxic and more potent than the disappointing first- and second-generation MDR modulators.

Here in this study we have demonstrated that 6G is an inhibitor of ABCB1-EP and can be regarded as a promising candidate, in co-treatments, to overcome drug resistance by overexpression of ABCB1.

3.3.2. Breast cancer cell lines

3.3.2.1. Introduction

Breast cancer is the second most frequent cancer in the world and one of the most common cancers worldwide in women, being the fifth most common cause of death by cancer in women. About 5% of women have metastatic cancer when they are first diagnosed with breast cancer. Breast cancer treatment usually involves surgery, radiotherapy, hormone therapy (e.g. tamoxifen, anastrazole, letrozole and exemestane), chemotherapy (e.g. doxorubicin, cyclophosphamide, docetaxel, fluorouracil, epirubicin and methotrexate) and targeted therapy (e.g. trastuzumab or lapatinib). Frequently the three types of therapy are used together, or in a combination with different chemotherapy drugs, in order to achieve better outcomes. Chemotherapy is the standard of care in triple-negative breast cancer treatment (158), usually requiring a combination of two or three drugs. However, both efficacy and safety of chemotherapy is problematic because of toxicity, side effects and frequent emergence of resistance.

The membrane ABC transporter proteins, such as ABCB1, play a crucial role in the development of multidrug-resistant phenotype of cancer cells due to drug efflux of multiple unrelated drugs. Inhibition of extrusion (efflux) results in the build-up of cytoplasmic concentration of anti-cancer agents to levels able to inhibit cell replication and eventual cell death. The overexpression of ABCB1 is involved in the process of resistance to several chemotherapeutic agents such as epipodophyllotoxins derivatives (e.g. etoposide and teniposide), antibiotics (e.g. actinomycin D), vinca alkaloids (e.g. vinblastine and vincristine), tyrosine kinase inhibitors (e.g. imatinib and erlotinib), taxanes (e.g. paclitaxel and docetaxel) and anthracyclines (e.g. doxorubicin) (60, 159, 160).

However, because of the intrinsic efflux activity present in healthy tissues, clinical trials with ABCB1 modulators have shown disappointing results due to the serious side effects observed. Therefore, there is an urgent need for the development of new therapeutic strategies in order to reverse drug resistance (DR) in cancer.

Reactive oxygen species (ROS) have important roles in normal physiology and also in disease, particularly cancer. Malignant cells have elevated levels of reactive oxygen species (ROS), most of them generated by the mitochondria, which are counteracted by an increase of the antioxidant defense mechanism, making cancer cells more sensitive than normal cells to ROS accumulation (161, 162). Many chemotherapeutic agents like doxorubicin induces the generation of intracellular ROS, which play a critical role in cell cytotoxicity (163-165). However, doxorubicin-induced ROS generation is described as being involved in ABCB1 expression promoting the development of MDR phenotypes.

In recent years, natural compounds have been studied as alternative chemotherapy agents, due to their low toxicity and similar efficacy. Most of these agents have been extracted from plants.

Interestingly, the first natural compounds that were clinically used as anti-tumors were the vinca alkaloids vinblastine and vincristine, and the diterpene extracted from the bark of the Pacific yew, *Taxus brevifolia* known as paclitaxel and their analogs (eg. Docetaxel) (166, 167). Doxorubicin, an anthracycline antibiotic, is obtained from a bacterium of the genus *Streptomyces* (*S. peucetius*).

Other plants, such as Ginger (rhizome of *Zingiber officinale* Roscoe) and Grains of paradise (seeds of *Aframomum melegueta)* also have many bioactive compounds with pharmacological activities, including antitumor activity. However, there are few studies on the activity of these bioactive compounds activity in breast cancer chemoresistance. Moreover, 6-gingerol (6G) which is the most abundant bioactive compound in these plants, has been reported to have anti-cancerous activity, however by still unclear mechanisms. Preliminary reports have demonstrated the ability of 6G to inhibit the efflux of ABCB1 in neoplastic cells (168).

Therefore, the main objective of this chapter was to evaluate the effect of 6G in human breast cancer drug resistance and its potential role as a modulator of ABCB1 efflux pumps, in line and following the same rational of the previous chapters and sub-chapters.

3.3.2.2. Materials and Methods

- **Reagents**

All reagents for cell culture and verapamil were purchased from Sigma-Aldrich. Doxorubicin hydrochloride (DOX) was obtained by TEVA (Pharmachemie B.V. Netherlands), Paclitaxel (PAX) was obtained by Sigma Aldrich and dissolved in DMSO. $DiOC_2$ (2 $mg.ml^{-1}$ in DMSO) was obtained from Molecular ProbesTM. Verapamil (VP) stock solution was made by dissolving in water (10 mM), 0.22 µm filter sterilized and stored in aliquots at -20 ºC. Calcein-AM® (Molecular Probes) was dissolved in DMSO.

- **Cell lines**

Human breast adenocarcinoma cell lines MCF-7 (IC50 DOX=1.36 µM, SD: 0.39) and its doxorubicin-resistant subline KCR (IC50 DOX= 152.8 µM, SD: 8.8), were kindly provided by Professor Molnar, Szeged Foundation for Cancer Research, Hungary (169). MCF-7 and KCR were cultured in Minimal Essential Medium (MEM) supplemented with 10% (v/v) heat inactivated fetal bovine serum (FBS), 1.5 $g \times l^{-1}$ sodium bicarbonate, 1 mM sodium pyruvate, 0.1 mM nonessential aminoacids (Gibco), 1% penicillin-streptavidin

(100,000 units penicillin and 10 mg streptomycin per ml (Sigma-Aldrich). KCR cells were cultured in the presence of 1 μM of DOX every 3 passages in order to maintain the resistant phenotype. All cell lines were incubated at 37 ºC in a humidified 5% CO_2 chamber. Culture medium was replaced by fresh medium three times a week and subcultures were made by trypsinization (0.25 % trypsin-EDTA in media without serum, Gibco) when cell confluence reaches approximately 80%.

- **Immunolocalization**

MCF-7 and KCR cells were directly grown on coverslips. Then, coverslips were washed twice with PBS and left to dry before being fixed with ice-cold acetone for 10 minutes. Cells were blocked with 3% BSA in PBS for 1 h and incubated with anti-human ABCB1 (1:200) primary antibody (C219) for another hour at 37 ºC in a humid chamber followed by incubation with FITC-conjugated secondary antibody. Slides were washed twice with PBS, counter-stained with DAPI, following the protocol previously described by Armada A. et al. (149). Coverslips were mounted on the slides and imaged using a Nikon DS-Ri1 camera installed in Nikon eclipse 80i microscope using NIS-Elements BR 3.3 software. Fluorescence emissions were observed using specific filters set for DAPI (laser 405 nm/BP 420-480 nm) and FITC (ex 495 nm/BP 515 nm) dyes.

- **Cell viability assay**

Approximately 4000 cells were cultured in complete medium in 96-well plates. The cells were allowed to grow for 24 h and then exposed to different concentrations of 6G (dissolved in DMSO not exceeding 0.1% in concentrations of 0, 2.5, 5, 10, 20, 40, 80, 160, 320, 640 μM for 72 h) and VP (0, 1.25, 2.5, 5, 10, 20, 40, 80, 160, 320 μM). DMSO at 0.1 % (v/v) was added to the wells without chemical (control cultures for 6G).

The cytotoxic effects of 6G and VP was determined by MTT assay accordantly to the method described in chapter 2 (section 2.2.2). Cell viability is expressed as [A_{570} of treated wells/A_{570} of untreated wells × 100]. At least three independent experiments were performed.

IC50-values were obtained using a non-linear dose–response curve fitting analysis via GraphPad Prism v.6.0 software. Absolute IC50 is defined as the drug concentration required to reduce absorbance by 50% of that of the control (untreated cells).

- **Assessment of ROS formation**

The cell permeant fluorogenic dye dihydrorhodamine 123 (DHR) was used for the detection of reactive oxygen species (ROS) by fluorescence microscopy (150). After being uptake by cells, non-fluorescent DHR is oxidized by ROS (such as peroxide and peroxynitrite) and converted to the green fluorescent rhodamine 123 that accumulates in the mitochondria.

Cells were seeded on sterile glass coverslips placed into 12-well culture plates. Adherent cells were loaded with 3 µM DHR (Molecular Probes) in complete RPMI medium for 30 min at 37 ºC. After removing medium with DHR, cells were incubated in RPMI medium with VP and 6G for 4 h. At the end of the incubation period, slides were rinsed twice in PBS and then cells were examined by fluorescence microscopy with excitation wavelength of 485 nm and emission filter (green fluorescence) of 530/30 nm.

- **Checkerboard microplate method**

Checkboard method was applied to study the effects of drug interactions between resistance modifiers and cytotoxic compound on cancer cells. After treatment with 6G and VP, the viability of doxorubicin (200 nM) and paclitaxel (1000 nM) was evaluated in KCR cancer cell lines. Cells were seeded (100 µl of total volume containing 5×10^4 cells per well) and, plates were incubated for 72 h at 37 °C in a humidified atmosphere with 5% CO_2. Cell growth rate was determined by MTT staining and, the intensity of blue color was measured on a micro ELISA reader.

- **Calcein-AM uptake assay**

In order to determine *in vitro* ABCB1-inhibitory potential ($IC50_{IP}$), calcein acetoxymethlyl ester (Calcein-AM®, Molecular Probes) uptake assay was performed. In

this assay, ABCB1 transport activity is inversely proportional to the accumulation of the intracellular fluorescent calcein obtained by ester hydrolysis of the MDR1 non-fluorescent substrate Calcein-AM. Calcein-AM is a substrate of ABCB1 efflux pumps.

Cells were resuspended in RPMI 10% FBS at a concentration of 1×10^6 cells.ml^{-1} and viability was assessed using the trypan blue exclusion method. 96-well plates were seeded with 5×10^5 cells/well in 100 µl of RPMI 10% FBS. Then, medium was removed from each well and fresh medium with 0.25 µM Calcein AM was added to KCR cells and 0.125 µM to MCF-7 in RPMI in the presence and absence of serial dilutions of VP and 6G. After 10 minutes of incubation, cells were placed on ice and fluorescence was quantified using a TRIADTM 1065 microplate fluorometer (DYNEX Technologies, E.U.A.), at excitation and emission wavelengths of 490 and 515 nm, respectively. The effectiveness of inhibitors on ABCB1 efflux activity was expressed as the amount of drug that can give 50% inhibition of Calcein AM efflux (EC_{50}).

The relative inhibition of each compound on Calcein AM efflux was calculated by the following equation:

$$\%\ Calcein\ retention = \frac{calcein\ fluorescence\ of\ treated\ cells}{calcein\ fluorescence\ of\ untreated\ cells}\ X\ 100$$

Modulator concentrations required for cells to achieve 50% of the calcein-specific fluorescence was determined from the dose-response curves and defined as EC_{50}. EC_{50} values towards calcein-AM ABCB1 inhibition were determined for 6G by non-linear regression analysis of calcein accumulation, using GraphPad Prism 6 (GraphPad Software, Inc.).

- **$DiOC_2$ efflux assay**

Microscopy efflux assays were done according to the method described in chapter 2 (2.2.4). Cells were seeded on sterilized glass coverslips in 6-well culture plates at a density of 5×10^5 cells.ml^{-1} and allowed to grow overnight for 12 h at 37 ºC. Then, medium was removed and fresh medium with 6G (32 µg.ml^{-1}) or VP (10 µM) was added to duplicate wells and plate was incubated for 30 min. In parallel, fresh medium EI-free was also added. $DiOC_2$ (1 µg.ml^{-1}) was added and plates were incubated for 1 h at 37 ºC. Afterward, medium was removed and dye free medium was added in the presence or absence of VP for another 1 h. Slides were rinsed twice in PBS and then cells were examined by fluorescence microscopy with excitation wavelength of 485 nm and emission filter (green fluorescence) of 530/30 nm, accordantly to the protocol described in chapter 2 (2.2.4), (106).

- **ABCB1 efflux assay by cytometry**

Cells were distributed at a concentration of 2×10^6 cells.ml^{-1} and pre-incubated in either control medium or in the presence of 6G (108 and 217 µM) and 10 µM VP (positive control), for 30 min at 37 ºC. Then, $DiOC_2$ was added to a final concentration of 1 µg.ml^{-1} and incubation continued for 1 h at 37 ºC. Cells were centrifuged, resuspended in 500 µl of fresh dye free medium in the presence and absence of VP and incubated for another period of 1 h. The cells were then washed twice with ice cold PBS, spin down, and resuspended in 500 µl cold PBS. Fluorescence retention was measured by flow cytometry using CytoFlex flow cytometer (Beckman Coulter) equipped with a blue (488 nm) laser, and the signals were registered in the FL1/FITC (530/30 filter) channel, following the protocols previously described in chapter 2 (2.2.5), (106). Data analysis was performed using FlowJo v10 software (Tree Star, Inc., Ashland, OR).

- **Chemomodulatory effect of 6-gingerol and verapamil to DOX and PAX within KCR resistant cell line**

The chemomodulatory effect of 6G and VP was evaluated in human breast cancer DOX resistant KCR cell line treated with DOX and PAX. 96-well plates were seeded with KCR cells as described in chapter 2 (2.2.2). After 24 h of incubation, cells were treated with

200 nM of DOX or 1000 nM PAX plus 6G (40 and 80 µM) or VP for 72 h. Afterwards, cell viability were assessed by MTT assay as previously described (2.2.2).

- **Statistical Analysis**

Significant differences were determined using the non-parametric Wilcoxon test for two paired samples (GraphPad Prism v 6.0, GraphPad Software, Inc, USA). A significance level of 5% ($p < 0.05$) was used to evaluate statistical significance. Results from three independent experiments and samples evaluated in triplicate are represented by graph bars (as mean and standard error).

3.3.2.3. Results

- **Characterization of ABCB1 efflux pumps in KCR cells**

ABCB1 overexpression on KCR cells was confirmed by immunolocalization (Fig. 29). In MCF-7 sensitive cell line, as expected, the presence of ABCB1 was not detected.

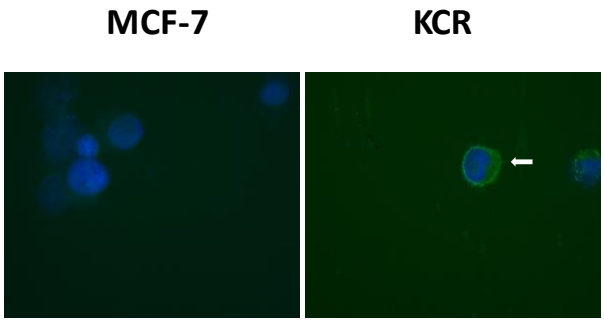

Figure 29: Imunolocalization of ABCB1 efflux pumps in human breast cancer MCF-7 and KCR cell lines. Cells incubated with C219 primary antibody followed by FITC-conjugated secondary antibody and counter-stained with DAPI were observed by fluorescence microscopy and pictures were acquired. DNA nuclear – blue; ABCB1 - green.

- **6-gingerol is more cytotoxic towards resistant cell lines**

The cytotoxic effect of 6G and VP on the viability of breast cancer cell lines KCR and MCF-7 were assessed by the MTT assay, in a dose-response manner. For comparison, the cytotoxicity of 6G and VP were also evaluated on PMA-stimulated human macrophage cell line (THP-1) as representative of cells of the immune system. The tested compounds showed diverse cytotoxicities against these cell lines, however THP-1 cells were relatively more resistant (Table 11).

Table 11: Cytotoxicity parameters (IC50) of 6-gingerol and verapamil against human breast cancer cell lines and human MØ cell line.

	Human cell lines	6-gingerol (µM)	verapamil (µM)
Breast cancer	**MCF-7**	≥ 320	≥ 160
	KCR	152	≥ 160
MØ	**THP-1**	473	134.3

6G and VP showed weak cytotoxicity to MCF-7 breast cancer cells. However, KCR cells were more sensitive to 6G.

Furthermore, 6G concentrations above 40 µM were more cytotoxic towards KCR cells than the corresponding MCF-7 sensitive cell line (Fig. 30A).

Although it was not possible to calculate the exact IC50 value for verapamil, MCF-7 cells treated with 160 µM VP showed cell viability below 70 %. (Fig. 30B). MCF-7 cells treated with VP concentrations ranging between 40-160 µM displayed a decrease in cell survival compared with the resistant KCR breast cancer cell line treated with the same concentrations of VP.

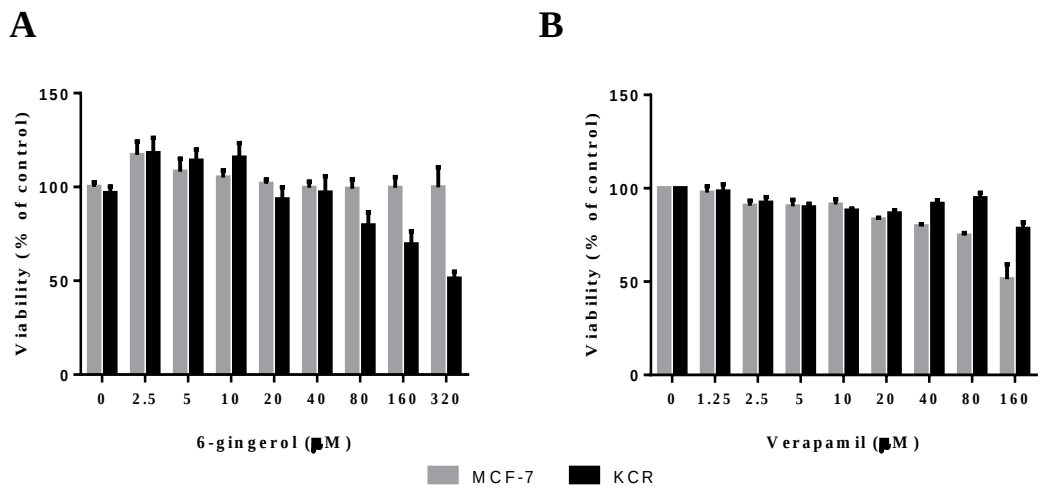

Figure 30: Viability of MCF-7 and KCR cells treated with 6-gingerol (A) and verapamil (B). Cells were treated with EIs for 72 h and viability determined by MTT assay. In parallel untreated cells (0 µm) were also evaluated. Results are expressed as a percentage of viable cells calculated over the control (non-treated cells). Data are shown as mean ± SEM from three independent experiments and three replicates per samples.

- **6G treatment induces ROS production**

Many natural chemotherapeutic agents induce intracellular ROS formation which plays a critical role in cell cytotoxicity. Therefore, the effect of 6G in ROS generation by MCF-7 and KCR cells was evaluated. The baseline of endogenous ROS in KCR cells was higher than observed in MCF-7 cells (Fig. 31). However, 6G induced a slightly increase of ROS in KCR cells but had no effect in MCF-7 cells (Fig. 31). These results suggest that 6G acts by inducing cell stress leading to an increase of ROS in resistant cells, as seen in previous chapters with the macrophages.

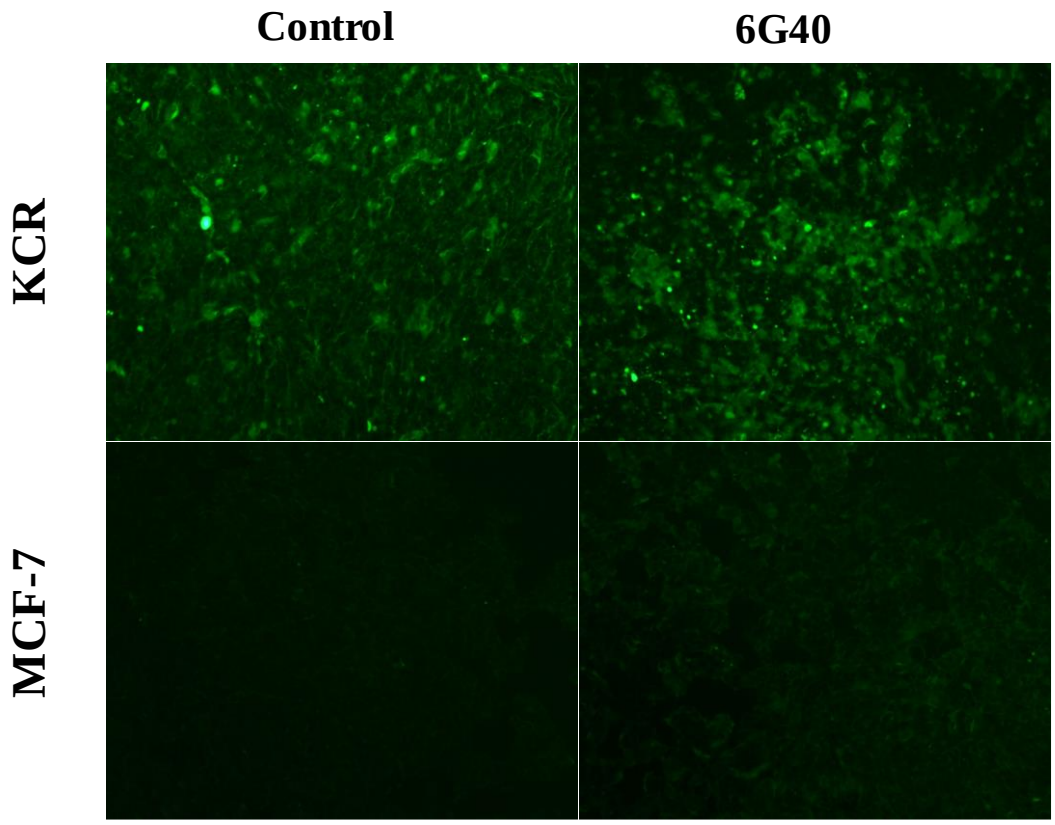

Figure 31: Effect of 6G in ROS production by cancer cell lines. MCF-7 and KCR cell lines treated with 6G were stained with dihydrorhodamine 123. Cells were observed by fluorescence microscopy and images were acquired. In parallel, untreated cells were also observed (100 × magnification).

- **6-gingerol is a modulator of ABCB1 efflux pumps in KCR cells**

In the present chapter, in order to detect whether 6G still interferes with the functional activity of ABCB1 efflux pumps of DOX resistant breast cancer cell line, an assay using the fluorescent probe $DiOC_2$ and flow cytometry were used. VP is a well-known modulator of ABCB1 that was used as a reference molecule.

Based on $DiOC_2$-fluorescence efflux assay, it was evidenced that both 6G and VP inhibited the activity of ABCB1 transporters in KCR cells (Fig. 32). KCR cells treated with VP showed an increased accumulation of $DiOC_2$ when compared to the control. As expected, in the MCF-7 cell line, which does not express ABCB1 efflux pumps, the accumulation of $DiOC_2$ was not affected by VP or by 6G.

The concentration of 6G that inhibited $DiOC_2$ efflux on KCR cells was 217 µM (64 µg.ml^{-1}) by fluorescence microscopy and 108 µM (32 µg.ml^{-1}) by flow cytometry (Fig. 33). The inhibitory concentration of 6G that inhibited the efflux on KCR cells by flow cytometry was similar to the concentration of 6G that was cytotoxic for 50% of the cells (IC50 114 µM, Fig. 33). However, VP (10 µM) caused a strong inhibition with only 1/8 of the IC50.

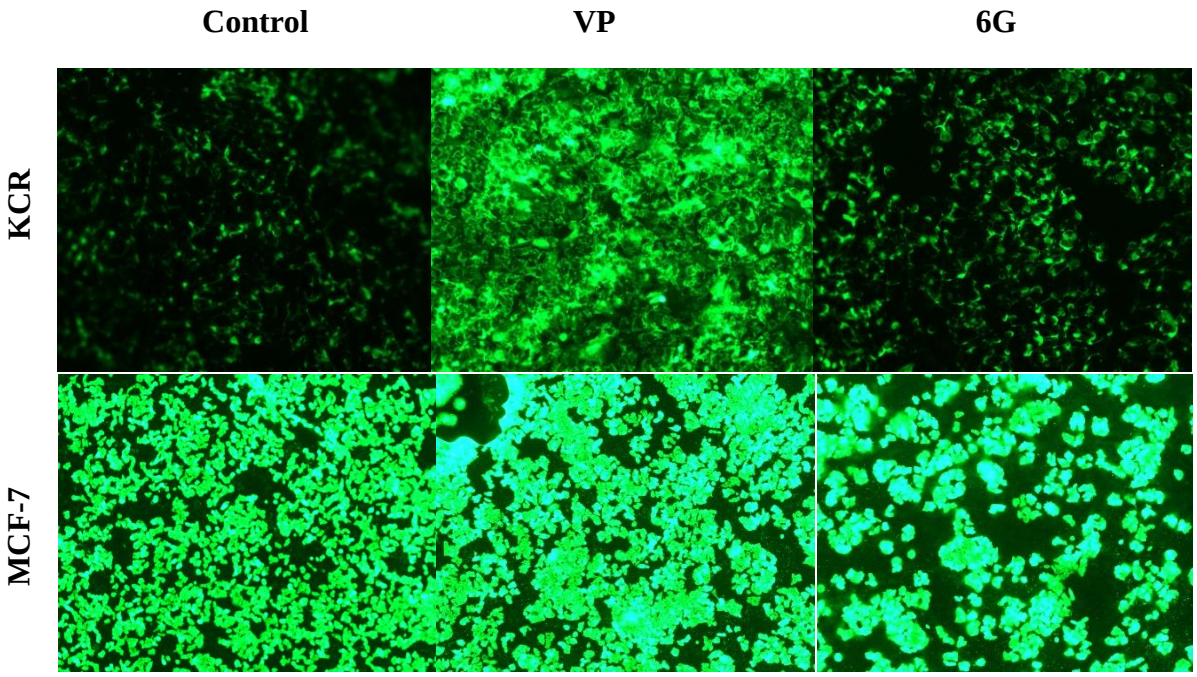

Figure 32. Accumulation of $DiOC_2$ in MCF-7 and KCR breast cancer cell lines Cells loaded with $DiOC_2$ were treated with VP (10 µM) and 6G (217 µM). Cells were examined by fluorescence microscopy and images were acquired. In parallel, non-treated cells were also evaluated (Control). VP: verapamil; 6G: 6-gingerol.

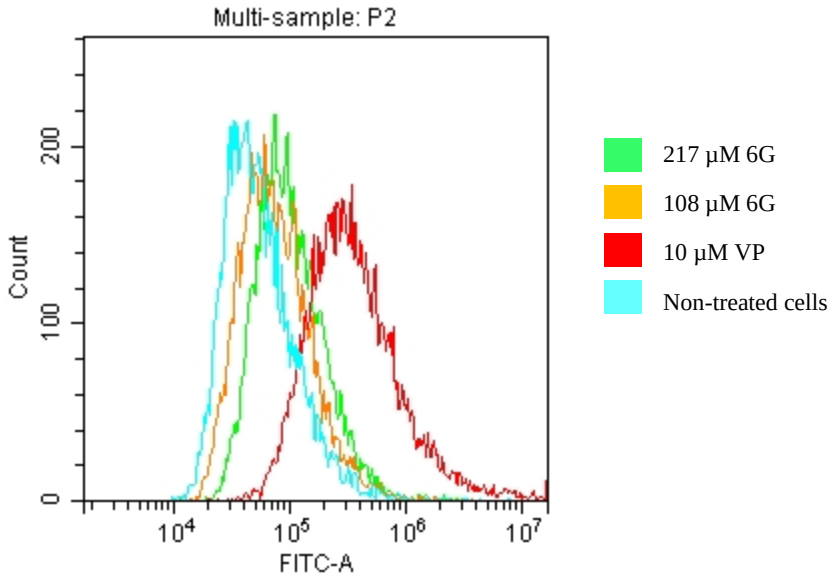

Figure 33: Flow cytometry analysis of $DiOC_2$ accumulation in KCR breast cancer cells. Cells loaded with $DiOC_2$ were treated with verapamil (VP) and 6-gingerol (6G) and evaluated by flow cytometry. In parallel, non-treated cells were also evaluated. Representative results of cell fluorescent emission are expressed by histogram. Blue line - non-treated cells, orange line - 108 µM 6G-treated cells, green line - 217 µM 6G treated cells and red line - 10 µM VP-treated cells.

These results indicate that 6G induced more cytotoxicity to resistant cells when compared to the MCF-7 cell line, however at a lower concentration than its ABCB1 inhibitory effect.

To investigate whether PAX and DOX are actively effluxed from drug-resistant cells, we compared the ability of MCF-7 and KCR cells to efflux the ABCB1 substrate Calcein AM. Calcein AM efflux is increased in the presence of ABCB1, thus limiting intracellular esterase cleavage and consequently fluorescent calcein production which was reflected by a decrease on intracellular accumulation.

We then assessed the accumulation of the intracellular calcein fluorescence in the presence of increasing concentrations of VP and 6G. VP and 6G treatment did not influence Calcein AM efflux in drug-sensitive MCF-7 cells, which do not express ABCB1, but caused a dose-dependent decrease in Calcein AM efflux (assessed by increased intracellular fluorescent calcein) in KCR cells (Fig. 34).

The use of different substrates interacting specifically with diverse drug binding sites of ABCB1 pumps should be taken in consideration in order to accurately characterize the putative ABCB1 inhibitory potential of a given drug.

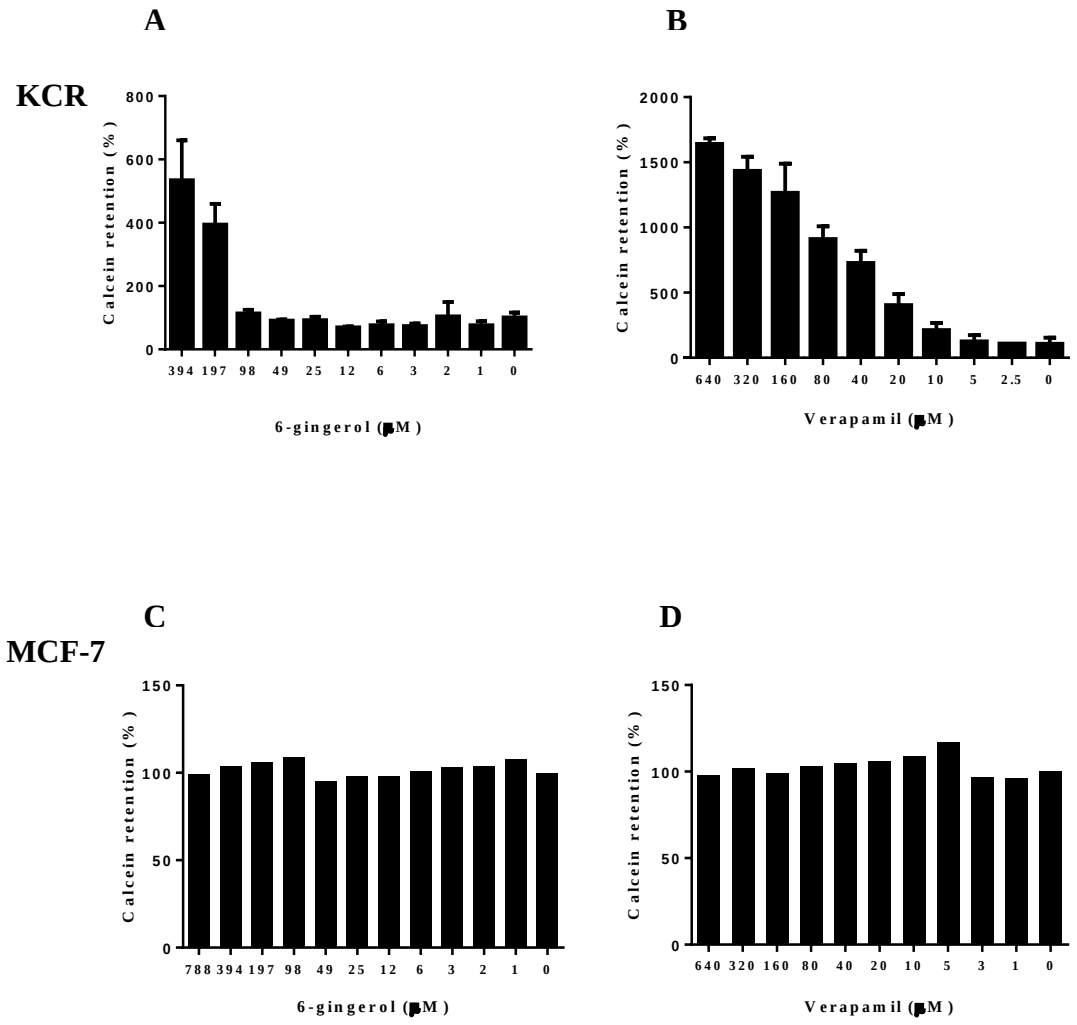

Figure 34: Intracellular accumulation of calcein in KCR and MCF-7 cells treated with 6-gingerol (6G) and verapamil (VP). Cells loaded with calcein were treated with 6G ranging from 1 µM to 788 µM and with VP ranging from 1 µM to 640 µM. Fluorescence was evaluated in a fluorometer and calcein intracellular concentration estimated.

In KCR cells, the EC_{50} towards ABCB1 mediated transport of calcein was 162.6 µM for 6G and 64.53 µM for VP. In contrast, VP and 6G did not manage to interfere in the intracellular accumulation of calcein in MCF-7 cells.

Subsequent cell viability tests were done using 10 µM of VP, in combination with PAX concentrations ranging from 16 to 1000 nM (Fig. 35). Cells treated with PAX stayed viable, even with higher concentrations of PAX. However, the combination of PAX and VP caused an important decrease of KCR cell viability. At higher concentration (1000 nM) of PAX ~75% of the cells were dead. Thus, this concentration was used to study cell viability of combined treatment of 6G and VP on KCR cells.

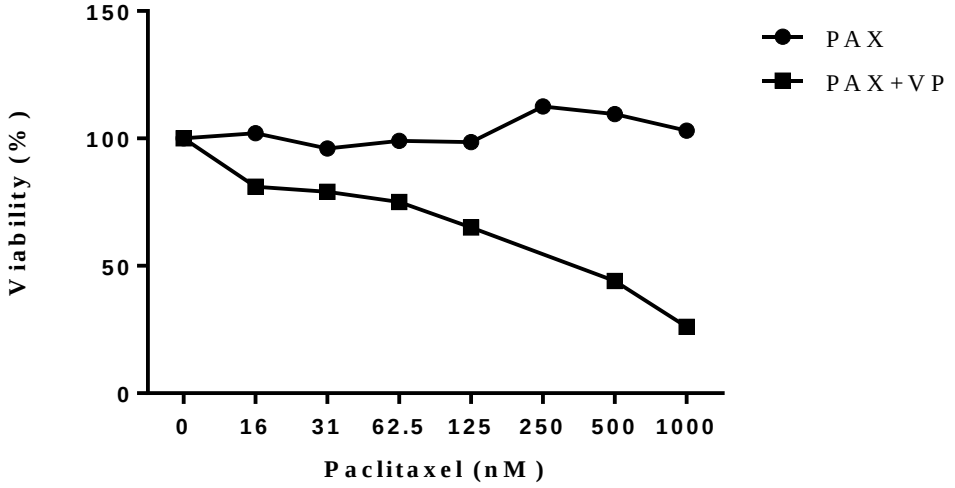

Figure 35: Checkerboard microtiter assay. KCR cells were treated for 72 h with paclitaxel (PAX) at concentrations ranging from 16 nM -100 nM and with PAX +10 µM VP. Non-treated cells (0) were also evaluated after 72 h. VP: verapamil.

Cell viability tests were done by using two different concentrations of 6G (40 and 80 µM) in combination with 1000 nM of PAX and 200 nM of DOX. KCR cells treated with 40 µM of 6G (a sub toxic concentration), 90% of cells were viable. KCR cells treated with 6G at 80 µM exhibited a cell viability lower than for the sensitive cell line.

Cells treated with DOX and PAX were used as reference of chemotherapeutic agents that are known substrates of ABCB1. Verapamil (10 µM) was used as a positive control.

The viability values obtained for the combination 6G+DOX and PAX are presented in (Fig. 36). The combined treatment, 6G80+DOX and 6G80 + PAX after 72 h had no effect on KCR cells treated with DOX or PAX.

However, combined treatment of PAX with 6G or VP at a subtoxic concentration reduced cell viability by 20 % and 36 %, respectively when compared to PAX treated cells.

Statistically significant differences were observed between untreated cells and cells treated with 80 µM of 6G alone. 6G treatment increased cell death ($p < 0.05$) by approximately 32 % and was more effective than combined treatment.

Although not statistically different, we can observe that the combination of 6G at subtoxic concentration (40 µM) and PAX induced a synergistic interaction by reducing cell viability.

No significant difference was observed between treated and untreated cells. Values are expressed as mean ± SEM from three independent experiments (n = 3).

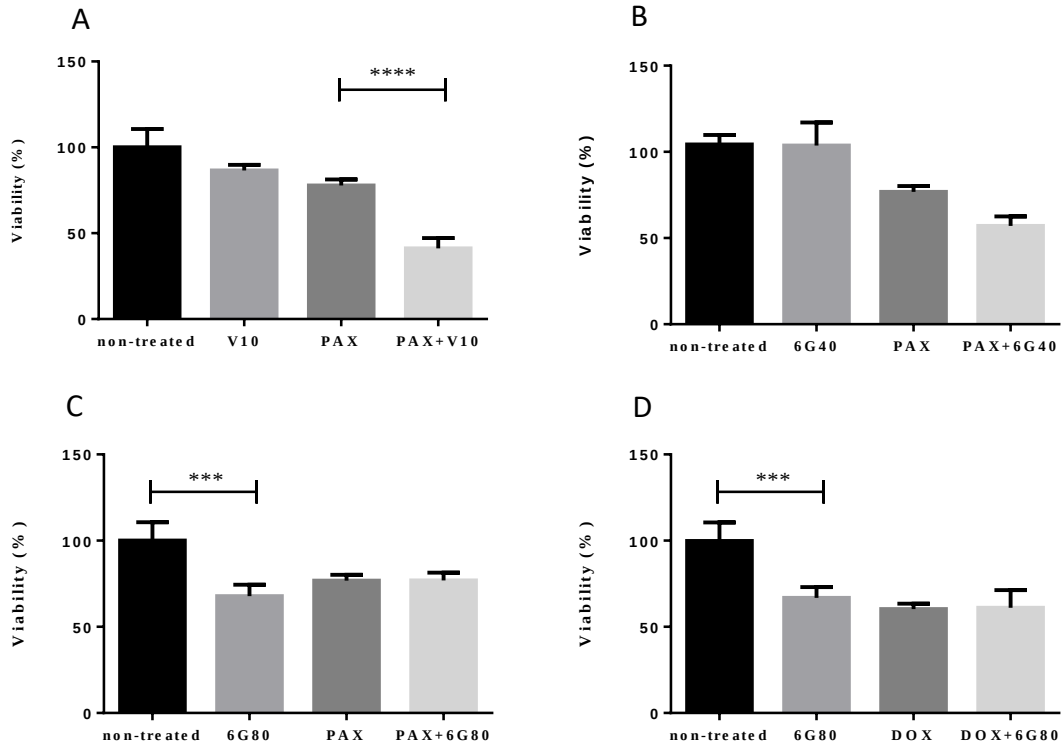

Figure 36: Cytotoxic effect of paclitaxel (A, B, C) and doxorubicin (D) in combination with VP (A) and 6G (B, C, D) on KCR cells. Cells were treated with 1000 nM of PAX (A, B and C) or with 200 nM DOX (D) plus 10 µM of VP (A) or 40 µM (B) and 80 µM of 6G (C and D). Cell viability was determined by MTT assay. Non-treated cells and cells treated with PAX and DOX were used as controls. *P < 0.05, **P < 0.01, ***P < 0.001 indicate significance differences when comparing non-treated cells vs treated cells. PAX: paclitaxel; DOX: doxorubicin; 6G: 6-gingerol; V: verapamil.

- **Discussion and Conclusions**

During the development of cancer, drug resistance can emerge during treatment. Chemo-resistance has proven to be a major clinical obstacle to the successful treatment of breast cancer. The overexpression of ABCB1 efflux pumps has been recognized as one of the main mechanisms associated to drug resistance in breast cancer. Although, the mechanisms linked to drug resistance phenotype are not yet completely understood, its presence is an indicator of a poor prognosis.

Here in this chapter we have demonstrated the presence of ABCB1 transporter in a breast cancer cell line resistant to DOX, which was in agreement to what is described in the literature (170). ABCB1 efflux is responsible for the reduction of intracellular drug concentrations with the consequent decrease in cell cytotoxicity of a broad spectrum of antitumor drugs, including DOX and PAX.

Thus, one of the strategies to circumvent drug resistance is by using natural compounds as non-toxic chemosensitizing agents against drug resistant cells.

Dietary phytochemicals, which can interfere with tumor promotion and progression, usually have multiple molecular targets. This pleiotropic effect can constitute an advantage in the treatment of chemo-resistant breast cancer. 6G, a bioactive component present in certain plants that are part of our diet, has been putatively recognized as having anti-cancer and anti-inflammatory properties. This present work demonstrated that 6G is a potential modulator of ABCB1 transporters in breast cancer cells, reinforcing the previous preliminary observations in the literature. However, 6G presented an EI50 concentration higher than VP and close to the corresponding IC50 for the drug resistant cell line (KCR). As expected, 6G did not show any efflux inhibitory effect on the sensitive cell line (MCF-7), which does not express ABCB1 transporters, reinforcing its potential role as a pump inhibitor in drug resistance due to ABCB1 overexpression.

6G was more cytotoxic towards drug-resistant breast cancer cell line (IC50 = 114 µM) than the sensitive cell line (IC50 = 320 µM). Curiously, MDA-MB-231 cell line, which represents a tumor cell line with metastatic capability, has a 6G IC50 (105 µM) similar to the 6G IC50 for tumor cell line resistant to doxorubicin (KCR) (data not shown).

The cytotoxic effect of 6G to different types of cancer has already been reported, being associated with different mechanisms of action. Although reported concentrations of 6G responsible for cell cytotoxicity differ considerably, this phytochemical seems to be more toxic to cancer cells than to normal cells. Previous studies have already demonstrated differences between the effect of 6G on human colon cancer cell line and normal intestinal epithelial cells (171).

The activity of 6G against drug resistant breast cancer cells has been poorly investigated. Here, in this chapter, the sensitivity of a resistant cancer cell line to 6G can possibly be related to ROS production. The cytotoxic effect of 6G on KCR cells became more evident at a concentration lower than the IC50. At non-toxic concentrations, 6G may act as a cell stressor by inducing resistant cells to display oxidative burst. When resistance to one drug confers cell hypersensitivity to another drug, it is denominated collateral sensitivity (117, 172). In the case of KCR drug-resistant cancer cells, collateral sensitivity to 6G may have occurred.

ABCB1 positive cells were shown to be collaterally sensitive to certain drugs that were less toxic to ABCB1-negative cancer cells and to normal cells (117, 172, 173). Also, ROS generating agents have been shown to elicit collateral sensitivity (172).

Besides its protective function, ABCB1 has also been implicated in resistance to apoptosis, promoting cell survival. ROS has been implicated in the regulation of ABCB1 (174). Many natural chemotherapeutic agents induce the generation of intracellular ROS, which plays a critical role in cell cytotoxicity (163-165) as in the case of DOX. 6G which has also been described as inducing ROS production by leukemia cells (175-177).

These findings are in agreement with the hypothesis previously described sensitivity of ABCB1 overexpressing cells being associated to oxidative cell death (178).

The dual role of efflux inhibitors, as ABCB1 modulators and anti-tumor activity (cytotoxic agents), has been previously described and the capability of 6G in reverting resistance to PAX and DOX was demonstrated for the first time in this work at a concentration above their IC50, the same concentration that favored a slight increase of intracellular ROS. Because of DOX spectral characteristics, PAX, a known inhibitor of ABCB1, was the chemotherapeutic drug used in this preliminary study. These findings

suggest that despite its potential as an inhibitor of ABCB1 cell transporters, 6G has also a promising potential to target drug-resistant breast cancer cells, promoting drug sensitivity. This is a mechanism that can be explored as an important approach to exploit resistance by identifying compounds that are selectively cytotoxic to MDR cells (117, 179). Also this study highlights the emerging strategy of treating breast cancer by targeting ROS homeostasis (180).

Taken into account that the level of ABCB1 in cell lines is much higher than that in human tissues, lower concentrations of ABCB1 modulators should be effective inhibitors of ABCB1 efflux pumps *in vivo*, when compared to *in vitro* studies. Therefore, a low therapeutic dose of 6G that is considered to be non-toxic, could be advantageous in future *in vivo* studies (181, 182).

4. Regulation of ABCB1 expression by miR-200c and miR-203a in breast cancer cells

4.1. Introduction

Breast cancer is the most common cancer in women. Data reported in 2012 by WHO revealed that each year there are about 1,7 million new cases worldwide (http://gco.iarc.fr/today/home). Up to 30 % of women diagnosed with early-stage breast cancer will eventually progress to metastatic breast cancer (MBC) (183).

Depending on its type and stage, breast cancer treatment can be local or systemic. Systemic therapy usually includes a combination of 2 or 3 chemotherapy drugs such as anthracyclines (doxorubicin and epirubicin), taxanes (paclitaxel, docetaxel), 5-fluorouracil (5-FU), cyclophosphamide and carboplatin, hormone therapy (tamoxifen, fulvestrant, aromatase inhibitors) and target therapy (trastuzumab, lapatinib). (https://www.cancer.org/cancer/breast-cancer/).

Emergence of resistance to the available chemotherapeutic drugs is inevitable when recurrence occurs. Cancer drug resistance (CDR) is deemed to be the cause of treatment failure in over 90 % of patients with MBC. In order to overcome CDR resistance, treatment strategies are established, taking into account the tumour phenotype (184). In fact, drug resistance to the available chemotherapeutic drugs is dependent on biological factors, involving multiple pathways (185).

Epithelial-Mesenchymal Transition (EMT) is an adaptation process where cells lose their epithelial characteristics and acquire a mesenchymal phenotype with migratory and invasive capabilities. In tumour cells, the induction of EMT is frequently associated with tumour progression, metastasis development and drug resistance (186, 187). The metastatic cells that have undergone EMT usually exhibit a cancer stem cell-like phenotype normally resistant to chemotherapy due to deregulation of several genes, including the overexpression of ATP-dependent efflux pumps (ABC-transporter

proteins), which promotes the efflux of a broad range of anticancer drugs through the cellular membrane (188). In healthy tissues, the presence of this transporter associated with bio-transformation pathways is widely distributed, having a role as a "first responder" to compounds that passively cross the membranes, protecting cells from the intracellular accumulation of toxic products. Under drug pressure, cells undergo genetic and protein adaptations by using diverse molecular mechanisms, such as the activation of survival signaling pathways and/or an increase in drug efflux.
The presence of these transporters frequently occurs in cancers that developed from liver, pancreas, kidney, adrenocortical and colon tissues where they are naturally present before treatment or is an acquired process as a consequence of chemotherapy, similar to what occurs in leukemia, lymphomas, neuroblastoma and breast cancers (189).

ABCB1 (P-glycoprotein or P-gp, MDR1), MRP1 and BCRP proteins are the most prevalent ABC proteins in breast cancer, having the capacity to confer multi-drug resistance (MDR). These proteins are part of a complex network of cellular factors or tissue features which promotes the development of drug resistance in cancer cells, and their presence is correlated with resistance (190). Overexpression of ABCB1 is commonly the first mechanism of resistance, preceding the development of other mechanisms like an increase of drug metabolism, change of specific drug targets, activation of DNA repair mechanisms, suppression of apoptosis and EMT, as cells proliferate and adapt to drug regimens (191).

Approximately 50% of human cancers express ABCB1 at an adequate amount to confer CDR. Thus ABCB1 protein, which is the most prevalent transporter associated with breast CDR phenotype, confers resistance to a broad range of anticancer drugs, including the classic (genotoxic drugs) and the new generation of cytostatic compounds (173) , such as taxanes, anthracyclines, antibiotics, vinca alkaloids and tyrosine kinase inhibitors (60, 192).

Several strategies to overcome drug resistance by regulating the activity of ABCB1 have been widely explored, especially through the use of efflux pumps inhibitors in combination to anticancer drugs. However, because of the intrinsic efflux activity present in healthy tissues, clinical trials with ABCB1 modulators have shown disappointing results due to the serious side effects observed. Therefore, there is an urgent need for the

development of new therapeutic strategies in order to reverse drug resistance (DR) as stressed in previous chapters of this thesis.

Given that the expression of ABCB1 is also under control of other factors, including epigenetic regulation, another strategy to overcome MDR mediated by ABCB1 is to silence the activity of ABCB1 efflux pumps or reduce its expression by interfering with gene regulation by using for example non-coding RNAs. Dysregulated expression of miRNAs, often seen in diverse type of cancers, has been recognized as a specific miRNA signature. The investigation of mechanisms that lead to miRNAs dysregulation could establish an association between the expression level of a particular miRNA to drug resistance. These associations can lead to treatments using specific therapy, and/or use a specific miRNA as a possible drug target in order to revert the process that lead to MDR (53).

MicroRNAs (miRNAs, miRs) are small noncoding RNAs that negative regulate gene expression by post-transcriptionally targeting the 3'-UTR region of mRNA. They act as master regulators of protein expression by blocking translation (193) and due to their small size (22-25 nucleotides), miRNAs can bind to several different mRNAs, while the same mRNA can be targeted by several miRNAs. The extend of complementary of the miRNA recognition sequence (seed region) with its target mRNA determines mRNA cleavage with subsequent degradation, when there is a perfect match, or translational repression if the interaction is partially complementary.

The relevance of miRNAs in regulating the expression of ABC transporters in CDR has been recently reviewed (194, 195) specifically the expression pattern of miRNAs seems to have a critical role in DR (196). In fact, several miRNAs have been reported to have a direct or indirect role in the regulation of the expression (52, 194, 197) or activity (198) of ABCB1 in DR in different cancers.

The process that drives DR acquisition during treatment or tumour progression may be connected to EMT and the emergence of stem cell-like features, which, in part, can be linked to the regulatory role of dysregulated miRNAs (199). In particular, miR-200c and miR-203a have been linked to drug resistance in different tumours (200-204) and also to EMT transition (194, 205-207). Recent studies conducted by our team have shown that there was a significant downregulation of miR-203a and miR-200c with increased stage

in invasive lobular carcinomas (187). In addition, down-regulation of miR-200c was also observed in MCF-7 breast cancer cell line resistant to doxorubicin being associated with a poor chemotherapy response in human breast cancer patients in part by a possible regulation of ABCB1 expression (208). Also, there is growing evidence supporting a correlation between EMT and the induction of drug resistance (209). Interestingly, during EMT the expression of ABC transporters can change continuously (210).

Further studies have shown an association of miR-203 with drug chemotherapeutic resistance (203, 204, 211), invasiveness (212, 213), proliferation (212, 214-216), and metastases (216, 217). However, the role of miR-203 as a putative regulator of ABCB1 in drug resistance remains unknown. Therefore, we hypothesized that miR-203 could also be a potential modulator for breast cancer therapeutics resistance.

Thus, in the present study we have investigated the role of miR-200c and miR-203 in the modulation of ABCB1 in drug resistance by using a doxorubicin resistant breast cancer cell line and $DiOC_2$ as a specific fluorescence substrate of this transporter. These cells constitutively overexpress ABCB1 gene and exhibit a gene expression pattern compatible with EMT (169, 218).

4.2. Material and Methods

4.2.1. Bioinformatics microRNA target prediction

The web interface of Target Scan release 7.1 (http://www.targetscan.org/) prediction program was used to search for putative miR-203 and miR-200c binding sites within the 3′-UTR regions of human ABCB1 mRNA (219).

4.2.2. **Reagents**

All reagents for cell culture and verapamil (VP) were purchased from Sigma-Aldrich. Doxorubicin hydrochloride (DOX) was obtained by TEVA (TEVA 2 $mg.ml^{-1}$; Pharmachemie B.V. Netherlands), $DiOC_2$ (2 $mg.ml^{-1}$ in DMSO) was obtained from Molecular Probes™. VP stock solution was prepared in water (10 mM), 0.22 µm filter sterilized and stored in aliquots at -20 ºC.

4.2.3. **Cell culture**

Human breast adenocarcinoma cell lines MCF-7 and its doxorubicin-resistant subline KCR, were kindly provided by Professor Joseph Molnar, Szeged Foundation for Cancer Research, Hungary (169). MCF-7 cell line exhibits some features of differentiated mammary epithelium and KCR cell line exhibits epithelial-mesenchymal transition gene expression pattern (220). MCF-7 and KCR were cultured in Minimal Essential Medium (EMEM) supplemented with 10% (v/v) heat inactivated fetal bovine serum (FBS), 1.5 $g \times l^{-1}$ sodium bicarbonate, 1 mM sodium pyruvate, 0.1 mM nonessential aminoacids (Gibco), 1% streptavidin-penicillin (100,000 unit's penicillin and 10 mg streptomycin per ml, Gibco). KCR cells were cultured in the presence of 1 µM of DOX every 3 passages in order to maintain the resistant phenotype. All cell lines were incubated at 37 ºC in a humidified 5% CO_2 chamber. Culture medium was replaced three times a week and subcultured by trypsinization (0.25 % trypsin in media without serum, Gibco) when confluence reaches approximately 80%.

4.2.4. Ectopic expression and inhibition of miR-203 and miR-200c

Mimetic miRNAs (Pre-miR™ miRNA Precursor hsa-miR-200c-3p # PM11714 and hsa-miR-203a #PM10152; Life Technologies) and miRNAs inhibitors (Anti-miR™ miRNA Inhibitor hsa-miR-200c-3p # AM11714 and hsa-miR-203a-3p # AM10152; Life Technologies) were transfected in KCR and MCF-7, respectively.

As negative controls we used Pre-miR™ miRNA Precursor Negative Control #1 (Life Technologies # AM17110) and Anti-miR™ miRNA Inhibitor Negative Control #1 (Life Technologies # AM17010). These negative controls are oligonucleotides similar to miRNA precursors and miRNA inhibitors but without any biological effect.

The transfection complex (oligo + transfection agent) was prepared in EMEM without any supplementation and incubated at room temperature for 15 min. After this time, the transfection complex was added to the cells that already had complete culture medium in a proportion of 1:1.

Adherent cells were transfected with a mixture of 0.3 % (v/v) FuGENE HD transfection reagent (Promega) with mimic/anti-miR-203a and mimic/anti-miR-200c (Life Technologies) or non-specific pre/anti-miRNA controls at a final concentration of 30 nM and 50 nM for KCR/MCF-7 respectively, for 24 h, 48 h and 72 h, at 37 ºC, according to the manufacturers' recommendations.

After the incubation time, functional analysis was done and total RNAs and proteins were purified.

4.2.5. Immunofluorescence

Cells were washed twice with PBS and resuspended in a small amount of PBS. Cells in suspension were spotted on a multi-well slide and left to dry before being fixed with ice-cold acetone for 10 min. Cells were blocked with 3 % BSA in PBS for 1 h and then incubated with C219 (1:200) primary antibody for another hour at 37 ºC in a humid chamber followed by incubation with FITC-conjugated antibody. Slides were washed twice with PBS, counter-stained with DAPI, following the protocol previously described (149). Coverslips were mounted on the slides and imaged using a Nikon DS-Ri1 camera installed in Nikon eclipse 80i microscope using NIS-Elements BR 3.3 software. Fluorescence emissions were acquired using specific filters set for DAPI (laser 405 nm/BP 420-480 nm), FITC dyes (ex 495 nm/BP 515 nm).

4.2.6. Evaluation of ABCB1 activity by fluorescence microscopy

Cells were seeded on sterilized glass coverslips in 6-well culture plates (for microscopy fluorescence assays) at a density of 2.5×10^5 cells.ml^{-1} (24 h, 48 h transfection assay) and 10^5 cells.ml^{-1} (72 h transfection assay), and allowed to grow overnight at 37 ºC. The following day, ABCB1 efflux pump activity of transfected cells was evaluated as previously described by the author (106) (chapter 2, 2.2.4). Briefly, after the transfection time (24 h, 48 h and 72 h), medium was removed from coverslips and fresh medium with and without 10 µM verapamil was added to each duplicated experiment well and incubated for 30 minutes before addition of 1 µg.ml^{-1} of $DiOC_2$ for 1 h at 37 ºC. Subsequently, medium was removed and dye free medium was added with the presence or absence of VP for another 1 h. Slides were rinsed twice in PBS and then cells were examined using a fluorescence microscopy. Cells were examined at 485 nm excitation laser and 530/30 nm emission filter (green fluorescence).

4.2.7. Quantification of $DiOC_2$ cell retention by Flow cytometry

After 24 h of transfection, KCR cells were seeded on duplicated T25 flasks (with scramble NC, mimic-miR-203a and mimic-miR-200c), at a density of 2.5×10^5 cells.ml^{-1} and incubated for 48 h at 37 ºC in a humidified atmosphere of 5 % CO_2. Then, cells were harvested using trypsin, resuspended in complete medium and viable cells quantified by direct microscopy, using a Neubauer-chamber and trypan blue exclusion dye. Cells were placed in eppendorf tubes at a concentration of 5×10^5 cells.ml^{-1} and pre-incubated in medium (control cells) or treated with 10 µM VP, for 30 min at 37 ºC and $DiOC_2$ (1 µg.ml^{-1}) was added and cells were incubated for 1 h at 37 ºC. To keep efflux pumps inhibited, cells were then resuspended in 500 µl of fresh medium in the presence and absence of VP and incubated for another hour. Cells were washed twice with cold PBS, spin down, resuspended in 500 µl cold PBS and fluorescence retention was measured by flow cytometry, using CytoFlex flow cytometer (Beckman Coulter) at an excitation wavelength of 488 nm and emission recorded in 525/40 BP (FITC-A channel). Data was collected for at least 10,000 events per sample and analysed using FlowJo v10 software (Tree Star, Inc., Ashland, OR).

In order to remove bad flow (questionable events), a FITC-A vs time plot parameter was used (Fig. 37A). The area exhibiting a poor flow was excluded from areas of good flow by time gating. Forward scatter area (FSC-A) vs side scatter-area (SSC-A) density plot was used to remove debris and pyknotic cells in the lower left-hand portion of the plot as well as the very large (off scale) debris found in the upper right-hand portion (Fig. 37B). Breast cancer cells (KCR) population was identified based on FSC-A vs SSC-A gate. Singlet gate was used to define the non-clumping cells based on pulse geometry forward scatter height (FSC-H) vs FSC-A eliminating the doublets (Fig. 37C). Then, gated cells corresponding to viable KCR cells was represented on one-parameter histogram by plotting FL1-A/$DiOC_2$ vs the number of events (Fig. 37D). Results were expressed by the median of fluorescence intensity.

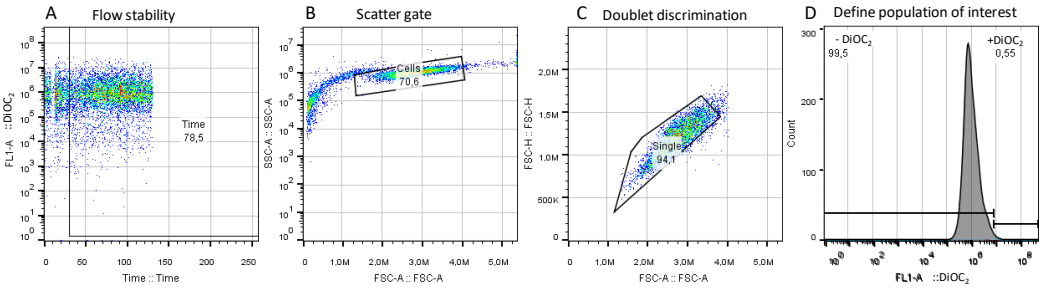

Figure 37: Gating strategy used to select the population of interest. (A) Flow stability; (B) Scatter gate; (C) Doublet discrimination and (D) Representative histogram of positive and negative fluorescent regions.

4.2.8. **Nucleic acid purification**

Total RNA and miRNAs from cell lines were purified with All Prep DNA/RNA Mini kit (Qiagen # 80204) and RNeasy MinElute Cleanup Kit (Qiagen # 74204), accordantly to what is described by the manufacture. Briefly, $6x10^6$ cells were harvested and lysed in 700 µl of RLT plus buffer and loaded into an AllPrep DNA spin column and centrifuged for 30 s at ≥8000 × g. The flow-through was used for RNA purification and the DNA spin column stored at room temperature until further use. One volume of 70% ethanol was added to the flow-through and mixed by pipetting. Up to 700 µl of the sample, was loaded into an RNeasy spin column and centrifuged for 30 s at ≥8000 × g. The flow-through was stored at room temperature for later use for miRNAs purification. RNeasy spin column was washed by adding 700 µl of RW1 buffer and centrifuged for 30 s at ≥8000 × g. The flow-through was discarded. A second wash with 500 µl of RPE buffer was done, followed by a centrifugation for 30 s at ≥8000 × g. The flow-through was also discarded. A third wash with 500 µl of RPE buffer was done, followed by a centrifugation for 2 min at ≥8000 × g. The flow-through was again discarded. Next, 30 µl of nuclease-free water was added directly to the spin column membrane and centrifuged for 1 min at ≥8000 × g to elute the RNA. This RNA was then stored at -80 °C until further use. One volume of 100% ethanol was added to the flow-through previously stored for miRNAs purification. This mixture was then loaded into an RNeasy MinElute Cleanup column and

centrifuged for 30 s at ≥8000 × g. The flow-through was discarded. A wash was done by adding 500 µl of RPE buffer and centrifuged for 30 s at ≥8000 × g and discarding the flow-through. A second wash with 500 µl of 80% ethanol was done and centrifuged for 2 min at ≥8000 × g. The flow-through was discarded and a centrifugation for 5 min at full speed was done in order to dry the filter. Next, 14 µl of nuclease-free water was added to the column and centrifuged for 1 min at full speed. The miRNAs were then stored at -80 °C until further use. All samples were quantified using a NanoDrop™ spectrophotometer.

4.2.9. Reverse transcription qPCR for miRNA

The relative expression of miRNA was quantified by Reverse transcription qPCR (RT-qPCR) by using Universal cDNA synthesis kit II and ExiLENT SYBR® Green master mix from Exiqon in a real time PCR 7300 system (ABI), accordantly to the protocol described by the manufacturer and described by Bruno Gomes et al. (193). The primers used according to Bruno G. PhD thesis (2016)[3]: hsa-miR-203 (Exiqon, LNA™ PCR primer set # 204285); hsa-miR-200c-3p (Exiqon, LNA™ PCR primer set # 204482) and as endogenous control U6 snRNA (Exiqon, PCR primer set # 203907).

This methodology was performed to detect miR-200c and miR-203 expression levels in MCF-7 and KCR cell lines after ectopic inhibition or over-expression of both miRNAs. The relative amount of miRNA was normalized with the internal control U6 snRNA using the equation $2^{-\Delta CT}$, where ΔCT = CT miR-203 - CT U6.

[3] Bruno Daniel da Costa Gomes. 2016. MicroRNA involvement in breast cancer susceptibility and progression. PhD Nova Medical School.

4.2.10. ABCB1 protein expression by Western Blot

Forty-eight hours after transfection with mimics of miR-203 and miR-200c, cells were harvested, washed with PBS and membrane proteins were isolated by using Mem-PER^{M} Membrane Protein Extraction Kit (Thermofisher) following the manufacture's protocol. Proteins were quantified by the Bradford assay (Bio-Rad Laboratories) and approximately 3 µg of protein from each sample was mixed with equal amounts of Laemmli sample buffer (Bio-Rad Laboratories) and boiled before being separated by electrophoresis precast gels (4–20% Mini-PROTEAN® TGX™ Precast Protein Gels, Bio-Rad #4561093S). Proteins were transferred onto polyvinylidene difluoride (PVDF) membranes, according to the protocol previously described[4]. Blots were done using the WesternDot^{TM} 625 Goat anti-Mouse Western Blot Kit (#W10132) and probed with anti-human ABCB1 (dilution 1:1000) (D11: # sc-55510, Santa Cruz Biotechnology) and anti-β-actin primary antibodies (Santa Cruz # sc-47778).

The immunoblots were visualized under ultra-violet light and the chemiluminescence signal was captured by ChemiDoc^{TM} Touch Imaging System (BioRad), accordantly to the protocol described by the manufacture (Invitrogen).

4.2.11. Real-time RT-qPCR quantification of mRNA

Quantification of ABCB1 mRNA was done by polymerase chain reaction (RT-qPCR). Total RNA was extracted as previously described and purity ratios 260/280 and 260/230 were determined by using nanodrop spectrophotometer. Single-stranded cDNA was

[4] Carlos N, Martins TM, Prata S, Lopes A, Armada A. Gene sequencing, modelling and immunolocalization of the protein disulfide isomerase from *Plasmodium chabaudi*. 2009;45(4):399-406.

synthesized from 1µg of total RNA using the High Capacity cDNA Reverse Transcription Kits (Applied Biosystems) in a final reaction volume of 20 µl according to the manufacturer's instructions.

The reaction mixture was then used as a template in a TaqMan Fast real-time quantitative PCR assay using Taqman Universal PCR Master Mix and the 7300 Real-Time PCR System (Applied Biosystems). The predeveloped Taq-man assays (Assay-on-Demand products from Applied Biosystems) were ABCB1, Hs00184491_m1 and the human GAPDH, 4352934E as the reference gene. All PCR reactions were done in a total volume of 10 µl by using TaqMan® Universal Master Mix II, ROX as an internal reference dye and TaqMan DNA polymerase. Template controls and reverse transcriptase controls (RT negative) for each cDNA synthesis were included.

Thermal cycler conditions were 50 ºC for 2 min; 95 ºC for 10 min followed by 40 cycles at 95 ºC for 15 s and at 60 ºC for 1 min (221). The mean values of the triplicate RT-qPCR reactions for each assay were normalized with the expression values for each gene. Relative expression of ABCB1 was performed by the comparative $2^{-(\Delta\Delta Ct)}$ method using the expression of GAPDH in the cDNA by using the standard curve method described by the manufacturer (Applied Biosystems).

4.2.12. **Statistical analyses**

Significant differences were determined using the non-parametric Wilcoxon test for two paired samples (GraphPad Prism 6.0, GraphPad Software, Inc, USA). A significance level of 5% ($p < 0.05$) was used to evaluate statistical significance. The mean and standard error of at least three independent experiments and triplicate samples are represented by bar-charts.

4.3. **Results**

4.3.1. **ABCB1 is only expressed in the doxorubicin resistant breast cancer cell line and is inversely correlated with the expression of miR-203 and miR-200c**

According to the authors who developed this cell line (169), the KCR resistant subline expresses both ABCC1 (Multidrug resistance-associated protein, MRP-1) and ABCB1 genes and its parental cell line MCF-7 only expresses MRP-1. By RT-qPCR, KCR cell line showed an increase of 100 000-fold change of ABCB1 mRNA expression levels relative to MCF-7 doxorubicin sensitive cells (Fig. 38A). As illustrated, the protein expression levels of ABCB1 efflux pumps was also significantly up-regulated in KCR cells when analysed by immunofluorescence and western blotting, whereas in MCF-7 it was not detectable (Fig. 38B and C).

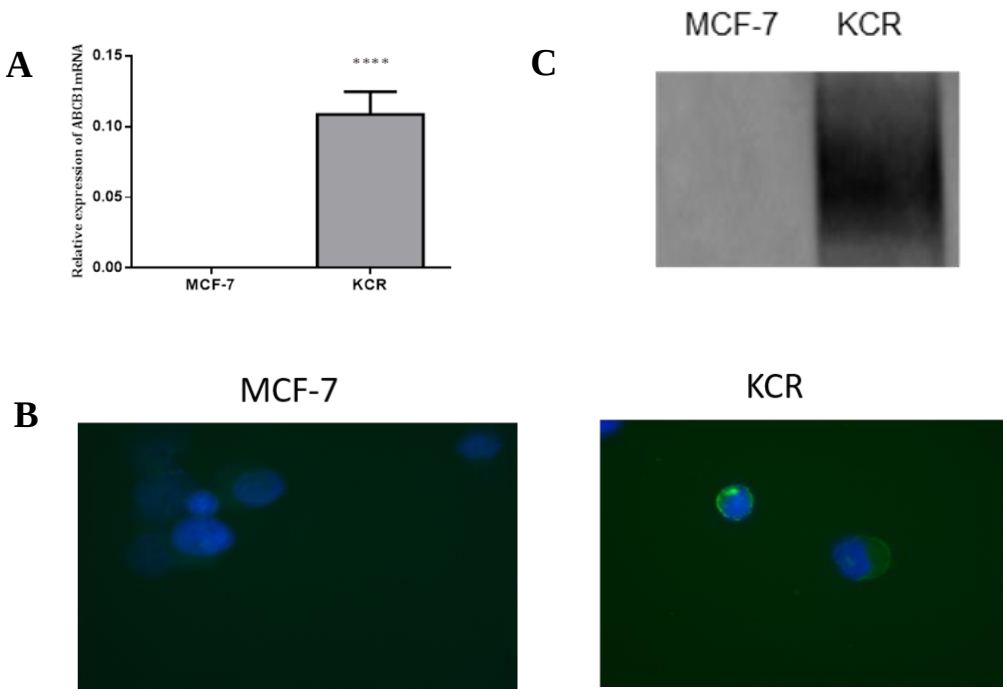

Figure 38: Expression levels of ABCB1/MDR1 in breast cancer cell lines (KCR and MCF-7). The mRNA and protein expression levels were analysed by RT-qPCR (A), immunofluorescence (B) and western blotting (C). The average fold change of ABCB1 mRNA expression compared to parental MCF-7 cells ± SEM (n=4) was calculated using $2^{-(\Delta\Delta Ct)}$ method from real-time RT–PCR data.

In order to evaluate the role of miR-203 and miR-200c in the MDR phenotype, the basal levels of miR-203 and miR-200c in MCF-7 and DOX resistant sublines cells (KCR) were assessed by RT-qPCR.

Gene expression level of miR-203 in KCR resistant cell line was significantly down-regulated, more than 150 fold-change, compared with the parental wild-type MCF-7 where the expression of ABCB1 was not detected (Fig. 39). These results suggest that miR-203 expression may have a role in the doxorubicin resistant phenotype mediated by ABCB1 efflux pumps.

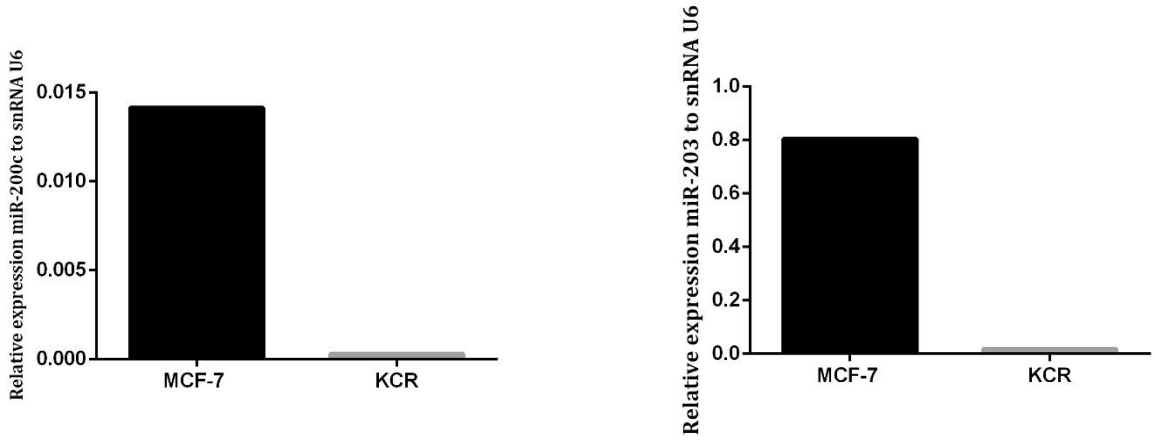

Figure 39: Expression levels of miR-200c and miR-203 in MCF-7 and KCR cell lines. miRNA was assessed by RT-qPCR and values are represented as the mean relative expression of three independent experiments and three replicates per sample normalized to U6 snRNA ± standard deviation. Both miRNAs showed different patterns of gene expression in MCF-7 and KCR cells, miR-200c and miR-203 are downregulated in the resistant cell line (KCR) that overexpresses ABCB1.

Using TargetScan informatics analysis we identified that mRNA of ABCB1 (ENST00000265724.3) is a putative target of miRNA-203 (Fig. 40).

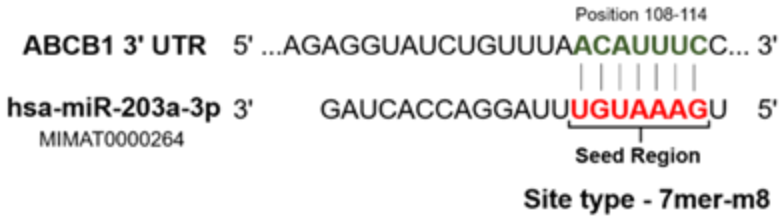

Figure 40: TargetScan prediction for a miR-203 target site inside human sequence ABCB1-3'UTR. Predicted sites on the 3'UTR regions of human ABCB1 (Gene bank ENST00000265724.3) target by 5'-end of hsa-miR-203a using bioinformatics algorithms TargetScan Release 7.2 (http://www.targetscan.org/).

In order to investigate the role of miRNA-203a in the regulation of ABCB1 expression in drug resistance, we proceeded to transiently transfection of mimics and antagomirs of miR-203a and miR-200c in KCR and MCF-7 cell lines, respectively and analysed the efflux transport activity of ABCB1 efflux pumps in living cells using a ABCB1 specific fluorescent substrate.

Figure 41 shows the expression of miR-200c and miR-203a after transfection with pre-miR-200c and pre-miR-203 in the KCR cell line. This graph demonstrates an effective transfection of these precursors.

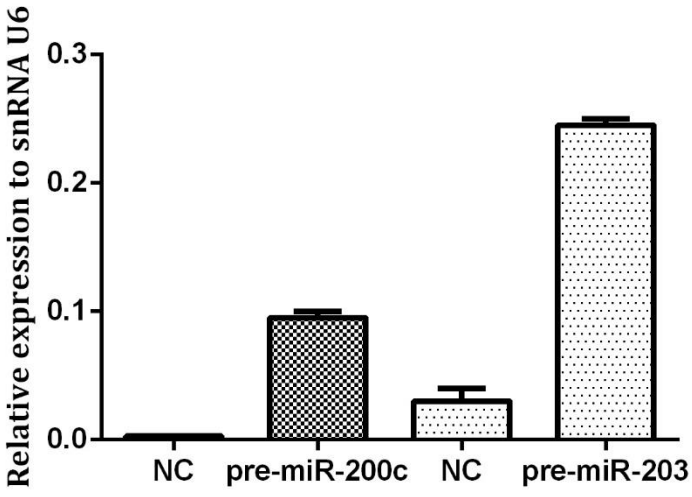

Figure 41: Expression of miR-200c and miR-203a on KCR cell. Insertion was done through pre-miRNAs transfection by using FUGENE HD. Values represent mean values of two independent experiments ± standard deviation.

4.3.2. Mimic-miR-203a and miR-200c impaired the activity of ABCB1 in KCR cells

The results obtained suggest that these microRNAs may play a role in the regulation of expression of the ABCB1 transporter. Thus, to understand whether miR-203 is involved in the regulation of ABCB1 membrane transporters in drug resistance, the transport activity of the ABCB1 efflux pumps in the phenotype of miRNA transfected cells was evaluated by indirectly measuring the intracellular accumulation of the ABCB1 specific fluorescent substrate $DiOC_2$, according to previously described techniques (106).

KCR cells, which have downregulation of miR-203 and miR-200c, and MCF-7 which have upregulation of miR-203 and miR-200c, were transfected, respectively, with mimics/antagomiRs of miR-203, miR-200c and recommended mimic-miR and anti-miR precursors (NC) without any biological function, as negative controls, for 24 h, 48 h and 72 h. After that, transfected cells were analysed for the ability to retain $DiOC_2$ in the presence and absence of VP.

By fluorescent microscopy there were no perceptible differences in the accumulation of $DiOC_2$ in MCF-7 cells. However, after 48 h of transfection, KCR cells showed an increase in the accumulation of $DiOC_2$ (Fig. 42), This period after transfection was chosen to proceed our work by quantifying the intracellular accumulation of fluorescence by flow cytometry.

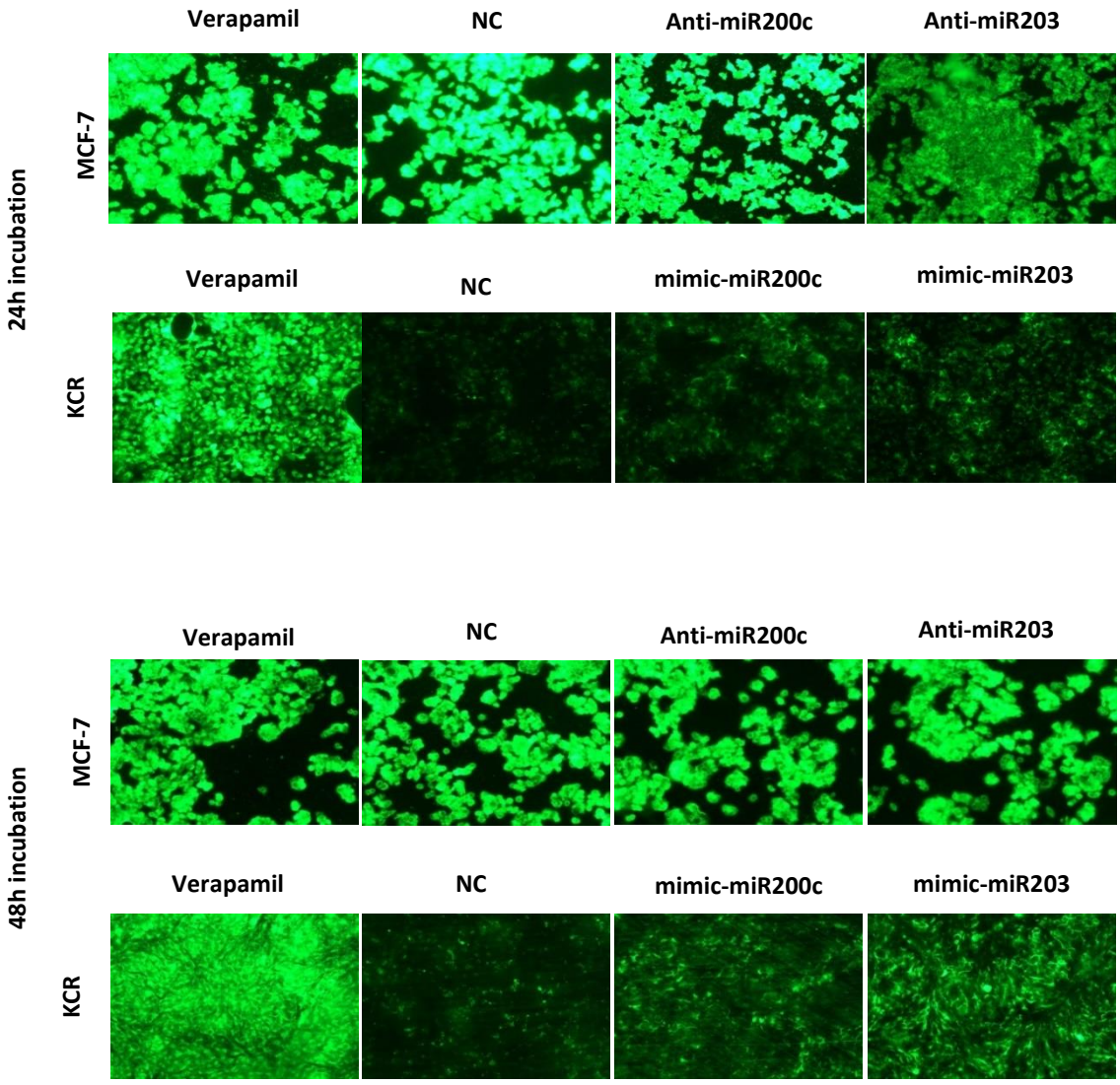

Figure 42: Fluorescence images of $DiOC_2$ accumulation using a dye retention assay in KCR cells. Cells were ectopic transient transfected with mimic-miR-NC and 203 (KCR). After 24 h, 48 h and 72 h of transfection (not shown), cells were observed under a fluorescent microscope (×100 magnification) and images were acquired. In parallel, cells treated with verapamil were also evaluated. Green colour reflects the accumulation of $DiOC_2$ inside the cell.

Flow cytometry analysis of KCR cells transfected with miR-203, miR-200c and NC mimics allowed the quantification of the accumulation of $DiOC_2$ after efflux in the presence and absence of VP, a known inhibitor of ABCB1 efflux pumps. The activity of ABCB1 efflux pumps in mimic-miR-203 KCR transfected cells was significantly impaired compared to the control NC (Fig. 43).

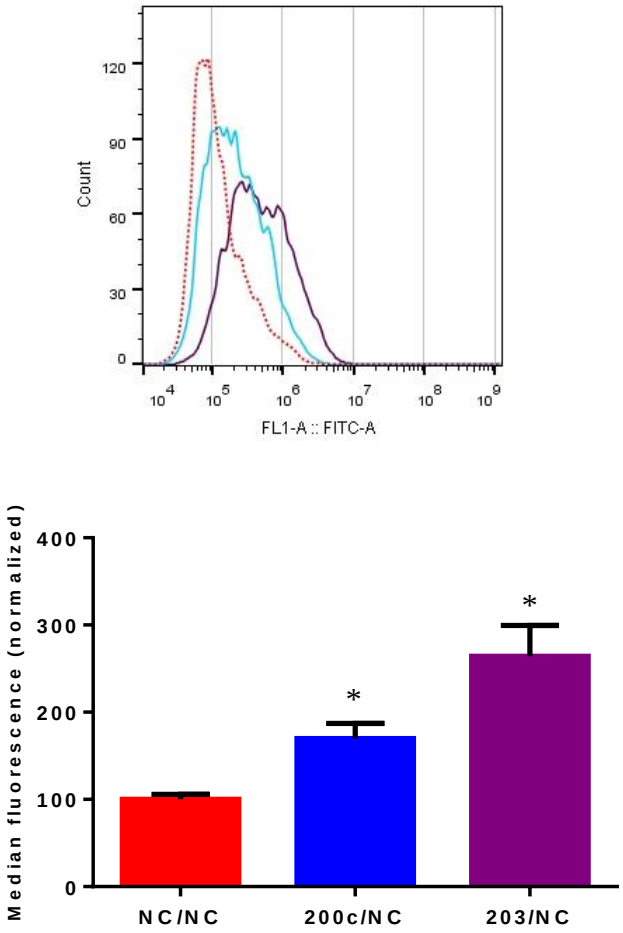

Figure 43: $DiOC_2$ accumulation in KCR transfected cells. $DIOC_2$ accumulation, in KCR cells transfected for 48 h with mimic-miR-negative control (NC), mimic-200c and mimic-miR-203 mimics were evaluated by flow cytometry analysis. Results are expressed by fluorescent means of three independent assays and triplicate per sample. Histogram of a representative experiment is also shown: Red line - negative control (NC), blue line-miR-200c and purple line-miR-203 transfected cells. Data are expressed as the mean ± SEM of four separate experiments (n = 3). * ($p<0.05$) indicate statistical significant differences.

The ABCB1 efflux activity, 48 h after transfection with pre- miR-203 and miR-200c, was verified by the capacity of transfected cells to retain $DiOC_2$ in the presence of VP, a known inhibitor of ABCB1 efflux pumps. VP didn't show a significant inhibitory effect in miR-203 and miR-200c transfected cells as shown in the representative histograms in Fig. 44.

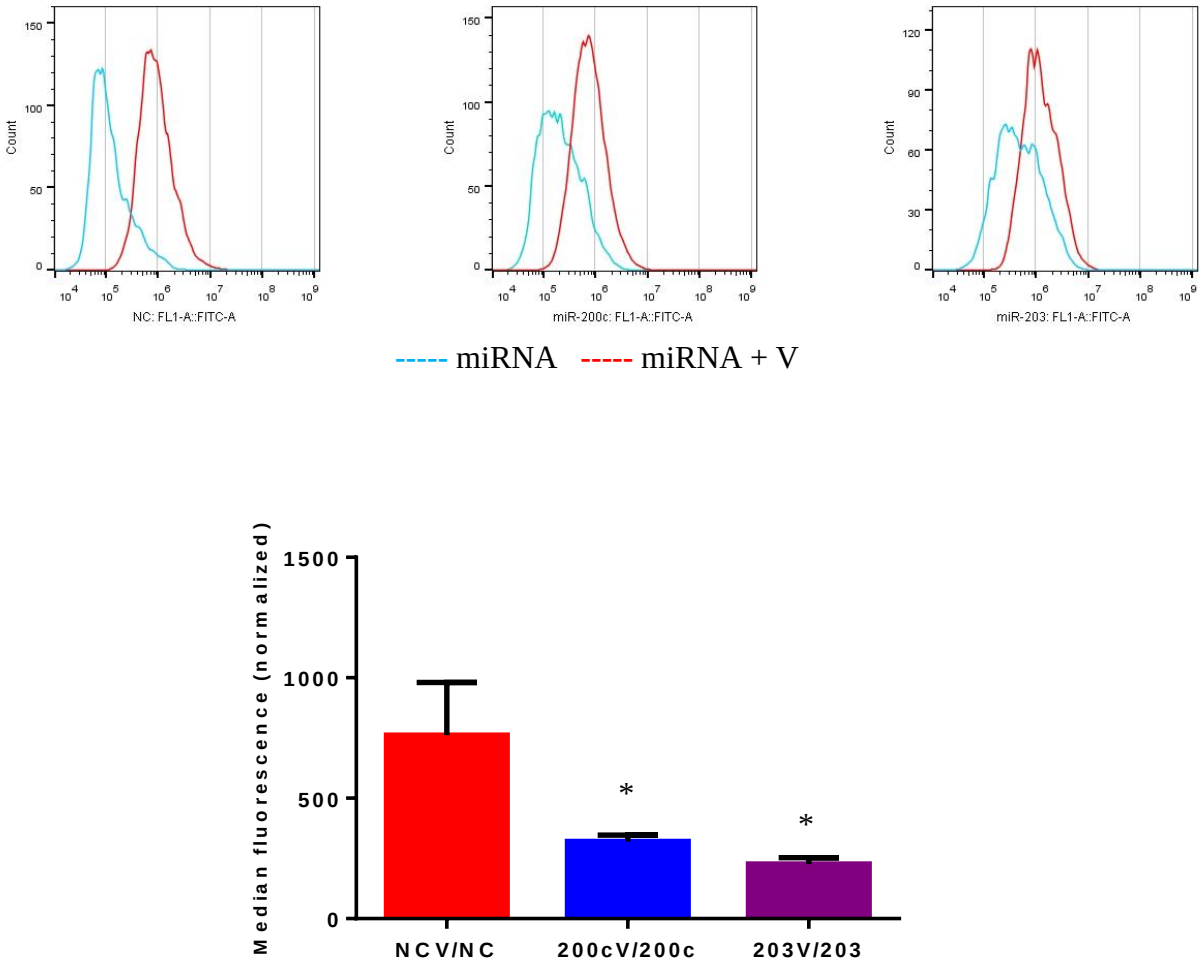

Figure 44: Levels of $DiOC_2$ accumulation in KCR transfected cells in the presence of VP. $DIOC_2$ accumulation, in KCR cells transfected for 48 h with mimics of miR-negative control (NC) and miR-203 and treated with VP, were evaluated by flow cytometry analysis. In parallel untreated cells, untreated transfected KCR cells (NC) and KCR cells treated with VP were also evaluated. Results are expressed by fluorescent means of four independent assays and triplicates per sample normalized to the respective untreated transfected cell. Representative histograms are also shown. Red line – transfected cells in the presence of VP; Blue line – Untreated transfected cells. Results were statistically analyzed by GraphPad Prism 6 software. * ($p<0.05$) indicates significant differences when compared with untreated KCR cells.

However, VP had a more pronounced inhibitory effect in the negative control cells (NC) measured by an increased fluorescent retention inside the cells, which reflects functional efflux of ABCB1 efflux pumps. These results suggest that miR-transfected cells have reduced activity of ABCB1 efflux pumps, most probably and as expected derived from low expression/activity of the ABCB1 (more accumulation indicates less efflux).

4.3.3. Expression of ABCB1/*MDR1* in KCR transfected cells

The ABCB1 expression levels of both mRNA and proteins after cell transfection with miRNA-203a and miR-200c mimics were quantified by RT-qPCR and western blot.

There were no significant differences in ABCB1 expression levels between transfected cells and negative control.

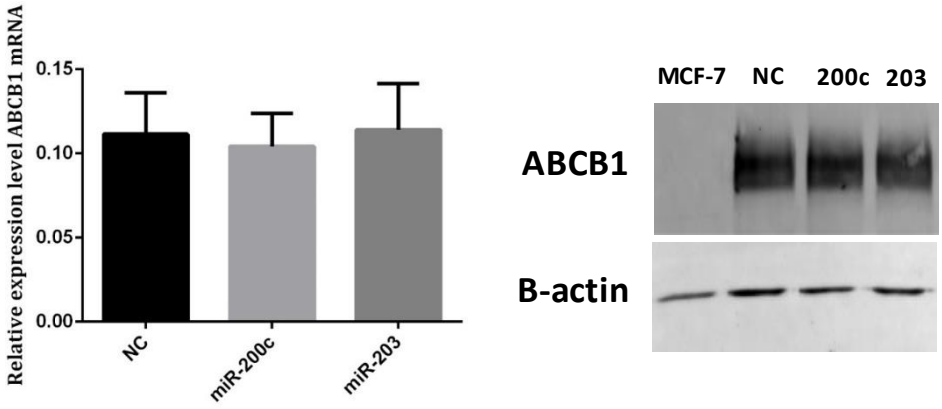

Figure 45: Expression levels of ABCB1 in KCR transfected cells. KCR cells were transfected with mimics-miRs (NC, miR-200c and miR-203) for 48 h. (A) Relative expression levels of ABCB1 mRNA by RT-qPCR in KCR transfected cells. Expression was normalized with respect to the house keeping gene GAPDH. (B) Western blot analysis for protein expression of ABCB1 in MCF-7 and KCR transfected cells. β-actin was used as an internal control. All cells were at passage 4 (n=3, mean values ±SD). There were no significant differences between negative (NC) control and over-expression of miR-200c and miR-203 in KCR cell lines.

Western Blot analysis of membrane proteins of MCF-7, mimic-NC, miR-200c and 203 transfected cell using an anti-MDR1 monoclonal antibody (C219). The 170 kDa band corresponds to ABCB1 protein. In this study the concentration of miRNAs applied were non-toxic, however they exerted just a slight antiproliferative effect during a period of 72 h (Fig. 45).

4.4. **Discussion and Conclusions**

The molecular mechanisms underlying drug resistance in cancer cells still need to be clarified. The MDR phenotype can be triggered by physiological stress signalling pathways induced by chemotherapeutic agents, which enable cancer cells to survive against the harmful action of cytotoxic drugs (222).

Chemotherapeutic drugs like doxorubicin and paclitaxel, described as ABCB1 substrates, can induce the up-regulation of ABCB1 efflux pumps during treatment, directing the upsurge of different acquired resistance mechanisms (223). The mechanisms underlying efflux pump overexpression still need to be elucidated in order to find a strategy to overcome drug resistance. However, it has been observed that this over-expression usually occurs as an early event in the development of MDR, which takes place before other mechanisms are established, such as the modification of drug metabolism, activation of DNA repair mechanisms or apoptotic death prevention. Thus, an important strategy to overcome MDR would be to target the overexpression of ABCB1. One possibility is to use non-coding RNAs that target ABCB1.

Small noncoding microRNAs modulate a great number of biological processes in a post-transcriptional manner by negatively regulating protein expression.

In the present chapter, the modulating effect of miR-203 and miR-200c on the expression and activity of ABCB1 efflux pumps in DOX resistant breast cancer cells that constitutively over-express ABCB1 efflux pumps, was investigated.

We have demonstrated that DOX resistant breast cancer cells (KCR), which over-express ABCB1mRNA and present high levels of ABCB1 have a low expression level of miR-203a and miR-200c compared to its parental sensitive cell line MCF-7. These findings indicate a possible role for miR-203 and miR-200c in DOX resistance and consequently in the phenotype exhibited by breast cancer cell lines.

Recent studies demonstrated that miRNAs can directly or indirectly regulate ABCB1 gene expression (52, 194). In fact, bioinformatics analysis indicates that miR-200c and miR-203 are putative regulators of ABCB1, but only miR-200c has been experimentally

validated (194, 202). Although miR-203 is known to have multiple targets, its role in drug resistance has been linked to different cancers (211).

To confirm the hypothesis of the potential role of miR-203 in drug resistance by over-expression of ABCB1, the activity of this pump was assessed by cell uptake of the fluorescence dye $DiOC_2$, a specific substrate of ABCB1 transporter.

Our findings indicate that miR-203 and miR-200c have a negative role in the regulation of ABCB1 efflux pumps. This was reflected in the significantly higher capacity of miR-203 KCR transfected cells retain $DiOC_2$ when compared to miR-200c transfected cells and to the control cells. The fact that ABCB1 mRNA levels were not significantly changed by transfection corroborates the hypothesis of post-transcriptional regulation of ABCB1 by miR-203 and miR-200c. Furthermore, using a specific efflux inhibitor of ABCB1 pumps, we were able to show that the increased intracellular accumulation of the dye was probably associated with a small decrease of the number of functional ABCB1 efflux pumps in miR-203 and miR-200c transfected cells. However, WB analysis did not show significant differences in the expression of ABCB1 in both miR-203 and miR-200c transfected cells, raising the hypothesis that ABC expression levels do not always correlate with their functional activity (224).

On the other hand, the significant overexpression of ABCB1 in KCR cells may not allow the assessment of a downregulation by these miRNAs. Katayama et al. (225) demonstrated that the half-life of endogenously expressed ABCB1 is 26.7 ± 1.1 h in human colorectal cancer HCT-15 cells. Thus the kinetics of downregulation of ABCB1 expression after transfection by pre-miRNAs may need a substantial period to reduce the levels of ABCB1 protein, over the 48 h period chosen in this experimental setup.

It is also possible that WB analysis might not have been sensitive enough to distinguish small variations in the protein levels. If so, small changes in ABCB1 expression could be enough to reduce the efflux activity, in order to be detected by the functional assays but not noticed by WB. Previous studies have reported differences in the expression level of ABCB1 protein after transfection with miR-200c (208). However, in the present study the methodological conditions were different. Differences include miRNA concentration used in the transfection, transfection agent, membrane extraction method and the origin of the resistant cells, hampering comparisons. In addition, we must be aware that working

with high concentrations of miRNAs mimics can cause non-specific changes in gene expression of cells (226).

These findings are in agreement with what was described by Lebedeva et al. (227) and point out that drug transport activity can be significantly affected even when there are minor changes in the ABCB1 expression levels. Tomonto et al. (198) has recently demonstrated, in lung cancer cell lines, that over-expression of the transcription factor SNAI1 is responsible, indirectly, for the enhanced activity of ABCB1 without affecting ABCB1 protein expression levels by WB. Interesting is that the Snail Family Transcriptional Repressor 1 (SNAI1), one of the key regulatory element of EMT, seems to be involved in the reduction of the promoter activity of miR-203 and miR-200c (216, 228), which can lead to a down-regulation of both miRNAs in drug resistance.

Together with the fact that KCR cells exhibit an EMT gene expression pattern (220), these results indicate a possible indirect role for miR-203 and miR-200c in the negative regulation of the expression/activity of ABCB1 efflux pumps in multidrug-resistance, suggesting that down regulation of both miRNAs are related to drug resistance by over-expression of ABCB1 transporters.

To the best of our knowledge, this is the first time that miR-203 is described as a regulator of ABCB1 in breast cancer drug resistance. Nevertheless, the underlying mechanism responsible for the altered expression of both miR-203 and miR-200c and ABCB1 in doxorubicin resistance breast cancer and their role in the activity of the efflux pump in drug resistance, still need to be addressed in the future. Also, tumors and adjacent normal tissue of patients with breast cancer expressing downregulation of miR-200c and miR-203 should be analyzed in order to highlight the potential role of both miRNAs as biomarkers of drug resistance. This would lead to our final goal that is to establish a miRNA expression level threshold for tumour cells compared to adjacent tissue in order to predict the development of a MDR phenotype by over-expression of ABCB1.

Taken together, these findings raise the hypothesis that miR-203 and miR-200c might be potential markers for DOX resistance in breast cancer cells.

5. Final remarks

Chemotherapy resistance is a major concern in infectious diseases and in cancer patients. The ABCB1 transport system that has been associated with drug resistance in several clinical situations (such as infectious diseases and cancer) is a conserved system in different organisms, ranging from prokaryotic to superior eukaryotic cells.

In the second chapter of the thesis we have adapted, improved, developed and validated new methodologies to evaluate potential modulators of ABC transporters in eukaryotic cell models to be tested in the subsequent chapters.

Subsequently, we have shown in chapter three, for the first time, that ABCB1-like efflux pumps are expressed and functionally active in adult PZQ-resistant *Schistosoma mansoni* worms, a multicellular parasite that causes human disease. The overexpression of functionally active ABCB1 transporters was also demonstrated in cells transformed by malignancy and in mouse macrophages altered in consequence of an infection caused by the intracellular protozoa *Leishmania*.

Furthermore, the ion-channel blocker verapamil, a well-known inhibitor of efflux pumps, is competent in modulating the efflux systems of these different cell models, indicating that ABCB1, at a molecular level, has a similar function, thus the similitude of ABCB1 transporters among eukaryotic and prokaryotic cells makes the application of these methodologies, that were initially optimized for bacteria, possible in eukaryotic cells.

The demonstration of this hypothesis during this thesis is highly relevant, as it shows as a consequence of drug pressure, most of the cells, if not all cells, overexpress ABCB1-like efflux pumps, highlighting how any eukaryotic cell can become resistant to a simple medication by efficient efflux of the drug by all cells. These findings raised some questions and concerns. If this happens in parasites, it is probable that the same occurs in the human body. Chemotherapeutics can induce efflux pump overexpression in target and non-target cells and chemical inhibitors, like VP, can also interact with all cells expressing

ABCB1. The use of VP to revert drug resistance has never reached clinical settings because of the serious side effects that it can cause. However, treating patients with a combination of an efflux inhibitor and a chemotherapeutic, such as PZQ, can be a chemotherapeutic alternative to be used in the future aimed at re-sensitizing resistant cells, as we have demonstrated with therapeutic concentrations of PZQ and drug resistant *Schistosoma mansoni*, thus avoiding unwanted side effects to the human host. The use of natural inhibitors as adjuvants could also be explored in the treatment of schistosomiasis. Treating the long-standing neglected parasite diseases, as in the case of leishmaniasis has also been a challenge explorer in this thesis, following the previous overarching rational. *Leishmania* amastigote parasites live within the phagolysosome of mammalian macrophages, being protected from most drugs. Therefore, total parasite elimination is barely achieved and relapses are common. The efficient modulation of efflux pump activity could facilitate drug access to the intracellular form of the parasite, improving the success of leishmaniasis drug therapy.

Also in the third chapter of this thesis we have been able to demonstrate that the phytochemical 6G has a dual activity in *Leishmania*-infected macrophages. It can modulate efflux pumps, although at high concentrations like OUAB and the other synthetic inhibitors (VP, TZ and CPZ) evaluated in the present study, and it can modulate macrophage immune response to *L. infantum*. To avoid being killed after uptake by macrophages, *Leishmania* parasites regulate macrophage microbicide mechanisms. Thus, taking advantage of the pleiotropic effect of ABCB1 efflux pump inhibitors to counteract parasite effect and stimulate macrophage microbicide mechanisms is a possible new therapeutic strategy for leishmaniasis. To the best of our knowledge, this is the first study that has investigated the immune activity of natural and synthetic inhibitors in *Leishmania*- infected macrophages.

Expanding the rational to human cancer cells in the final sections of chapter three, the pleiotropic effect of natural compounds in mammalian cells, and in the present thesis, was confirmed, and we have been able to demonstrate that the natural compound 6-gingerol inhibits the activity of human ABCB1 efflux pumps, at high but nontoxic concentrations. ABCB1 overexpression in cancer is one of the most common phenotypes associated to drug resistance responsible for treatment failure.

It has widely demonstrated that cell homeostasis can be affected by disease (e.g. cancer; intracellular infections) and by drugs (e.g. anti-cancer drugs). In order to survive, affected cells activate protective responses and make the adjustments needed to preserve a stable internal environment. Cancer cells are able to develop heightened anti-oxidant systems to survive in high oxidative stress environments. These common phenotypic changes also include the overexpression of efflux pumps. Cell homeostasis is an evolutionary mechanism that when disturbed, can result in detrimental outcomes. Ion-channel blockers and 6G have been shown to have the ability to disturb the cell environment, by mechanisms still to be addressed, however ROS, pH and normal function of ABCB1 efflux pumps are involved.

Collateral hypersensitivity emerged during this study, when VP was shown to induce hypersensitivity to PZQ-resistant adult worms, and 6G revealed to be more cytotoxic to drug-resistant cancer cells than to their corresponding sensitive parental cells.

Cellular mechanisms of drug resistance in cancer cells arise by genetic and epigenetic regulation mechanisms that can alter drug sensitivity. MicroRNAs can play a key regulatory role in MDR by modulating pathways linked to drug resistance such as dysregulation of expression of drug transporters.

Our studies carried out in chapter four of this thesis, enable us to conclude that miR-200c and miR-203 are differentially expressed in breast cancer cell lines. Specifically, miR-200c and miR-203 are downregulated in KCR resistant cells while they are over expressed in the MCF-7 cells. According to our data, miR-203 and miR-200c negatively regulate the functionality of ABCB1, however, probably as a result of an indirect target mechanism, as the target sequences of these miRNAs were not identified in available databases. Further studies must now be performed by analyzing tumor and adjacent normal tissue of the same patient in order to validate the *in vitro* data regarding miRNAs expression in drug resistance by overexpression ABCB1 in order to use miR-200c and miR-203 as biomarkers of drug resistance or treatment follow-up.

As one of the major conclusions of this thesis, our work highlighted the need to continue and expand our knowledge by exploring the dual effect of efflux inhibitors, used either in monotherapy or in combination therapy, to overcome drug resistance and treatment failure focusing on cancer cell vulnerabilities and on parasite-host interplay. Moreover,

the findings that phytochemicals, with pleiotropic potential, can modulate ABC transporters and specifically target resistant and infected cells, presenting a lower toxicity *in vitro* to healthy cells. Our findings, many of which still preliminary, opens now an avenue for the research and development of a new line of phytochemical based compounds and miRNAs based adjuvant therapies to prevent and modulate drug resistance in parasitic infections and cancer.

6. Bibliography

1. Gillet JP, Gottesman MM. Mechanisms of multidrug resistance in cancer. Methods in Molecular Biology. 2010;596:47-76.

2. Baguley BC. Multiple drug resistance mechanisms in cancer. Molecular Biotechnology. 2010;46(3):308-16.

3. Housman G, Byler S, Heerboth S, Lapinska K, Longacre M, Snyder N, et al. Drug resistance in cancer: an overview. Cancers. 2014;6(3):1769-92.

4. Ouellette M, Legare D, Papadopoulou B. Multidrug resistance and ABC transporters in parasitic protozoa. Journal of Molecular Microbiology and Biotechnology. 2001;3(2):201-6.

5. Piddock LJ. Clinically relevant chromosomally encoded multidrug resistance efflux pumps in bacteria. Clinical Microbiology Reviews. 2006;19(2):382-402.

6. Van Veen HW, Venema K, Bolhuis H, Oussenko I, Kok J, Poolman B, et al. Multidrug resistance mediated by a bacterial homolog of the human multidrug transporter MDR1. Proceedings of the National Academy of Sciences of the United States of America. 1996;93(20):10668-72.

7. El-Awady R, Saleh E, Hashim A, Soliman N, Dallah A, Elrasheed A, et al. The role of eukaryotic and prokaryotic ABC transporter family in failure of chemotherapy. Frontiers in Pharmacology. 2016;7:535.

8. Vasiliou V, Vasiliou K, Nebert DW. Human ATP-binding cassette (ABC) transporter family. Human Genomics. 2009;3(3):281-90.

9. Dean M, Annilo T. Evolution of the ATP-binding cassette (ABC) transporter superfamily in vertebrates. Annual Review of Genomics and Human Genetics. 2005;6:123-42.

10. Wilkens S. Structure and mechanism of ABC transporters. F1000 Prime Reports. 2015;7:14.

11. Duraisingh MT, Cowman AF. Contribution of the *pfmdr1* gene to antimalarial drug-resistance. Acta Tropica. 2005;94(3):181-90.

12. Gomez C, Perez DG, Lopez-Bayghen E, Orozco E. Transcriptional analysis of the EhPgp1 promoter of *Entamoeba histolytica* multidrug-resistant mutant. The Journal of Biological Chemistry. 1998;273(13):7277-84.

13. Maser P, Kaminsky R. Identification of three ABC transporter genes in *Trypanosoma brucei* spp. Parasitology Research. 1998;84(2):106-11.

14. Shahi SK, Krauth-Siegel RL, Clayton CE. Overexpression of the putative thiol conjugate transporter TbMRPA causes melarsoprol resistance in *Trypanosoma brucei*. Molecular Microbiology. 2002;43(5):1129-38.

15. da Costa KM, Valente RC, Salustiano EJ, Gentile LB, Freire-de-Lima L, Mendonca-Previato L, et al. Functional characterization of ABCC proteins from *Trypanosoma cruzi* and their involvement with thiol transport. Frontiers in Microbiology. 2018;9:205.

16. Coelho AC, Beverley SM, Cotrim PC. Functional genetic identification of PRP1, an ABC transporter superfamily member conferring pentamidine resistance in *Leishmania major*. Molecular and Biochemical Parasitology. 2003;130(2):83-90.

17. Cortes-Selva F, Munoz-Martinez F, Ilias A, Jimenez AI, Varadi A, Gamarro F, et al. Functional expression of a multidrug P-glycoprotein transporter of *Leishmania*. Biochemical and Biophysical Research Communications. 2005;329(2):502-7.

18. Perez-Victoria JM, Di Pietro A, Barron D, Ravelo AG, Castanys S, Gamarro F. Multidrug resistance phenotype mediated by the P-glycoprotein-like transporter in *Leishmania*: a search for reversal agents. Current Drug Targets. 2002;3(4):311-33.

19. Perez-Victoria JM, Cortes-Selva F, Parodi-Talice A, Bavchvarov BI, Perez-Victoria FJ, Munoz-Martinez F, et al. Combination of suboptimal doses of inhibitors targeting different domains of LtrMDR1 efficiently overcomes resistance of *Leishmania* spp. to Miltefosine by inhibiting drug efflux. Antimicrobial Agents and Chemotherapy. 2006;50(9):3102-10.

20. Castanys-Munoz E, Alder-Baerens N, Pomorski T, Gamarro F, Castanys S. A novel ATP-binding cassette transporter from *Leishmania* is involved in transport of phosphatidylcholine analogues and resistance to alkyl-phospholipids. Molecular Microbiology. 2007;64(5):1141-53.

21. Dohmen LC, Navas A, Vargas DA, Gregory DJ, Kip A, Dorlo TP, et al. Functional validation of ABCA3 as a miltefosine transporter in human macrophages: Impact on intracellular survival of *Leishmania (viannia) panamensis*. The Journal of Biological Chemistry. 2016;291(18):9638-47.

22. Pinto-Almeida A, Mendes T, Armada A, Belo S, Carrilho E, Viveiros M, et al. The role of efflux pumps in *Schistosoma mansoni* praziquantel resistant phenotype. PLoS One. 2015;10(10):e0140147.

23. Lismond A, Tulkens PM, Mingeot-Leclercq MP, Courvalin P, Van Bambeke F. Cooperation between prokaryotic (Lde) and eukaryotic (MRP) efflux transporters in J774 macrophages infected with *Listeria monocytogenes*: studies with ciprofloxacin and moxifloxacin. Antimicrobial Agents and Chemotherapy. 2008;52(9):3040-6.

24. Sharom FJ. ABC multidrug transporters: structure, function and role in chemoresistance. Pharmacogenomics. 2008;9(1):105-27.

25. Biedler JL, Riehm H. Cellular resistance to actinomycin D in Chinese hamster cells *in vitro*: cross-resistance, radioautographic, and cytogenetic studies. Cancer Research. 1970;30(4):1174-84.

26. Riordan JR, Deuchars K, Kartner N, Alon N, Trent J, Ling V. Amplification of P-glycoprotein genes in multidrug-resistant mammalian cell lines. Nature. 1985;316(6031):817-9.

27. Locher KP. Review. Structure and mechanism of ATP-binding cassette transporters. Philosophical Transactions of the Royal Society of London Series B, Biological Sciences. 2009;364(1514):239-45.

28. Sauna ZE, Ambudkar SV. About a switch: how P-glycoprotein (ABCB1) harnesses the energy of ATP binding and hydrolysis to do mechanical work. Molecular Cancer Therapeutics. 2007;6(1):13-23.

29. Genovese I, Ilari A, Assaraf YG, Fazi F, Colotti G. Not only P-glycoprotein: Amplification of the ABCB1-containing chromosome region 7q21 confers multidrug resistance upon cancer cells by coordinated overexpression of an assortment of resistance-related proteins. Drug Resistance Updates : Reviews and commentaries in Antimicrobial and Anticancer Chemotherapy. 2017;32:23-46.

30. Paolini A, Baldassarre A, Del Gaudio I, Masotti A. Structural features of the ATP-binding cassette (ABC) transporter ABCA3. International Journal of Molecular Sciences. 2015;16(8):19631-44.

31. Lelong-Rebel IH, Cardarelli CO. Differential phosphorylation patterns of P-glycoprotein reconstituted into a proteoliposome system: insight into additional unconventional phosphorylation sites. Anticancer Research. 2005;25(6b):3925-35.

32. Kim CW, Asai D, Kang JH, Kishimura A, Mori T, Katayama Y. Reversal of efflux of an anticancer drug in human drug-resistant breast cancer cells by inhibition of protein kinase Calpha (PKCalpha) activity. Tumour biology: The Journal of the International Society for Oncodevelopmental Biology and Medicine. 2016;37(2):1901-8.

33. Chen Z, Shi T, Zhang L, Zhu P, Deng M, Huang C, et al. Mammalian drug efflux transporters of the ATP binding cassette (ABC) family in multidrug resistance: A review of the past decade. Cancer Letters. 2016;370(1):153-64.

34. Montanari F, Ecker GF. Prediction of drug-ABC-transporter interaction-recent advances and future challenges. Advanced Drug Delivery Reviews. 2015;86:17-26.

35. Higgins CF, Linton KJ. The ATP switch model for ABC transporters. Nature Structural & Molecular Biology. 2004;11(10):918-26.

36. Strouse JJ, Ivnitski-Steele I, Waller A, Young SM, Perez D, Evangelisti AM, et al. Fluorescent substrates for flow cytometric evaluation of efflux inhibition in ABCB1, ABCC1, and ABCG2 transporters. Analytical Biochemistry. 2013;437(1):77-87.

37. Martinez L, Arnaud O, Henin E, Tao H, Chaptal V, Doshi R, et al. Understanding polyspecificity within the substrate-binding cavity of the human multidrug resistance P-glycoprotein. The FEBS Journal. 2014;281(3):673-82.

38. Michaelis M, Rothweiler F, Wurglics M, Aniceto N, Dittrich M, Zettl H, et al. Substrate-specific effects of pirinixic acid derivatives on ABCB1-mediated drug transport. Oncotarget. 2016;7(10):11664-76.

39. Ferreira RJ, Ferreira MJ, dos Santos DJ. Molecular docking characterizes substrate-binding sites and efflux modulation mechanisms within P-glycoprotein. Journal of Chemical Information and Modeling. 2013;53(7):1747-60.

40. Martin C, Berridge G, Higgins CF, Mistry P, Charlton P, Callaghan R. Communication between multiple drug binding sites on P-glycoprotein. Molecular Pharmacology. 2000;58(3):624-32.

41. Zeino M, Saeed ME, Kadioglu O, Efferth T. The ability of molecular docking to unravel the controversy and challenges related to P-glycoprotein-a well-known, yet poorly understood drug transporter. Investigational New Drugs. 2014;32(4):618-25.

42. Ferreira RJ, dos Santos DJ, Ferreira MJ. P-glycoprotein and membrane roles in multidrug resistance. Future Medicinal Chemistry. 2015;7(7):929-46.

43. Molnar J, Kars MD, Gunduz U, Engi H, Schumacher U, Van Damme EJ, et al. Interaction of tomato lectin with ABC transporter in cancer cells: glycosylation confers functional conformation of P-gp. Acta Histochemica. 2009;111(4):329-33.

44. Sharom FJ. Complex interplay between the P-glycoprotein multidrug efflux pump and the membrane: Its role in modulating protein function. Frontiers in Oncology. 2014;4:41.

45. Sarkadi B, Homolya L, Szakacs G, Varadi A. Human multidrug resistance ABCB and ABCG transporters: participation in a chemoimmunity defense system. Physiological Reviews. 2006;86(4):1179-236.

46. Calcagno AM, Salcido CD, Gillet JP, Wu CP, Fostel JM, Mumau MD, et al. Prolonged drug selection of breast cancer cells and enrichment of cancer stem cell characteristics. Journal of the National Cancer Institute. 2010;102(21):1637-52.

47. Vaidyanathan A, Sawers L, Gannon AL, Chakravarty P, Scott AL, Bray SE, et al. ABCB1 (MDR1) induction defines a common resistance mechanism in paclitaxel- and olaparib-resistant ovarian cancer cells. British Journal of Cancer. 2016;115(4):431-41.

48. Wang YC, Juric D, Francisco B, Yu RX, Duran GE, Chen GK, et al. Regional activation of chromosomal arm 7q with and without gene amplification in taxane-selected human ovarian cancer cell lines. Genes, Chromosomes & Cancer. 2006;45(4):365-74.

49. Henrique R, Oliveira AI, Costa VL, Baptista T, Martins AT, Morais A, et al. Epigenetic regulation of MDR1 gene through post-translational histone modifications in prostate cancer. BMC Genomics. 2013;14:898.

50. Hodges LM, Markova SM, Chinn LW, Gow JM, Kroetz DL, Klein TE, et al. Very important pharmacogene summary: ABCB1 (MDR1, P-glycoprotein). Pharmacogenetics and Genomics. 2011;21(3):152-61.

51. Lu JF, Pokharel D, Bebawy M. A novel mechanism governing the transcriptional regulation of ABC transporters in MDR cancer cells. Drug Delivery and Translational Research. 2017.

52. Kazuhiro Katayama KN, and Yoshikazu Sugimoto. Regulations of P-glycoprotein/ABCB1/MDR1 in human cancer cells. New Journal of Science. 2014;2014:10.

53. An X, Sarmiento C, Tan T, Zhu H. Regulation of multidrug resistance by microRNAs in anti-cancer therapy. Acta Pharmaceutica Sinica B. 2017;7(1):38-51.

54. Lopes-Rodrigues V, Seca H, Sousa D, Sousa E, Lima RT, Vasconcelos MH. The network of P-glycoprotein and microRNAs interactions. International Journal of Cancer Journal International du Cancer. 2014;135(2):253-63.

55. Kasinathan RS, Sharma LK, Cunningham C, Webb TR, Greenberg RM. Inhibition or knockdown of ABC transporters enhances susceptibility of adult and juvenile schistosomes to Praziquantel. PLoS Neglected Tropical Diseases. 2014;8(10):e3265.

56. Johnson DJ, Owen A, Plant N, Bray PG, Ward SA. Drug-regulated expression of *Plasmodium falciparum* P-glycoprotein homologue 1: a putative role for nuclear receptors. Antimicrobial Agents and Chemotherapy. 2008;52(4):1438-45.

57. Rybczynska M, Liu R, Lu P, Sharom FJ, Steinfels E, Pietro AD, et al. MDR1 causes resistance to the antitumour drug miltefosine. British Journal of Cancer. 2001;84(10):1405-11.

58. Amaral L, Spengler G, Martins A, Armada A, Handzlik J, Kiec-Kononowicz K, et al. Inhibitors of bacterial efflux pumps that also inhibit efflux pumps of cancer cells. Anticancer Research. 2012;32(7):2947-57.

59. Carroll RE, Benya RV, Turgeon DK, Vareed S, Neuman M, Rodriguez L, et al. Phase IIa clinical trial of curcumin for the prevention of colorectal neoplasia. Cancer Prevention Research (Philadelphia, Pa). 2011;4(3):354-64.

60. Gromicho M, Dinis J, Magalhaes M, Fernandes AR, Tavares P, Laires A, et al. Development of imatinib and dasatinib resistance: dynamics of expression of drug transporters ABCB1, ABCC1, ABCG2, MVP, and SLC22A1. Leukemia & Lymphoma. 2011;52(10):1980-90.

61. Yang K, Wu J, Li X. Recent advances in the research of P-glycoprotein inhibitors. Bioscience Trends. 2008;2(4):137-46.

62. Ding PR, Tiwari AK, Ohnuma S, Lee JW, An X, Dai CL, et al. The phosphodiesterase-5 inhibitor vardenafil is a potent inhibitor of ABCB1/P-glycoprotein transporter. PLoS One. 2011;6(4):e19329.

63. Mealey KL, Fidel J. P-glycoprotein mediated drug interactions in animals and humans with cancer. Journal of Veterinary Internal Medicine. 2015;29(1):1-6.

64. Palmeira A, Sousa E, Vasconcelos MH, Pinto MM. Three decades of P-gp inhibitors: skimming through several generations and scaffolds. Current Medicinal Chemistry. 2012;19(13):1946-2025.

65. Ozben T. Mechanisms and strategies to overcome multiple drug resistance in cancer. FEBS Letters. 2006;580(12):2903-9.

66. Joshi P, Vishwakarma RA, Bharate SB. Natural alkaloids as P-gp inhibitors for multidrug resistance reversal in cancer. European Journal of Medicinal Chemistry. 2017;138:273-92.

67. Shaffer BC, Gillet JP, Patel C, Baer MR, Bates SE, Gottesman MM. Drug resistance: still a daunting challenge to the successful treatment of AML. Drug resistance updates : Reviews and Commentaries in Antimicrobial and Anticancer Chemotherapy. 2012;15(1-2):62-9.

68. Kelly RJ, Draper D, Chen CC, Robey RW, Figg WD, Piekarz RL, et al. A pharmacodynamic study of docetaxel in combination with the P-glycoprotein antagonist tariquidar (XR9576) in patients with lung, ovarian, and cervical cancer. Clinical Cancer Research: an Official Journal of the American Association for Cancer Research. 2011;17(3):569-80.

69. Eichhorn T, Efferth T. P-glycoprotein and its inhibition in tumors by phytochemicals derived from Chinese herbs. Journal of Ethnopharmacology. 2012;141(2):557-70.

70. Zhu H, Liu Z, Tang L, Liu J, Zhou M, Xie F, et al. Reversal of P-gp and MRP1-mediated multidrug resistance by H6, a gypenoside aglycon from *Gynostemma pentaphyllum*, in vincristine-resistant human oral cancer (KB/VCR) cells. European Journal of Pharmacology. 2012;696(1-3):43-53.

71. Munagala S, Sirasani G, Kokkonda P, Phadke M, Krynetskaia N, Lu P, et al. Synthesis and evaluation of strychnos alkaloids as MDR reversal agents for cancer cell eradication. Bioorganic & Medicinal Chemistry. 2014;22(3):1148-55.

72. Lewandowska U, Gorlach S, Owczarek K, Hrabec E, Szewczyk K. Synergistic interactions between anticancer chemotherapeutics and phenolic compounds and anticancer synergy between polyphenols. Postepy Higieny i Medycyny Doswiadczalnej (Online). 2014;68(0):528-40.

73. Martins C, Doran C, Silva IC, Miranda C, Rueff J, Rodrigues AS. Myristicin from nutmeg induces apoptosis via the mitochondrial pathway and down regulates genes of the DNA damage response pathways in human leukaemia K562 cells. Chemico-Biological Interactions. 2014;218:1-9.

74. Dandawate P, Padhye S, Ahmad A, Sarkar FH. Novel strategies targeting cancer stem cells through phytochemicals and their analogs. Drug Delivery and Translational Research. 2013;3(2):165-82.

75. Singh BN, Singh HB, Singh A, Naqvi AH, Singh BR. Dietary phytochemicals alter epigenetic events and signaling pathways for inhibition of metastasis cascade: phytoblockers of metastasis cascade. Cancer Metastasis Reviews. 2014.

76. Indumathy S, Dass CR. Finding chemo: the search for marine-based pharmaceutical drugs active against cancer. The Journal of Pharmacy and Pharmacology. 2013;65(9):1280-301.

77. Bailey DG, Spence JD, Munoz C, Arnold JM. Interaction of citrus juices with felodipine and nifedipine. Lancet (London, England). 1991;337(8736):268-9.

78. Bansal T, Jaggi M, Khar RK, Talegaonkar S. Emerging significance of flavonoids as P-glycoprotein inhibitors in cancer chemotherapy. Journal of pharmacy & pharmaceutical sciences: a publication of the Canadian Society for Pharmaceutical Sciences, Societe Canadienne des Sciences Pharmaceutiques. 2009;12(1):46-78.

79. Yuan H, Li X, Wu J, Li J, Qu X, Xu W, et al. Strategies to overcome or circumvent P-glycoprotein mediated multidrug resistance. Current Medicinal Chemistry. 2008;15(5):470-6.

80. Khushnud T, Mousa SA. Potential role of naturally derived polyphenols and their nanotechnology delivery in cancer. Molecular Biotechnology. 2013;55(1):78-86.

81. Aggarwal B, Prasad S, Sung B, Krishnan S, Guha S. Prevention and treatment of colorectal cancer by natural agents from mother nature. Current Colorectal Cancer Reports. 2013;9(1):37-56.

82. Nabekura T. Overcoming multidrug resistance in human cancer cells by natural compounds. Toxins. 2010;2(6):1207-24.

83. Dorai T, Aggarwal BB. Role of chemopreventive agents in cancer therapy. Cancer Letters. 2004;215(2):129-40.

84. Martins A, Toth N, Vanyolos A, Beni Z, Zupko I, Molnar J, et al. Significant activity of ecdysteroids on the resistance to doxorubicin in mammalian cancer cells expressing the human ABCB1 transporter. Journal of Medicinal Chemistry. 2012;55(11):5034-43.

85. Kim TH, Shin YJ, Won AJ, Lee BM, Choi WS, Jung JH, et al. Resveratrol enhances chemosensitivity of doxorubicin in multidrug-resistant human breast cancer cells via increased cellular influx of doxorubicin. Biochimica et Biophysica Acta. 2014;1840(1):615-25.

86. Du G, Lin H, Yang Y, Zhang S, Wu X, Wang M, et al. Dietary quercetin combining intratumoral doxorubicin injection synergistically induces rejection of established breast cancer in mice. International Immunopharmacology. 2010;10(7):819-26.

87. Ansbro MR, Shukla S, Ambudkar SV, Yuspa SH, Li L. Screening compounds with a novel high-throughput ABCB1-mediated efflux assay identifies drugs with known therapeutic targets at risk for multidrug resistance interference. PLoS One. 2013;8(4):e60334.

88. Liu W, Zhou CL, Zhao J, Chen D, Li QH. Optimized microwave-assisted extraction of 6-gingerol from *Zingiber officinale* Roscoe and evaluation of antioxidant activity *in vitro*. Acta Scientiarum Polonorum Technologia Alimentaria. 2014;13(2):155-68.

89. Groblacher B, Maier V, Kunert O, Bucar F. Putative mycobacterial efflux inhibitors from the seeds of *Aframomum melegueta.* Journal of Natural Products. 2012;75(7):1393-9.

90. Clark R, Lee SH. Anticancer properties of capsaicin against human cancer. Anticancer Research. 2016;36(3):837-43.

91. Lv L, Chen H, Soroka D, Chen X, Leung T, Sang S. 6-gingerdiols as the major metabolites of 6-gingerol in cancer cells and in mice and their cytotoxic effects on human cancer cells. Journal of Agricultural and Food Chemistry. 2012;60(45):11372-7.

92. Geng S, Zheng Y, Meng M, Guo Z, Cao N, Ma X, et al. Gingerol reverses the cancer-promoting effect of capsaicin by Increased TRPV1 level in a urethane-induced lung carcinogenic model. Journal of Agricultural and Food Chemistry. 2016;64(31):6203-11.

93. Li H, Krstin S, Wang S, Wink M. Capsaicin and piperine can overcome multidrug resistance in cancer cells to doxorubicin. Molecules. 2018;23(3).

94. Kapoor V, Aggarwal S, Das SN. 6-Gingerol mediates its anti tumor activities in human oral and cervical cancer cell lines through apoptosis and cell cycle arrest. Phytotherapy Research : PTR. 2016;30(4):588-95.

95. Chen CY, Chen CH, Kung CH, Kuo SH, Kuo SY. [6]-gingerol induces Ca^{2+} mobilization in Madin-Darby canine kidney cells. Journal of Natural Products. 2008;71(1):137-40.

96. Mahady GB, Pendland SL, Yun GS, Lu ZZ, Stoia A. Ginger (*Zingiber officinale* Roscoe) and the gingerols inhibit the growth of Cag A+ strains of Helicobacter pylori. Anticancer Research. 2003;23(5a):3699-702.

97. Nabekura T, Kamiyama S, Kitagawa S. Effects of dietary chemopreventive phytochemicals on P-glycoprotein function. Biochemical and Biophysical Research Communications. 2005;327(3):866-70.

98. Kim TH, Shin S. Effects of phytochemical P-glycoprotein modulators on the pharmacokinetics and tissue distribution of doxorubicin in mice. Molecules. 2018;23(2).

99. Krishan A, Fitz CM, Andritsch I. Drug retention, efflux, and resistance in tumor cells. Cytometry. 1997;29(4):279-85.

100. Spengler G, Ramalhete C, Martins M, Martins A, Serly J, Viveiros M, et al. Evaluation of cucurbitane-type triterpenoids from *Momordica balsamina* on P-glycoprotein (ABCB1) by flow cytometry and real-time fluorometry. Anticancer Research. 2009;29(10):3989-93.

101. Spengler G, Viveiros M, Martins M, Rodrigues L, Martins A, Molnar J, et al. Demonstration of the activity of P-glycoprotein by a semi-automated fluorometric method. Anticancer Research. 2009;29(6):2173-7.

102. Viveiros M, Martins A, Paixao L, Rodrigues L, Martins M, Couto I, et al. Demonstration of intrinsic efflux activity of *Escherichia coli* K-12 AG100 by an automated ethidium bromide method. International Journal of Antimicrobial Agents. 2008;31(5):458-62.

103. Shapiro HM. "Cellular astronomy"--a foreseeable future in cytometry. Cytometry Part A : the journal of the International Society for Analytical Cytology. 2004;60(2):115-24.

104. Szakacs G, Paterson JK, Ludwig JA, Booth-Genthe C, Gottesman MM. Targeting multidrug resistance in cancer. Nature Reviews Drug Discovery. 2006;5(3):219-34.

105. Spengler G, Evaristo M, Handzlik J, Serly J, Molnar J, Viveiros M, et al. Biological activity of hydantoin derivatives on P-glycoprotein (ABCB1) of mouse lymphoma cells. Anticancer Research. 2010;30(12):4867-71.

106. Armada A, Martins C, Spengler G, Molnar J, Amaral L, Rodrigues AS, et al. Fluorimetric methods for analysis of permeability, drug transport kinetics, and inhibition of the ABCB1 membrane transporter. Methods in Molecular Biology (Clifton, NJ). 2016;1395:87-103.

107. Katz N, Coelho PM. Clinical therapy of *Schistosomiasis mansoni*: the Brazilian contribution. Acta Tropica. 2008;108(2-3):72-8.

108. Viveiros M, Rodrigues L, Martins M, Couto I, Spengler G, Martins A, et al. Evaluation of efflux activity of bacteria by a semi-automated fluorometric system. Methods in Molecular Biology. 2010;642:159-72.

109. Rodrigues L, Ramos J, Couto I, Amaral L, Viveiros M. Ethidium bromide transport across *Mycobacterium smegmatis* cell-wall: correlation with antibiotic resistance. BMC Microbiology. 2011;11:35.

110. Kasinathan RS, Goronga T, Messerli SM, Webb TR, Greenberg RM. Modulation of a *Schistosoma mansoni* multidrug transporter by the antischistosomal drug praziquantel. FASEB Journal : Official Publication of the Federation of American Societies for Experimental Biology. 2010;24(1):128-35.

111. Kasinathan RS, Morgan WM, Greenberg RM. *Schistosoma mansoni* express higher levels of multidrug resistance-associated protein 1 (SmMRP1) in juvenile worms and in response to praziquantel. Molecular and Biochemical Parasitology. 2010;173(1):25-31.

112. Messerli SM, Kasinathan RS, Morgan W, Spranger S, Greenberg RM. *Schistosoma mansoni* P-glycoprotein levels increase in response to praziquantel exposure and correlate with reduced praziquantel susceptibility. Molecular and Biochemical Parasitology. 2009;167(1):54-9.

113. Liang YS, Wang W, Dai JR, Li HJ, Tao YH, Zhang JF, et al. Susceptibility to praziquantel of male and female cercariae of praziquantel-resistant and susceptible isolates of *Schistosoma mansoni*. Journal of Helminthology. 2010;84(2):202-7.

114. Kasinathan RS, Greenberg RM. Pharmacology and potential physiological significance of *Schistosome* multidrug resistance transporters. Experimental Parasitology. 2012;132(1):2-6.

115. Ardelli BF, Prichard RK. Inhibition of P-glycoprotein enhances sensitivity of Caenorhabditis elegans to ivermectin. Veterinary Parasitology. 2013;191(3-4):264-75.

116. Kerboeuf D, Guegnard F, Le Vern Y. Analysis and partial reversal of multidrug resistance to anthelmintics due to P-glycoprotein in *Haemonchus contortus* eggs using *Lens culinaris* lectin. Parasitology Research. 2002;88(9):816-21.

117. Hall MD, Handley MD, Gottesman MM. Is resistance useless? Multidrug resistance and collateral sensitivity. Trends in Pharmacological Sciences. 2009;30(10):546-56.

118. Greenberg RM. ABC multidrug transporters in *Schistosomes* and other parasitic flatworms. Parasitology International. 2013;62(6):647-53.

119. Pica-Mattoccia L, Cioli D. Sex- and stage-related sensitivity of *Schistosoma mansoni* to *in vivo* and *in vitro* praziquantel treatment. International Journal for Parasitology. 2004;34(4):527-33.

120. Aly IR, Hendawy MA, Ali E, Hassan E, Nosseir MM. Immunological and parasitological parameters after treatment with dexamethasone in murine *Schistosoma mansoni*. Memorias do Instituto Oswaldo Cruz. 2010;105(6):729-35.

121. Bin Dajem SM, Mostafa OM, El-Said FG. Susceptibility of two strains of mice to the infection with *Schistosoma mansoni*: parasitological and biochemical studies. Parasitology Research. 2008;103(5):1059-63.

122. Manson P. Report of a case of bilharzia from the West Indies. British Medical Journal. 1902;2(2190):1894-5.

123. Leta S, Dao TH, Mesele F, Alemayehu G. Visceral leishmaniasis in Ethiopia: an evolving disease. PLoS Neglected Tropical Diseases. 2014;8(9):e3131.

124. Tiuman TS, Santos AO, Ueda-Nakamura T, Filho BP, Nakamura CV. Recent advances in leishmaniasis treatment. International Journal of Infectious Diseases : IJID : Official publication of the International Society for Infectious Diseases. 2011;15(8):e525-32.

125. Brito AM, Dos Santos D, Rodrigues SA, Brito RG, Xavier-Filho L. Plants with anti-*Leishmania* activity: Integrative review from 2000 to 2011. Pharmacognosy Reviews. 2013;7(13):34-41.

126. Singh N, Mishra BB, Bajpai S, Singh RK, Tiwari VK. Natural product based leads to fight against leishmaniasis. Bioorganic & Medicinal Chemistry. 2014;22(1):18-45.

127. Sifaoui I, Lopez-Arencibia A, Martin-Navarro CM, Chammem N, Reyes-Batlle M, Mejri M, et al. Activity of olive leaf extracts against the promastigote stage of *Leishmania* species and their correlation with the antioxidant activity. Experimental Parasitology. 2014;141:106-11.

128. Oryan A. Plant-derived compounds in treatment of leishmaniasis. Iranian Journal of Veterinary Research. 2015;16(1):1-19.

129. Cantacessi C, Dantas-Torres F, Nolan MJ, Otranto D. The past, present, and future of *Leishmania* genomics and transcriptomics. Trends in Parasitology. 2015;31(3):100-8.

130. Dean M. ABC transporters, drug resistance, and cancer stem cells. Journal of Mammary Gland Biology and Neoplasia. 2009;14(1):3-9.

131. Lage H. An overview of cancer multidrug resistance: a still unsolved problem. Cellular and Molecular Life Sciences : CMLS. 2008;65(20):3145-67.

132. Higgins CF. Multiple molecular mechanisms for multidrug resistance transporters. Nature. 2007;446(7137):749-57.

133. Gatti L, Beretta GL, Cossa G, Zunino F, Perego P. ABC transporters as potential targets for modulation of drug resistance. Mini Reviews in Medicinal Chemistry. 2009;9(9):1102-12.

134. Nagle AS, Khare S, Kumar AB, Supek F, Buchynskyy A, Mathison CJ, et al. Recent developments in drug discovery for leishmaniasis and human African Trypanosomiasis. Chemical Reviews. 2014;114(22):11305-47.

135. Miguel DC, Yokoyama-Yasunaka JK, Uliana SR. Tamoxifen is effective in the treatment of *Leishmania amazonensis* infections in mice. PLoS Neglected Tropical Diseases. 2008;2(6):e249.

136. Amaral L, Martins M, Viveiros M. Enhanced killing of intracellular multidrug-resistant *Mycobacterium tuberculosis* by compounds that affect the activity of efflux pumps. The Journal of Antimicrobial Chemotherapy. 2007;59(6):1237-46.

137. Martins M, Viveiros M, Amaral L. Inhibitors of Ca^{2+} and K^{+} transport enhance intracellular killing of *M. tuberculosis* by non-killing macrophages. In vivo. 2008;22(1):69-75.

138. Martins M, Viveiros M, Couto I, Amaral L. Targeting human macrophages for enhanced killing of intracellular XDR-TB and MDR-TB. The International Journal of Tuberculosis and Lung Disease : The Official Journal of the International Union against Tuberculosis and Lung Disease. 2009;13(5):569-73.

139. Viveiros M, Martins M, Couto I, Rodrigues L, Machado D, Portugal I, et al. Molecular tools for rapid identification and novel effective therapy against MDRTB/XDRTB infections. Expert Review of Anti-infective Therapy. 2010;8(4):465-80.

140. Reeves EP, Lu H, Jacobs HL, Messina CG, Bolsover S, Gabella G, et al. Killing activity of neutrophils is mediated through activation of proteases by K^+ flux. Nature. 2002;416(6878):291-7.

141. Ahluwalia J, Tinker A, Clapp LH, Duchen MR, Abramov AY, Pope S, et al. The large-conductance Ca^{2+}-activated K^+ channel is essential for innate immunity. Nature. 2004;427(6977):853-8.

142. Essodaigui M, Frezard F, Moreira ES, Dagger F, Garnier-Suillerot A. Energy-dependent efflux from *Leishmania* promastigotes of substrates of the mammalian multidrug resistance pumps. Molecular and Biochemical Parasitology. 1999;100(1):73-84.

143. Grigore D, Meade JC. A COOH-terminal domain regulates the activity of *Leishmania* proton pumps LDH1A and LDH1B. International Journal for Parasitology. 2006;36(4):381-93.

144. Pearson RD, Manian AA, Harcus JL, Hall D, Hewlett EL. Lethal effect of phenothiazine neuroleptics on the pathogenic protozoan *Leishmania donovani*. Science (New York, NY). 1982;217(4557):369-71.

145. Croft SL, Coombs GH. Leishmaniasis--current chemotherapy and recent advances in the search for novel drugs. Trends in Parasitology. 2003;19(11):502-8.

146. Mookerjee Basu J, Mookerjee A, Banerjee R, Saha M, Singh S, Naskar K, et al. Inhibition of ABC transporters abolishes antimony resistance in *Leishmania* Infection. Antimicrobial Agents and Chemotherapy. 2008;52(3):1080-93.

147. Haldar AK, Sen P, Roy S. Use of antimony in the treatment of leishmaniasis: current status and future directions. Molecular Biology International. 2011;2011:571242.

148. Singh N, Gupta R, Jaiswal AK, Sundar S, Dube A. Transgenic *Leishmania donovani* clinical isolates expressing green fluorescent protein constitutively for rapid and reliable *ex vivo* drug screening. The Journal of Antimicrobial Chemotherapy. 2009;64(2):370-4.

149. Armada A, Gazarini ML, Goncalves LM, Antunes S, Custodio A, Rodrigues A, et al. Generation of an antibody that recognizes *Plasmodium chabaudi* cysteine protease (chabaupain-1) in both sexual and asexual parasite life cycle and evaluation of chabaupain-1 vaccine potential. Experimental Parasitology. 2013;135(1):166-74.

150. Brito MA, Rosa AI, Falcao AS, Fernandes A, Silva RF, Butterfield DA, et al. Unconjugated bilirubin differentially affects the redox status of neuronal and astroglial cells. Neurobiology of Disease. 2008;29(1):30-40.

151. Paixao L, Rodrigues L, Couto I, Martins M, Fernandes P, de Carvalho CC, et al. Fluorometric determination of ethidium bromide efflux kinetics in *Escherichia coli*. Journal of Biological Engineering. 2009;3:18.

152. Song L, Cui R, Yang Y, Wu X. Role of calcium channels in cellular antituberculosis effects: Potential of voltage-gated calcium-channel blockers in tuberculosis therapy. Journal of Microbiology, Immunology, and Infection. 2015;48(5):471-6.

153. Meister S, Frey B, Lang VR, Gaipl US, Schett G, Schlotzer-Schrehardt U, et al. Calcium channel blocker verapamil enhances endoplasmic reticulum stress and cell death induced by proteasome inhibition in myeloma cells. Neoplasia. 2010;12(7):550-61.

154. Lee TY, Lee KC, Chen SY, Chang HH. 6-Gingerol inhibits ROS and iNOS through the suppression of PKC-alpha and NF-kappaB pathways in lipopolysaccharide-stimulated mouse macrophages. Biochemical and Biophysical Research Communications. 2009;382(1):134-9.

155. De Muylder G, Vanhollebeke B, Caljon G, Wolfe AR, McKerrow J, Dujardin JC. Naloxonazine, an amastigote-specific compound, affects *Leishmania* parasites through modulation of host-encoded functions. PLoS Neglected Tropical Diseases. 2016;10(12):e0005234.

156. Bruns H, Stegelmann F, Fabri M, Dohner K, van Zandbergen G, Wagner M, et al. Abelson tyrosine kinase controls phagosomal acidification required for killing of *Mycobacterium tuberculosis* in human macrophages. Journal of Immunology. 2012;189(8):4069-78.

157. Liang N, Sang Y, Liu W, Yu W, Wang X. Anti-inflammatory effects of gingerol on lipopolysaccharide-stimulated RAW 264.7 cells by inhibiting *NF-kappaB* signaling pathway. Inflammation. 2018; 41(3):835-845.

158. Guestini F, McNamara KM, Ishida T, Sasano H. Triple negative breast cancer chemosensitivity and chemoresistance: current advances in biomarkers indentification. Expert Opinion on Therapeutic Targets. 2016;20(6):705-20.

159. Tulsyan S, Mittal RD, Mittal B. The effect of ABCB1 polymorphisms on the outcome of breast cancer treatment. Pharmacogenomics and Personalized Medicine. 2016;9:47-58.

160. Kathawala RJ, Gupta P, Ashby CR, Jr., Chen ZS. The modulation of ABC transporter-mediated multidrug resistance in cancer: a review of the past decade. Drug resistance updates : Reviews and Commentaries in Antimicrobial and Anticancer Chemotherapy. 2015;18:1-17.

161. Liu J, Wang Z. Increased oxidative stress as a selective anticancer therapy. Oxidative Medicine and Cellular Longevity. 2015;2015:294303.

162. Ding S, Li C, Cheng N, Cui X, Xu X, Zhou G. Redox regulation in cancer stem cells. Oxidative Medicine and Cellular Longevity. 2015;2015:750798.

163. Kizaki M. New therapeutic approach for myeloid leukemia: induction of apoptosis via modulation of reactive oxygen species production by natural compounds. International Journal of Hematology. 2006;83(4):283-8.

164. Kelkel M, Jacob C, Dicato M, Diederich M. Potential of the dietary antioxidants resveratrol and curcumin in prevention and treatment of hematologic malignancies. Molecules (Basel, Switzerland). 2010;15(10):7035-74.

165. Pesakhov S, Khanin M, Studzinski GP, Danilenko M. Distinct combinatorial effects of the plant polyphenols curcumin, carnosic acid, and silibinin on proliferation and apoptosis in acute myeloid leukemia cells. Nutrition and Cancer. 2010;62(6):811-24.

166. Demain AL, Vaishnav P. Natural products for cancer chemotherapy. Microbial Biotechnology. 2011;4(6):687-99.

167. Kinghorn AD, EJ DEB, Lucas DM, Rakotondraibe HL, Orjala J, Soejarto DD, et al. Discovery of anticancer agents of diverse natural origin. Anticancer Research. 2016;36(11):5623-37.

168. Pereira MM, Haniadka R, Chacko PP, Palatty PL, Baliga MS. *Zingiber officinale* Roscoe (ginger) as an adjuvant in cancer treatment: a review. Journal of BUON : Official Journal of the Balkan Union of Oncology. 2011;16(3):414-24.

169. Kars MD, Iseri OD, Gunduz U, Ural AU, Arpaci F, Molnar J. Development of rational in vitro models for drug resistance in breast cancer and modulation of MDR by selected compounds. Anticancer Research. 2006;26(6b):4559-68.

170. Calcagno AM, Ambudkar SV. Molecular mechanisms of drug resistance in single-step and multi-step drug-selected cancer cells. Methods in Molecular Biology. 2010;596:77-93.

171. Radhakrishnan EK, Bava SV, Narayanan SS, Nath LR, Thulasidasan AK, Soniya EV, et al. [6]-Gingerol induces caspase-dependent apoptosis and prevents PMA-induced proliferation in colon cancer cells by inhibiting MAPK/AP-1 signaling. PLoS One. 2014;9(8):e104401.

172. Pluchino KM, Hall MD, Goldsborough AS, Callaghan R, Gottesman MM. Collateral sensitivity as a strategy against cancer multidrug resistance. Drug Resistance Updates : Reviews and Commentaries in Antimicrobial and Anticancer Chemotherapy. 2012;15(1-2):98-105.

173. Callaghan R, Luk F, Bebawy M. Inhibition of the multidrug resistance P-glycoprotein: time for a change of strategy? Drug Metabolism and Disposition: The Biological Fate of Chemicals. 2014;42(4):623-31.

174. Sita G, Hrelia P. P-glycoprotein (ABCB1) and Oxidative Stress: Focus on Alzheimer's disease. Oxidative Medicine and Cellular Longevity. 2017; 2017:7905486.

175. Zeng HL, Han XA, Gu C, Zhu HY, Huang XS, Gu JQ, et al. [Reactive oxygen species and mitochondrial membrane potential changes in leukemia cells during 6-gingerol induced apoptosis]. Journal of Chinese Medicinal Materials. 2010;33(4):584-7.

176. Rastogi N, Gara RK, Trivedi R, Singh A, Dixit P, Maurya R, et al. (6)-Gingerol induced myeloid leukemia cell death is initiated by reactive oxygen species and activation of miR-27b expression. Free Radical Biology & Medicine. 2014;68:288-301.

177. Lin CB, Lin CC, Tsay GJ. 6-Gingerol inhibits growth of colon cancer cell LoVo via induction of G2/M arrest. Evidence-Based Complementary and Alternative Medicine 2012;2012:326096.

178. Karwatsky J, Lincoln MC, Georges E. A mechanism for P-glycoprotein-mediated apoptosis as revealed by verapamil hypersensitivity. Biochemistry. 2003;42(42):12163-73.

179. Hall MD, Marshall TS, Kwit AD, Miller Jenkins LM, Dulcey AE, Madigan JP, et al. Inhibition of glutathione peroxidase mediates the collateral sensitivity of multidrug-resistant cells to tiopronin. The Journal of Biological Chemistry. 2014;289(31):21473-89.

180. Hecht F, Pessoa CF, Gentile LB, Rosenthal D, Carvalho DP, Fortunato RS. The role of oxidative stress on breast cancer development and therapy. Tumour Biology: The Journal of the International Society for Oncodevelopmental Biology and Medicine. 2016;37(4):4281-91.

181. Lopes-Rodrigues V, Sousa E, Vasconcelos MH. Curcumin as a modulator of P-glycoprotein in cancer: challenges and perspectives. Pharmaceuticals. 2016;9(4).

182. Ambudkar SV, Dey S, Hrycyna CA, Ramachandra M, Pastan I, Gottesman MM. Biochemical, cellular, and pharmacological aspects of the multidrug transporter. Annual Review of Pharmacology and Toxicology. 1999;39:361-98.

183. Milani A, Geuna E, Mittica G, Valabrega G. Overcoming endocrine resistance in metastatic breast cancer: current evidence and future directions. World Journal of Clinical Oncology. 2014;5(5):990-1001.

184. Marquette C, Nabell L. Chemotherapy-resistant metastatic breast cancer. Current Treatment Options in Oncology. 2012;13(2):263-75.

185. Tegze B, Szallasi Z, Haltrich I, Penzvalto Z, Toth Z, Liko I, et al. Parallel evolution under chemotherapy pressure in 29 breast cancer cell lines results in dissimilar mechanisms of resistance. PLoS One. 2012;7(2):e30804.

186. Singh A, Settleman J. EMT, cancer stem cells and drug resistance: an emerging axis of evil in the war on cancer. Oncogene. 2010;29(34):4741-51.

187. Gomes BC, Martins M, Lopes P, Morujao I, Oliveira M, Araujo A, et al. Prognostic value of microRNA-203a expression in breast cancer. Oncology Reports. 2016;36(3):1748-56.

188. Gottesman MM. Mechanisms of cancer drug resistance. Annual Review of Medicine. 2002;53:615-27.

189. Gottesman MM, Pastan IH. The role of multidrug resistance efflux pumps in cancer: Revisiting a JNCI publication exploring expression of the MDR1 (P-glycoprotein) gene. Journal of the National Cancer Institute. 2015;107(9).

190. Atalay C, Demirkazik A, Gunduz U. Role of ABCB1 and ABCC1 gene induction on survival in locally advanced breast cancer. Journal of Chemotherapy (Florence, Italy). 2008;20(6):734-9.

191. Gromicho M, Magalhaes M, Torres F, Dinis J, Fernandes AR, Rendeiro P, et al. Instability of mRNA expression signatures of drug transporters in chronic myeloid leukemia patients resistant to imatinib. Oncology Reports. 2013;29(2):741-50.

192. Gottesman MM, Fojo T, Bates SE. Multidrug resistance in cancer: role of ATP-dependent transporters. Nature Reviews Cancer. 2002;2(1):48-58.

193. Gomes BC, Rueff J, Rodrigues AS. MicroRNAs and cancer drug resistance. Methods in Molecular Biology. 2016;1395:137-62.

194. Haenisch S, Werk AN, Cascorbi I. MicroRNAs and their relevance to ABC transporters. British Journal of Clinical Pharmacology. 2014;77(4):587-96.

195. Ikemura K, Iwamoto T, Okuda M. MicroRNAs as regulators of drug transporters, drug-metabolizing enzymes, and tight junctions: implication for intestinal barrier function. Pharmacology & Therapeutics. 2014;143(2):217-24.

196. Riquelme I, Letelier P, Riffo-Campos AL, Brebi P, Roa JC. Emerging role of miRNAs in the drug resistance of gastric cancer. International Journal of Molecular Sciences. 2016;17(3):424.

197. Liang XJ, Chen C, Zhao Y, Wang PC. Circumventing tumor resistance to chemotherapy by nanotechnology. Methods in Molecular Biology. 2010;596:467-88.

198. Tomono T, Yano K, Ogihara T. Snail-induced epithelial-to-mesenchymal transition enhances P-gp-mediated multidrug resistance in HCC827 Cells. Journal of Pharmaceutical Sciences. 2017;106(9):2642-9.

199. Guo F, Parker Kerrigan BC, Yang D, Hu L, Shmulevich I, Sood AK, et al. Post-transcriptional regulatory network of epithelial-to-mesenchymal and mesenchymal-to-epithelial transitions. Journal of Hematology & Oncology. 2014;7:19.

200. Hamano R, Miyata H, Yamasaki M, Kurokawa Y, Hara J, Moon JH, et al. Overexpression of miR-200c induces chemoresistance in esophageal cancers mediated through activation of the Akt signaling pathway. Clinical Cancer Research : an official Journal of the American Association for Cancer Research. 2011;17(9):3029-38.

201. Ma C, Huang T, Ding YC, Yu W, Wang Q, Meng B, et al. MicroRNA-200c overexpression inhibits chemoresistance, invasion and colony formation of human pancreatic cancer stem cells. International Journal of Clinical and Experimental Pathology. 2015;8(6):6533-9.

202. Sui H, Cai GX, Pan SF, Deng WL, Wang YW, Chen ZS, et al. miR200c attenuates P-gp-mediated MDR and metastasis by targeting JNK2/c-Jun signaling pathway in colorectal cancer. Molecular Cancer Therapeutics. 2014;13(12):3137-51.

203. Liu Y, Gao S, Chen X, Liu M, Mao C, Fang X. Overexpression of miR-203 sensitizes paclitaxel (Taxol)-resistant colorectal cancer cells through targeting the salt-inducible kinase 2 (SIK2). Tumour Biology : The Journal of the International Society for Oncodevelopmental Biology and Medicine. 2016;37(9):12231-9.

204. Ru P, Steele R, Hsueh EC, Ray RB. Anti-miR-203 upregulates SOCS3 expression in breast cancer cells and enhances cisplatin chemosensitivity. Genes & Cancer. 2011;2(7):720-7.

205. Drago-Garcia D, Espinal-Enriquez J, Hernandez-Lemus E. Network analysis of EMT and MET micro-RNA regulation in breast cancer. Scientific Reports. 2017;7(1):13534.

206. Obayashi M, Yoshida M, Tsunematsu T, Ogawa I, Sasahira T, Kuniyasu H, et al. microRNA-203 suppresses invasion and epithelial-mesenchymal transition induction via targeting NUAK1 in head and neck cancer. Oncotarget. 2016;7(7):8223-39.

207. Taube JH, Malouf GG, Lu E, Sphyris N, Vijay V, Ramachandran PP, et al. Epigenetic silencing of microRNA-203 is required for EMT and cancer stem cell properties. Scientific Reports. 2013;3:2687.

208. Chen J, Tian W, Cai H, He H, Deng Y. Down-regulation of microRNA-200c is associated with drug resistance in human breast cancer. Medical Oncology. 2012;29(4):2527-34.

209. Saxena M, Stephens MA, Pathak H, Rangarajan A. Transcription factors that mediate epithelial-mesenchymal transition lead to multidrug resistance by upregulating ABC transporters. Cell Death & Disease. 2011;2:e179.

210. Jiang ZS, Sun YZ, Wang SM, Ruan JS. Epithelial-mesenchymal transition: potential regulator of ABC transporters in tumor progression. Journal of Cancer. 2017;8(12):2319-27.

211. Liao H, Bai Y, Qiu S, Zheng L, Huang L, Liu T, et al. MiR-203 downregulation is responsible for chemoresistance in human glioblastoma by promoting epithelial-mesenchymal transition via SNAI2. Oncotarget. 2015;6(11):8914-28.

212. Chen T, Xu C, Chen J, Ding C, Xu Z, Li C, et al. MicroRNA-203 inhibits cellular proliferation and invasion by targeting Bmi1 in non-small cell lung cancer. Oncology Letters. 2015;9(6):2639-46.

213. Zhang Z, Zhang B, Li W, Fu L, Fu L, Zhu Z, et al. Epigenetic silencing of miR-203 upregulates SNAI2 and contributes to the invasiveness of malignant breast cancer cells. Genes & Cancer. 2011;2(8):782-91.

214. Hailer A, Grunewald TG, Orth M, Reiss C, Kneitz B, Spahn M, et al. Loss of tumor suppressor mir-203 mediates overexpression of LIM and SH3 protein 1 (LASP1) in high-risk prostate cancer thereby increasing cell proliferation and migration. Oncotarget. 2014;5(12):4144-53.

215. Chi Y, Jin Q, Liu X, Xu L, He X, Shen Y, et al. miR-203 inhibits cell proliferation, invasion, and migration of non-small-cell lung cancer by downregulating RGS17. Cancer Science. 2017; 8(12):2366-2372.

216. Ding X, Park SI, McCauley LK, Wang CY. Signaling between transforming growth factor beta (TGF-beta) and transcription factor SNAI2 represses expression of microRNA miR-203 to promote epithelial-mesenchymal transition and tumor metastasis. The Journal of Biological Chemistry. 2013;288(15):10241-53.

217. Taipaleenmaki H, Browne G, Akech J, Zustin J, van Wijnen AJ, Stein JL, et al. Targeting of runx2 by miR-135 and miR-203 impairs progression of breast cancer and metastatic bone disease. Cancer Research. 2015;75(7):1433-44.

218. Iseri OD, Kars MD, Gunduz U. Two different docetaxel resistant MCF-7 sublines exhibited different gene expression pattern. Molecular Biology Reports. 2012;39(4):3505-16.

219. Agarwal V, Bell GW, Nam JW, Bartel DP. Predicting effective microRNA target sites in mammalian mRNAs. eLife. 2015;4.

220. Iseri OD, Kars MD, Arpaci F, Atalay C, Pak I, Gunduz U. Drug resistant MCF-7 cells exhibit epithelial-mesenchymal transition gene expression pattern. Biomedicine & Pharmacotherapy. 2011;65(1):40-5.

221. Gromicho M, Rueff J, Rodrigues AS. Dynamics of expression of drug transporters: methods for appraisal. Methods in Molecular Biology. 2016;1395:75-85.

222. Tiligada E. Chemotherapy: induction of stress responses. Endocrine-Related Cancer. 2006;13 Suppl 1:S115-24.

223. Xu F, Wang F, Yang T, Sheng Y, Zhong T, Chen Y. Differential drug resistance acquisition to doxorubicin and paclitaxel in breast cancer cells. Cancer Cell International. 2014;14(1):538.

224. Beck WT, Grogan TM, Willman CL, Cordon-Cardo C, Parham DM, Kuttesch JF, et al. Methods to detect P-glycoprotein-associated multidrug resistance in patients' tumors: consensus recommendations. Cancer Research. 1996;56(13):3010-20.

225. Katayama K, Kapoor K, Ohnuma S, Patel A, Swaim W, Ambudkar IS, et al. Revealing the fate of cell surface human P-glycoprotein (ABCB1): The lysosomal degradation pathway. Biochimica et Biophysica Acta. 2015;1853(10 Pt A):2361-70.

226. Jin HY, Gonzalez-Martin A, Miletic AV, Lai M, Knight S, Sabouri-Ghomi M, et al. Transfection of microRNA mimics should be used with caution. Frontiers in Genetics. 2015;6:340.

227. Lebedeva IV, Pande P, Patton WF. Sensitive and specific fluorescent probes for functional analysis of the three major types of mammalian ABC transporters. PLoS One. 2011;6(7):e22429.

228. Moes M, Le Bechec A, Crespo I, Laurini C, Halavatyi A, Vetter G, et al. A novel network integrating a miRNA-203/SNAI1 feedback loop which regulates epithelial to mesenchymal transition. PLoS One. 2012;7(4):e35440.